ISTANBUL TECHNICAL UNIVERSITY ★ INSTITUTE OF SCIENCE AND TECHNOLOGY

DYNAMIC PROPERTIES AND STATIC BEHAVIOR OF FIBER REINFORCED SAND

M.Sc. Thesis by
Hande GERKUŞ

Department : Civil Engineering

Programme : Soil Mechanics and Geotechnical Engineering

JUNE 2011

ISTANBUL TECHNICAL UNIVERSITY ★ INSTITUTE OF SCIENCE AND TECHNOLOGY

DYNAMIC PROPERTIES AND STATIC BEHAVIOR OF FIBER REINFORCED SAND

M.Sc. Thesis by
Hande GERKUŞ
501091321

Date of submission :   **06 May 2011**
Date of defence examination: **13 June 2011**

Supervisor (Chairman) :   **Prof. Dr. Ayfer ERKEN (ITU)**
Members of the Examining Committee :   **Prof. Dr. Atilla ANSAL (BU)**
Assoc. Prof. Dr. Recep İYİSAN (ITU)

JUNE 2011

İSTANBUL TEKNİK ÜNİVERSİTESİ ★ FEN BİLİMLERİ ENSTİTÜSÜ

FİBER İLE GÜÇLENDİRİLMİŞ KUM ZEMİNLERİN DİNAMİK ÖZELLİKLERİ VE STATİK DAVRANIŞLARI

YÜKSEK LİSANS TEZİ
Hande GERKUŞ
(501091321)

Tezin Enstitüye Verildiği Tarih :   06 Mayıs 2011
Tezin Savunulduğu Tarih :   13 June 2011

Tez Danışmanı :   Prof. Dr. Ayfer ERKEN (İTÜ)
Diğer Jüri Üyeleri :   Prof. Dr. Atilla ANSAL (BÜ)
Doç. Dr. Recep İYİSAN (İTÜ)

HAZİRAN 2011

FOREWORD

This master of thesis has been prepared for submission to Istanbul Technical University, Civil Engineering Department-Geotechnical Engineering Program.

I would like to express my sincere thanks to my advisor Prof. Dr. Ayfer ERKEN, for sharing her knowledge, for her guidance and efforts to help me complete this thesis on time. I would to thank Prof. Dr. Atilla ANSAL and Assoc. Prof. Dr. Recep İYİSAN, for contributing to my thesis with their valuable comments.

I would like to present my special thanks to Mojtaba TORABİ (B.Sc.) for his support during the experimental part of my study.I would like to thank Research Assistant Mustafa HATİPOĞLU for his advices throughout my study. I would also like to thank ITU Soil Mechanics Laboratory staff for all their support.

Finally, I present my deepest appreciation to my mother Semra GERKUŞ and my brother Halit GERKUŞ, for being my greatest support throughout my life. I present my special thanks to Berkay KOÇAK (B.Sc.) for his support and encouragement.

May 2011   Hande GERKUŞ

                                                Civil Engineer

TABLE OF CONTENTS

ABBREVIATIONS

ASTM   **:** American Society for Testing and Materials
CD   **:** Consolidated drained
CU   **:** Consolidated undrained
In.   **:** Inch
kN   **:** Kilonewton
kPa   **:** Kilopascal
MPa   **:** Megapascal
PVD   **:** Prefabricated vertical drain
P.W.P.   **:** Pore water pressure
Psi   **:** Pounds per square inch
SP   **:** Poorly graded sand
Wt   **:** Weight

x

LIST OF TABLES

LIST OF FIGURES

SYMBOL LIST

A_R **:** Cross sectional area of all fibers crossing the shear plane
A **:** total cross-sectional area of the failure plane
c : Cohesion
c' : Effective stress cohesion intercept
C_u : Coefficient of uniformity
C_c : Coefficient of curvature
d : Fiber diameter
D **:** Damping ratio
D_{10} **:** Effective size
D_{30} **:** Diameter corresponding to 30% finer
D_{60} **:** Diameter corresponding to 60% finer
D_r **:** Relative density
e **:** Void ratio
E **:** Elasticity modulus, Young's modulus
E_{max} **:** Maximum Elasticity modulus, Maximum Young's modulus
E_r **:** Fiber Modulus
G **:** Shear Modulus
i **:** Fiber orientation angle
k **:** Shear distortion ratio
L : Length
p : Total mean stress
p^* : Effective mean stress
q : Deviatoric stress
u : Pore water pressure
N_s : Average number of fibers intersecting a unit area
t_R **:** Mobilized tensile strength of fiber per unit area of soil
V **:** Volume
V_r **:** Volume of fibers in a specimen
ω **:** Angle of distortation
w **:** Water content
x **:** Shear displacement parallel to the shear zone
z **:** Thickness
β_f **:** Volume fraction
$\Delta\sigma$ **:** Deviator stress
ΔS_R **:** Shear strength increase
$\varepsilon, \varepsilon_l, \varepsilon_a$ **:** Axial strain
ε_q **:** Shear strain
ε_v **:** Volumetric strain
ϕ **:** Shear strength angle, internal friction angle
ϕ' **:** Effective stress friction angle
ϕ^*_m **:** Mobilized friction angle
θ **:** Angle of distortation
ζ **:** Empirical coefficient

μ	**:** Poisson's ratio
τ	**:** Shear stress
γ	**:** Shear strain
σ₁	**:** Major principle stress
σ₃	**:** Minor principle stress
σₐ	**:** Axial stress
σc, σconf	**:** Confining stress
σcrit	**:** Critical stress
σn	**:** Normal stress
σr	**:** Radial stress
σR	**:** tensile stress developed in the fiber at the shear failure
ρ	**:** Fiber content by the percentage of weight
μ	**:** Poisson's ratio
η	**:** Aspect ratio

DYNAMIC PROPERTIES AND STATIC BEHAVIOR OF FIBER REINFORCED SAND

SUMMARY

In the recent years, very high loads are applied on soil deposits as a result of developing technology, raising population and increasing demand for giant structures. In most of the constructions, the soil properties need to be improved in order to enable safe and economical constructions. Soil improvement techniques are used to improve the engineering properties of soils. Different methods are preffered according to the requirements and soil type. One of the most commonly used soil improvement type is the addition of substances such as polypropylene fibers.

In scope of this research, the dynamic properties and static behavior of fiber reinforced sand is determined by performing labaratory tests. Conducted laboratory tests are cyclic triaxial test, static triaxial test and direct shear test. The maximum Elasticity Modulus, the stress-strain response under monotonic loading and shear strength parameters are determined for unreinforced and reinforced sand specimens. While the type of fiber and sand is kept constant, effect of different parameters are tested in each test. The main aim is to find the effect of fiber inclusion on the behavior of tested sand.

The cyclic triaxial test is performed to determine the maximum Elasticity Modulus at two different confining pressures. The static triaxial test is performed at different strain rates on saturated specimens. The consolidated undrained and consolidated drained triaxial tests are performed. Also samples prepared at certain water content are subjected to static triaxial test. In the second part of the experimental study, direct shear tests are performed on unreinforced and randomly distributed fiber reinforced samples. The effect of different fiber contents on the behavior of sand is tested during the experimental study. The effect of fiber inclusion on the shear strength parameters are discussed by using the experimental results obtained from direct shear and triaxial tests.

In general, the results obtained from laboratory tests showed that fiber reinforcement improves the static behavior of sand, depending on the test type and tested fiber content. On the other hand, the effect of strain rate on the triaxial test results can be considered insignificant.

FİBERLE GÜÇLENDİRİLEN KUM ZEMİNLERİN DİNAMİK ÖZELLİKLERİ VE STATİK DAVRANIŞI

ÖZET

Gelişen teknoloji ve artan nüfusa bağlı olarak günümüzde zeminler yüksek miktarda yüklere maruz kalmaktadırlar. Birçok inşaat projesinde, güvenli ve ekonomik çözümler geliştirebilmek için zeminlerin mühendislik özelliklerinin iyileştirilmesi gerekmektedir. Zemin iyileştirme yöntemleri de zeminlerin mühendislik parametrelerini iyileştirmek için geliştirilen yöntemlerdir. Uygulanan zemin iyileştirme yöntemi, zemin cinsine ve uygulamanın gerekliliklerine bağlıdır. Günümüzde en çok kullanılan zemin iyileştirme yöntemlerinden biri de çeşitli zemine çeşitli malzemeler katılarak zemin iyileştirilmesidir. Özellikle polipropilen fiberler sıkça kullanılmaktadır.

Bu çalışma kapsamında fiber katılmış kum zeminin dinamik özellikleri ve statik davranışı laboratuvar deneyleri ile incelenmiştir. Dinamik üç eksenli deney sistemi, statik üç eksenli deney sistemi ile kesme kutusu deney sistemi kullanılarak zeminin davranışı belirlenmiştir. Temiz kum ve fiberle güçlendirilmiş kum için maksimum Elastisite Modülü, statik yük altında gerilme-deformasyon davranışı ve kayma mukavemeti parametreleri belirlenmiştir. Deneylerde kullanılan fiber ve kum çeşidi sabit tutularak çeşitli parametrelerin etkisi incelenmiştir. Öncelikle her deneyde fiberin zeminin davranışına etkisi incelenmiştir.

Dinamik üç eksenli deney sisteminde, numunelerin maksimum Elastisite Modülleri iki farklı konsolidasyon basıncı altında belirlenmiştir. Statik üç eksenli deney sisteminde ise değişik deformasyon hızlarında doygun numuneler test edilmiştir. Numunelere, konsolidasyonlu drenajsız ve konsolidasyonlu drenajlı deneyler yapılmıştır. Aynı zamanda belirli bir su muhtevasında hazırlanmış ve doygunluğa ulaşmamış numunelerde de statik üç eksenli basınç deneyleri yapılmıştır. Deneysel çalışmanın ikinci bölümünde ise saf kum ve dağınık liflerle rastgele donatılı kumlar kesme kutusu deneyi ile test edilmişlerdir. Deneysel çalışmada farklı fiber oranlarının kumun davranışına etkisi incelenmiştir. Fiber eklemenin kayma mukavemeti parametreleri üzerine etkisi, üç eksenli deney ve kesme kutusu deney sonuçları karşılaştırılarak yorumlanmıştır.

Genel olarak, laboratuvar deney sonuçları fiber eklemenin kumun statik davranışını iyileştirdiğini ve bu iyileşmenin fiber miktarı ile deney çeşidine bağlı olduğunu göstermiştir. Bunun yanı sıra, üç eksenli deneyler test edilen hızlar için deney hızının sonuçlar üzerine önemli bir etkisi olmadığı gözlemlenmiştir.

1. INTRODUCTION

Soil improvement techniques have essential importance for Soil Mechanics and Foundation Engineering Applications. By using different methods, it is possible to improve the engineering properties of soils and thus safer and more economical solutions can be developed.

Addition of substances to improve soil properties dates back to ancient times when sun-dried soil bricks were the primary building materials (Freitag, 1985). As a result of developing technology, adding different substances to improve soil properties became a common application. Fly ash, lime, cement and fibers are the most common additives preferred. The idea of reinforcing soil with adding fibers is derived from the tree root-soil mechanism (Waldron, 1977). Natural and synthetic types of fibers are mixed into soil and their effects are determined by different testing methods.

In scope of this thesis, dynamic properties and static behavior of fiber reinforced sand is determined by performing laboratory tests. For the experimental study, random distribution of fibers is preferred as sample preparation only requires simply mixing fibers into sand and random distribution of fibers provide strength isotropy (Yetimoglu and Salbas, 2002).

First, brief information about the most commonly used soil improvement techniques are presented. Secondly, dynamic properties and static behaviour of sand is presented along with the previous studies on fiber reinforced sand samples. Considering the information obtained from literature study, the experimental program has been prepared.

In the experimental part of this study, cyclic triaxial test, static triaxial test and direct shear test are performed. The engineering properties of Akpınar sand are determined. One type of polypropylene fiber is chosen to mix into poorly graded Akpınar sand. The effect of fiber on the dynamic properties and static behavior of sand is analysed.

The maximum Elasticity Modulus is determined by conducting cyclic triaxial test. The static behavior of randomly distributed fiber reinforced sand and unreinforced sand are analysed by performing static triaxial tests at different strain rates. The saturated and unsaturated specimens prepared at certain water content are used in the experimental study. The direct shear test is performed to determine the effect of fiber inclusions on the shear strength parameters of sand. The shear strength parameters calculated from static triaxial tests conducted on unsaturated samples are compared with the parameters calculated from the direct shear tests. The result of the experimental study will be discussed to present the effect of fiber inclusion on the behaviour of sand.

2. SOIL IMPROVEMENT

2.1 Introduction

Soil improvement techniques are used to improve the engineering properties of soils. These techniques vary by the application methods and soil types that can be improved. These methods are required not only when the top soil is not able to support structures but also when the deeper layers need to be improved. In general, the aim of soil improvement methods is to (Das, 2007):

1. Improve the shear strength of soils and increase the bearing capacity of shallow foundations
2. Reduce the shrinkage and swelling of soils
3. Reduce the settlement of structures
4. Increase the factor of safety for possible slope failure of embankments and earth dams.

Any change that renders parameters of the soil or rock to the required strength or permeability properties by the field construction is classified as stabilization. On the other hand, modification means a minor change in the parameters of soil. Modification of granular soils consists of changing the volume of voids, replacing the void material or application of both. For cohesive soils, modification requires mixing with stabilizers and preloading to reduce settlement.

In scope of soil improvement methods, ground water can be removed with different drainage methods. Methods such as grouting, freezing, mixing and jet piling are used for changing the void fluid (Karol, 2003). In scope of this thesis a general description of widely used methods for soil improvement are stated. It is possible to use only one method or a combination of methods depending on the soil profile and required properties for the construction site.

In this part of the thesis, brief information about soil improvement techniques are presented. Application of methods and their effects on soil properties are decribed briefly.

2.2 Soil Improvement Methods

2.2.1 Mechanical Stabilization

The aim of this method is to change the grain size distribution of the soil by adding binder materials that will fill the voids. In case of granular soils, the binder material adds cohesion to soil. Best results are obtained when the cohesive material occupies 75-90 % of the voids of granular material. For cohesive soils, the granular binder material is mixed with soil (Bowles, 1997).

2.2.2 Compaction

In this method, addition of water rearranges solid particles under compaction energy. The maximum dry unit weight at the optimum moisture content is calculated by applying Standard or Modified Proctor Tests at the laboratory. According to the results of the laboratory compaction tests, specifications for the in situ compaction are determined. In most cases, it is preferred to form a relative compaction of 90% or more based on the laboratory compaction test. The compaction is performed at the field by using rollers such as smooth wheel rollers, pneumatic rubber tired rollers, sheepsfoot rollers and vibratory rollers. Especially cohesive soils are well compacted by rollers (Das, 2007). Vibratory rollers are effective for cohesionless soils (Terzaghi et al., 1996). The soil is excavated until a certain depth, and the soil is backfilled by compacting in layers. The lift thickness should not exceed 75-100 mm for a successful compaction application (Bowles, 1997)

Dynamic compaction is a type of compaction method, which is performed by using a mobile crane to lift and drop a heavy tamper on to the soil. Depending on the height of the drop, weight of the mass and type of the soil, compaction can be performed successfully until a certain depth. This method can be used for compacting saturated soils that are classified as silty and/or clayey sand and gravels. The increase in the fine material content causes the decrease of the compaction. While partially saturated clays above ground water table level can be improved by this method, there can be no improvement for fully saturated clays (Bowles, 1997). The schematically drawing of the dynamic compaction method is shown in Figure 2.1.
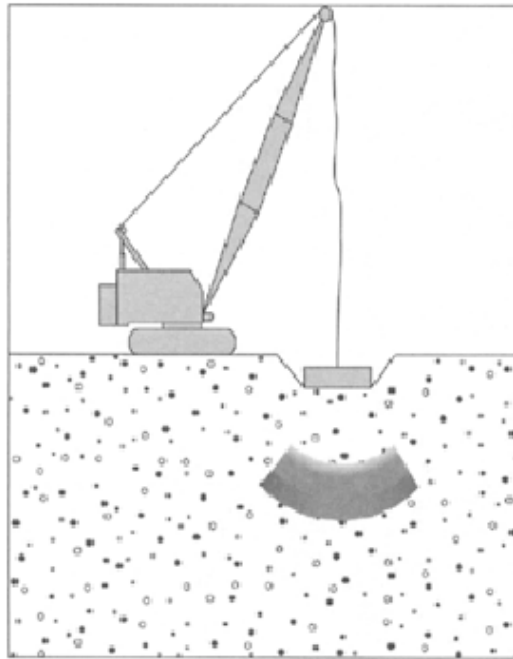
Figure 2.1: Dynamic Compaction Method (Gunaratme, 2006)

2.2.3 Vibro flotation

This method is used for compacting loose clean sand deposits that are above or below ground water table level. The cylindrical probe that includes an eccentric weight rotates about the vertical axis and transfers horizontal vibration to the probe. The sand particles moves and gets denser in a cylindrical zone as the vibrating probe lowers under its own weight The unit includes openings at the bottom and top for water jets and the vibrating unit is attached to the follow-up pipe. The method is applied for forming densified sand columns (Terzaghi et al., 1996).

The grain size distribution of the soil and the nature of the backfill used to fill the holes effects the efficiency of the vibro flotation method (Das,2007).

2.2.4 Blasting

This technique is used for the densification of granular soils. In this method, explosives such as 60 % dynamite are blasted at a certain depth in saturated soils. The explosives are placed at a depth of two-thirds of the thickness of the soil layer so that relative compaction values up to 80% can be achieved (Mitchell, 1970).

2.2.5 Freezing

In this method, a cold medium is contacted to the soil for a certain amount of time until the pore water is freezed. For application, pipes are placed into the soil. Pipes

are combined of two units, a small pipe concentric within a larger pipe. During the transfer of refrigerant through the inner pipe, the soil around the outer pipe is cooled. For using this method, the soil must be saturated and the groundwater movements should be slow. This method is preferred when temporary waterproof barriers are needed. Freezing soil increases the strength of soil but frozen soil masses subject to creep under load. As pollutants are not added to the soil, this method is environmentally friendly (Karol, 2003).

2.2.6 Precompression

Compressible soils such as soft clays, loose silts and most of the organic soils are consolidated by precompression method, which is also known as preloading method. The area is subjected to weight caused by the fill having a weight per unit area high enough to consolidate the soil. While the compressibility of the soil is decreased, the strength is increased. The factor of safety against undrained failure during the precompression application is achieved by determining adequate magnitude and rate for preloading (Terzaghi et al., 1996).

2.2.7 Drainage Methods

Different types of drainage methods are used to remove the water in the soil and thus increase the rate of settlements. In most of the natural deposits, the permeability of soil differentiates from point to point. Methods such as pumping of water from shafts in the excavation area, suction of water by well point method, deep well drainage method, drainage by electro-osmosis and vacuum method are also used (Terzaghi et al., 1996). Brief information about commonly used drainage methods are presented.

The sand drain method is used to accelerate the consolidation settlement of impermeable layers, especially soft, normally consolidated clay layers. The estimated rate of consolidation varies if horizontally discontinuous isolated sand layers exist in the compressible profile, as the drainage layers cannot be accurately determined. The installation of vertical drains is used in accordance with natural drainage layers (sand blankets) to increase the rate of consolidation. For this purpose, sand drains or fabric-encased sand drains are used (Terzaghi et al., 1996). The holes are drilled at regular intervals into the clay layers. After completing the backfilling with sand, a surcharge is applied at the ground surface and it increases the pore water pressure in the clay

layer. The excess pore water pressure is dissipated through sand drains and thus it accelerates the consolidation (Das, 2011).

The prefabricated vertical drains (PVDs), also known as wick drains, are used to enable the drainage of low-permeability soils under surface surcharge. These are produced with a channeled synthetic core enclosed by a geotextile filter (Das, 2011). The wick drains does not provide any strengthening effect on the soil except for that resulting from the water content and void ratio reduction (Bowles, 1997). The schematically drawing of the installation of PVDs is shown in Figure 2.2.
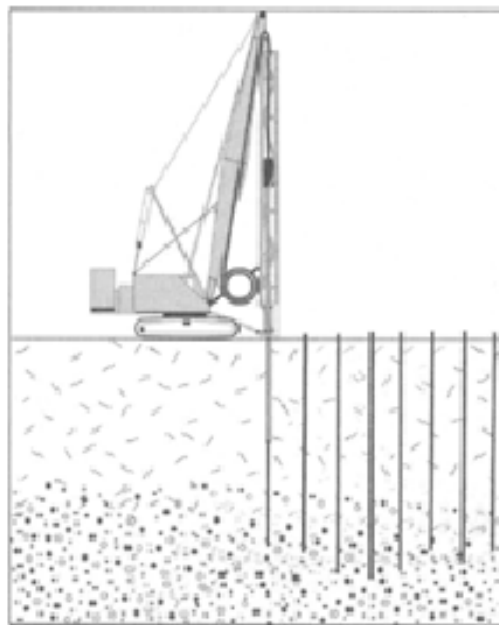
Figure 2.2: Installation of PVDs (Gunaratme, 2006)

2.2.8 Sand Columns

Sand columns are used to increase the stiffness of soils. This method is applicable in both sand and clay deposits. The amount of sand required, the density and spacing of columns are determined according to the present stiffness and target stiffness value. As this method enables the usage of in situ sand, this method can be considered economical in most of the cases (Bowles, 1997).

2.2.9 Stone Columns

This method is used to increase the load-bearing capacity of shallow foundations on soft clay layers (Das, 2011). While the stone columns can be used in sand deposits, it is usually preferred for soft, inorganic, cohesive soils. The vibroflot is used to

produce stone columns. The vibroflot is raised and lowered repeatedly as it cleans the cohesive cuttings by jetting. Then the backfill material is placed in stages by vibrating (Terzaghi et al., 1996). The size of the gravel used as the backfill material ranged between 6 to 40 mm. Stone columns are usually constructed with diameters about 0.5 to 0.75 m. After the construction of stone columns, the fill material is placed over the ground surface and it is compacted (Das, 2011).

2.2.10 Jet Grouting

The jet grouting method consists of injecting cement slurry into the soil at a high velocity in order to create a soil-cement matrix (Das, 2011). A special drill bit with vertical and horizontal high-pressure water jets is used for excavating through soil. The cement slurry is then injected into the soil where it is mixed with the remaining foundation material loosened during excavation (Bowles, 1997). The single, double and triple rod systems are developed for the jet grouting system. The erodibility of the soil effects in jet grout columns. While the high plasticity clays are difficult to erode, gravelly soil and clean sand are highly erodible (Burke, 2004; Welsh and Burke, 1991). The schematically drawing of the jet grout application is shown in Figure 2.3.
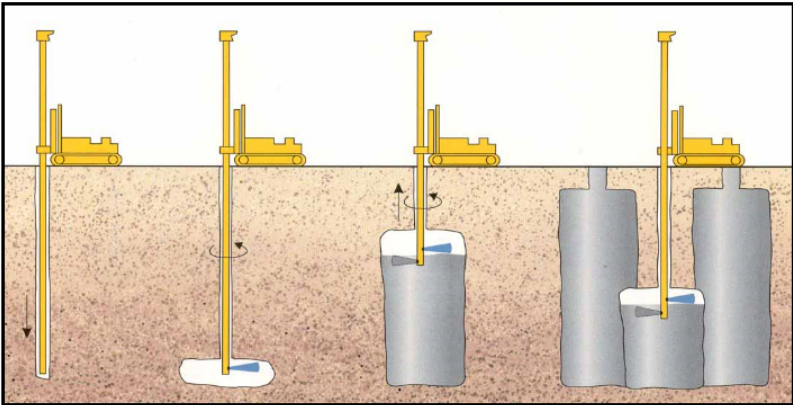
Figure 2.3: Jet Grouting Method (Baker)

2.2.11 Soil Nailing

This is an in situ technique for reinforcing and stabilizing deep cuts. Soil nailing is used for temporary or permanent support for excavations, retaining walls, stabilization of tunnel portals, stabilization of slopes and repairing retaining walls. This method is applicable to cohesive soils or weathered rock as this application requires the soil to temporarily stand in a near vertical face. The soil is excavated at a

certain depth. The soil is drilled and steel reinforcing bars, known as soil nails, are placed and a welded wire mesh is fastened to the steel bars and the excavated face is stabilized by shotcrete application. The schematic drawing of the soil nailing method is shown in Figure 2.4 (Gunaratme, 2006).
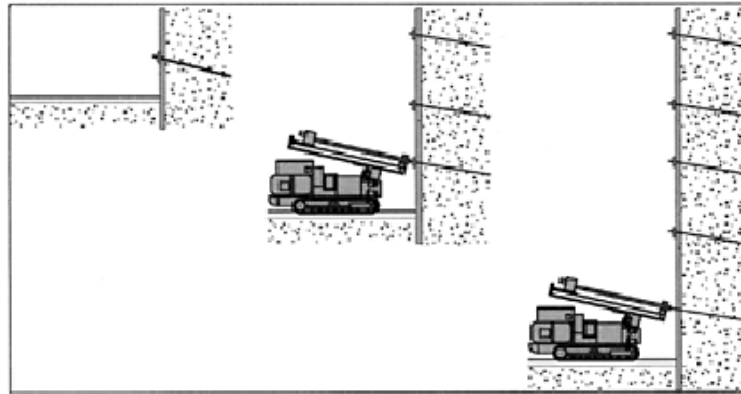
Figure 2.4 : Soil Nailing Process (Gunaratme, 2006)

2.2.12 Use of Geosynthetics

Different types of geosynthetics, synthetic fabric materials, are used to improve soil conditions. They are made from polyster, nylon, polyethylene and polypropylene. Geosynthetics are sufficiently durable materials and they can be used for different purposes (Bowles, 1997). Geosynthetic materials are used for several purposes. They are primarily used for separation, reinforcement, drainage, filtration and as a moisture barrier (Das, 2007).

They types of geosynthetics are geotextiles, geogrids, geonets, geomembranes, geosynthetic clay liners, geopipe and geocomposites. Geotextiles are used for erosion control applications as an alternative for granular soil filters. A typical geotextile application is shown in Figure 2.5. Geogrids are used for reinforcement. Geonets are preffered for drainage applications. Geomembranes are prefered due to their impervious nature. Geosynthetic clay liners are used as hydraulic barrier to water, leachate or other liquids. Geopipes are used for underground pipeline transmission of various types of liquid and gas. Geocomposites are combinations of different types of geosnyhtetic materials. They are used in combinations in order to provide required functions (Koerner, 1998).
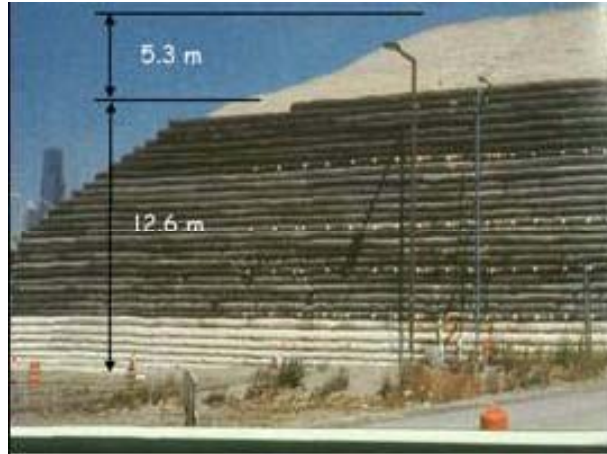
Figure 2.5 : Temporary geotextile wrapped-face wall (Bathurst)

2.2.13 Chemical Stabilization

Chemical admixtures, such as lime, cement, fly ash and their combinations are used to stabilize in situ soils, especially fine grained soils. The aim is to improve the strength and durability of the soil.

The addition of lime into the soil forms cementing material due to the puzzolonic reaction between soil and lime. There are different ways of performing lime stabilization in the field. One method is to mix in situ material with lime at the site and compact after the addition of moisture. The second method is to mix lime, soil and water in a plant and transfer the mixture to the site for compaction. The third method is to inject the lime slurry into the soil under pressure. The addition of lime to fine grained soil increases its unconfined compression strength and tensile strength in a considerable amount (Das, 2011).

Soil stabilization with addition of cement is preferred especially for the high way and earth dam constructions. It is used for stabilizing sand and clayey soils. The cement addition increases the strength of soil in a considerable amount. For field application, the required amount of cement and water are mixed with the soil and compacted (Das, 2011).

Fly ash is obtained from the pulverized coal combustion. It is a puzzolonic fine grained dust, which reacts with hydrated lime to produce cementitious products. Stabilized soil layers for highway bases and subbases are obtained by mixing soil with the lime-fly ash mixture and compacting under controlled conditions (Das, 2011).

2.2.14 Biotechnical and Fiber Reinforcement

Biotechnical reinforcement technique, also known as bioengineering, requires the usage of live vegetation to stabilize slopes against erosion and shallow mass movements (Gunaratme, 2006). The most common method of biotechnical reinforcement is to cover a part or the entire slope with small trees or low ground cover. Another biotechnical stabilization method is using microorganisms such as bacteria and fungi, to remove pollutants from soil and water. This method is known as bioremediation (Karol, 2003).The method of improving the engineering properties of soils by inclusions of various types of fibers is called fiber reinforcement. Randomly distributed discrete fibers are mixed into the soil to increase the strength and assist the soil in tension (Gunaratme, 2006).

2.3 Results

In this part of the thesis, brief description of soil improvement methods, their application and effects are presented. The most common methods are analysed. In scope of this thesis, soil improvement with fiber reinforcement method will be analysed in the following sections.

3. LITERATURE REVIEW

3.1 Introduction

In this part of the thesis, brief information about the dynamic properties of sand and sand behavior under static loading is included. In addition to this, previously conducted studies on sand specimens reinforced with randomly distributed fibers are presented. The effect of fiber inclusions on the static behavior of sand is demonstrated with the sample preparation methods, test methods and effect of different parameters on the test results.

3.2 Dynamic Properties of Sand

Soil behavior under cyclic loading conditions are governed by the dynamic properties of soil. Soil properties, stiffness, damping, Poisson's ratio and density influence the wave propagation and thus the behavior of soils under cyclic loading. Also the rate and number of cycles of loading are important parameters. Volume change characteristics are considered important especially at high strain levels (Kramer, 1996).

The most significant developments in the Soil Dynamics aim to determine elastic characteristics in a strain range between 10^{-6}-10^{-4}. This range respresents the strains encountered in earthquakes (Pecker, 2007). Dynamic properties can be determined directly by the field tests based on wave propagation velocities. The laboratory tests are performed to study soil behavior under controlled stress conditions. In the free vibration tests, an initial displacement is applied to the sample and this displacement is returned under free vibration. In the resonant tests, forced vibrations are applied to the sample and the frequency is tuned until the resonance occurs. The stress paths followed by a soil element in the field is duplicated by forced vibration tests which are cyclic triaxial test, cyclic simple shear test and torsional cyclic shear test (Pecker, 2007).

The cyclic triaxial test is used widely for the determination of cyclic strength and Young Modulus. The sample is isotropically consolidated and subjected to axial

stress in undrained condition. Young's modulus, shear modulus, shear strain and equivalent damping ratio are calculated by using stress strain relations and hysteresis loop. The stress controlled test is performed to determine the cyclic undrained strength of sand (Silver, 1976). Figure 3.1 shows the hysteresis loop obtained from a dynamic triaxial test. From the hysteresis loop the Young's Modulus is calculated as:

$$E = \frac{\Delta\sigma d}{\varepsilon}$$ (3.1)

where $\Delta\sigma_d$ is the deviatory stress and ε is the axial strain. The Shear Modulus (G) can be calculated as:

$$G = \frac{E}{2(1+\mu)}$$ (3.2)

where μ is the Poisson's ratio. The damping ratio is calculated as (Das, 1993):

$$D = \frac{1}{2\pi} \frac{area\ of\ the\ hysteresis\ loop}{area\ of\ the\ triangle\ OAB\ and\ OA'B'}$$ (3.3)
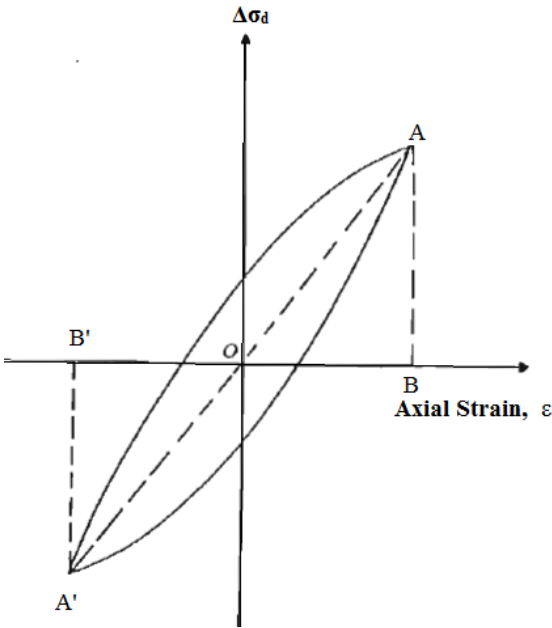
Figure 3.1 : Determination of damping ratio from cyclic triaxial test (Das, 1993)

The maximum modulus, E_{max}, is tangent to the stress-strain curve at the origin. The Figure 3.2 shows the stress-strain diagram that corresponds to the triaxial test and the definition of Young's modulus from the diagram (Sawicki and Swidzinski, 1998).

14
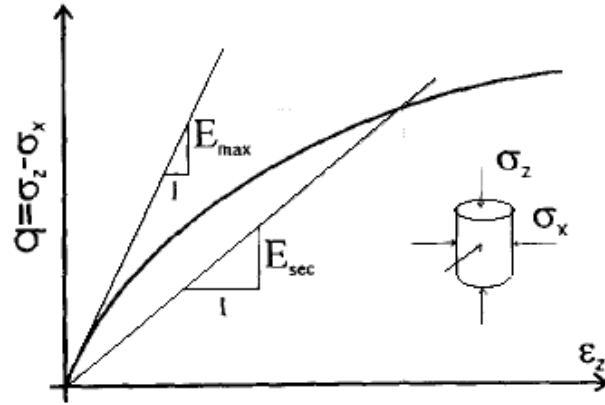
Figure 3.2 : Definition of Young's modulus (Tatsuoka et. al., 1994)

The cyclic simple shear test is performed to determine the behaviour of soils under pure shear stress fields (Silver, 1976). Especially shear modulus and damping ratio of soils can be determined by performing the cyclic simple shear test (Das, 1993). It is mostly used for liquefaction analysis. The device applies shear stress on the top and the bottom surfaces of the specimen (Kramer, 1996). Figure 3.3 shows the hysteresis loop obtained from the cyclic simple shear test. The shear modulus is determined as:

$$G = \frac{\text{amplitude of cyclic shear stress, } \tau}{\text{amplitude of cyclic shear strain, } \gamma'} \tag{3.4}$$

and the damping ratio is calculated as (Das, 2007) :

$$D = \frac{1}{2\pi} \frac{\text{area of the hysteresis loop}}{\text{area of the triangle OAB and OA'B'}} \tag{3.5}$$

For producing more homogeneous stress fields inside the sample and for having control on the radial stress, the torsional cyclic shear test is performed (Pecker, 2007). Cyclic shear stresses are applied on horizontal planes with continuous rotation of principal stresses at isotropic and anisotropic initial stress conditions. The stiffness and damping characteristics can be measure over a wide range of strains by torsional cyclic shear test (Kramer, 1996).

15
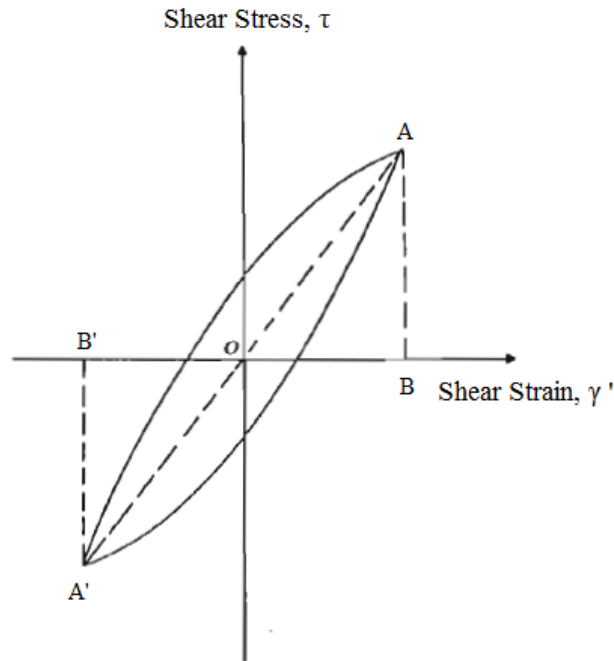
Figure 3.3 : Determination of damping ratio from hysteresis loop (Das, 1993)

3.3 Sand Behavior under Static Loading

Sand deposits are composed of solid particles that transmit inter-granular forces through points of contact. The term dilatancy is used to describe the volume change due to shear stress application. This volume change occurs as a result of slip-down and roll over movements of particles. While the volume reduction is observed at early stages of loading due to slip-down movement of particles, volume increase or dilation is induced at large deformations. Figure 3.4 shows the stress-strain relations of saturated sand specimens obtained from undrained shear tests. The strain hardening behavior is observed at large densities and the shear stress increases along with the shear strain. In this case, the dense sand sample is being dilative. The strain softening behavior is observed in the sample with a drop of shear stress followed by large strains. This behavior is preferred as flow type (Ishihara, 1996).

At moderate densities, the sand first shows strain-softening response at moderate strains. As the strain increases, strain hardening behavior is observed. This behavior is referred as flow type (Ishihara, 1996).

16
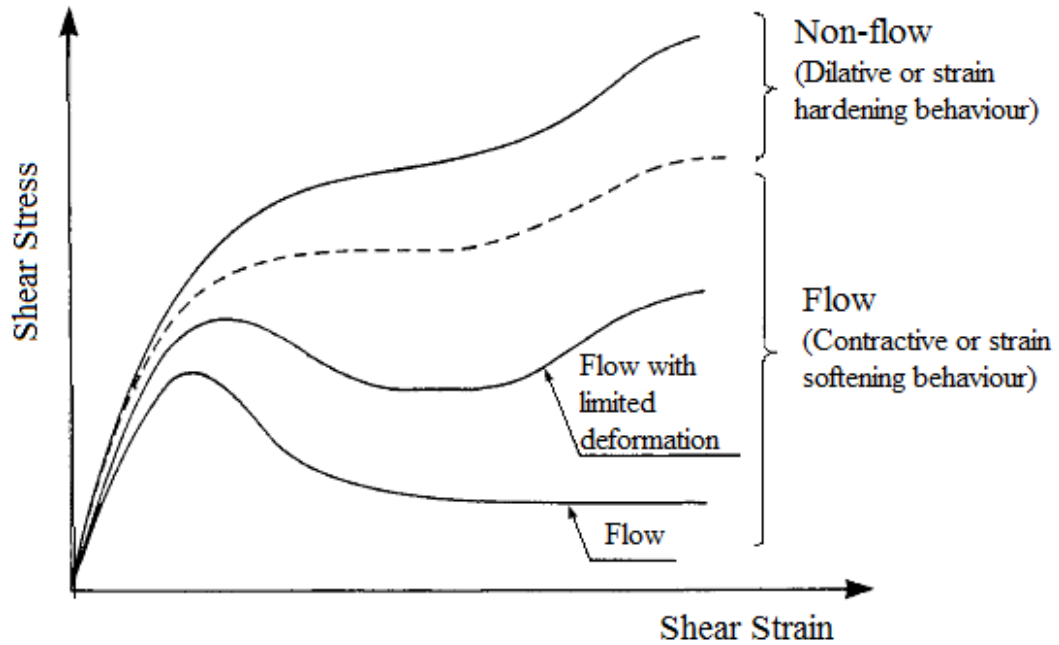
Figure 3.4 : Undrained behavior of sandy soils based on contractiveness and dilativeness (Ishihara, 1996)

The static shear strength of sands mostly depends on the density. Laboratory tests are performed to determine the static strength of sand. In addition, different correlations are developed by many researchers to determine the static strength of sands by using in-situ test results. (Srbulov, 2008).

3.4 Compression and Extension Tests on Sands Reinforced with Randomly Distributed Fibers

Babu et. al (2007) used coir fibers as reinforcement in their study. Coir is a biodegradable and thus environmentally friendly fiber and it is used to provide short term stability in the bund constructions. In this study, randomly distributed coir fibers are mixed with soil and triaxial compression tests were performed.

The samples subjected to triaxial tests included dry sand finer than 425 μm and coir fibers of 15 mm length and 0.25 mm average diameter. Soil samples are used with a diameter of 38 mm diameter and height of 76 mm. The samples were prepared by the method of dry mixing and according to observations, fibers mixed randomly within the soil. The triaxial tests were performed at confining pressures of 100 and 150 kPa with the fiber contents of 0%, 0.5%, 1.0% and 1.5%. The soil density was kept equal to 14.8 kN/m^3 in all the experiments. The application of deviatory stress continued until the specimen failed or a strain level of 10% is observed, whichever was earlier.

According to the triaxial test results, shown in Figure 3.5 (a)-(b), it is noted that the addition of fibers improved the stress-strain response of sand significantly.

In the second part of the research, the finite difference code of FLAC³ᴰ (2002) was used to analyze the behavior of coir fiber reinforced sand. Elastic-perfectly plastic Mohr-Coulomb model is used for the material behavior simulation, as the anticipated stress paths are mainly dominated by shear failure as a result of load application on the soil. Sand specimens with a diameter of 38 mm and a height of 76 mm are generated using cylindrical elements. The cable elements are used for the modeling of coir fibers as they cannot resist bending moments like fibers. A parameter, which is described as cross sectional area times Young's modulus divided by its length, is used to describe the axial stiffness of the cable element. The randomly oriented fibers within the sample domain are created by writing a numerical code using the built-in programming language FISH. Even though the cohesive strength of soil is practically zero, an amount of 0.1 kPa is used in order to establish numerical stability in the analysis.
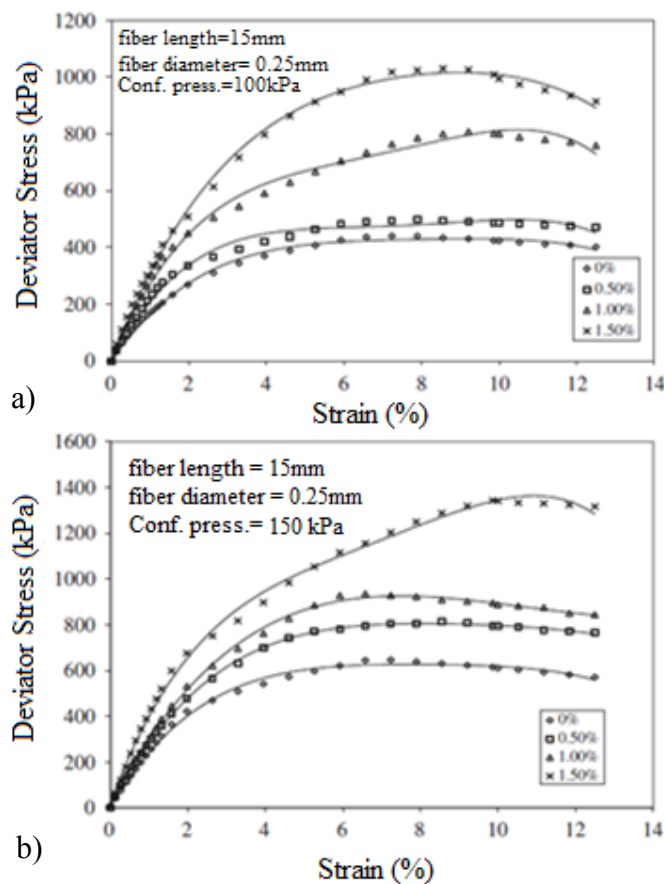
Figure 3.5 : Stress-strain curves for various fiber contents (Babu et al., 2007)

According to the stress-strain curves obtained from experiments and numerical simulations for the plain soil, it is noted that the results show good agreement. Figure 3.6 shows the stress-strain plots of both experiments and simulations. It is resulted that increase in confining stress causes increase of the failure deviatory stress and it leads to increase in shear strain. When shear stress exceeds the shear strength of soil, localization of strain causes the failure of soil sample. It is also stated that the addition of fibers results in the increase of deviatory stress by reducing the localization of strain to a broader area and creating additional frictional resistance in the soil. According to the numerical simulations, it is concluded that the stress-strain response of random-reinforced soil is governed by the pull-out resistance of fibers.
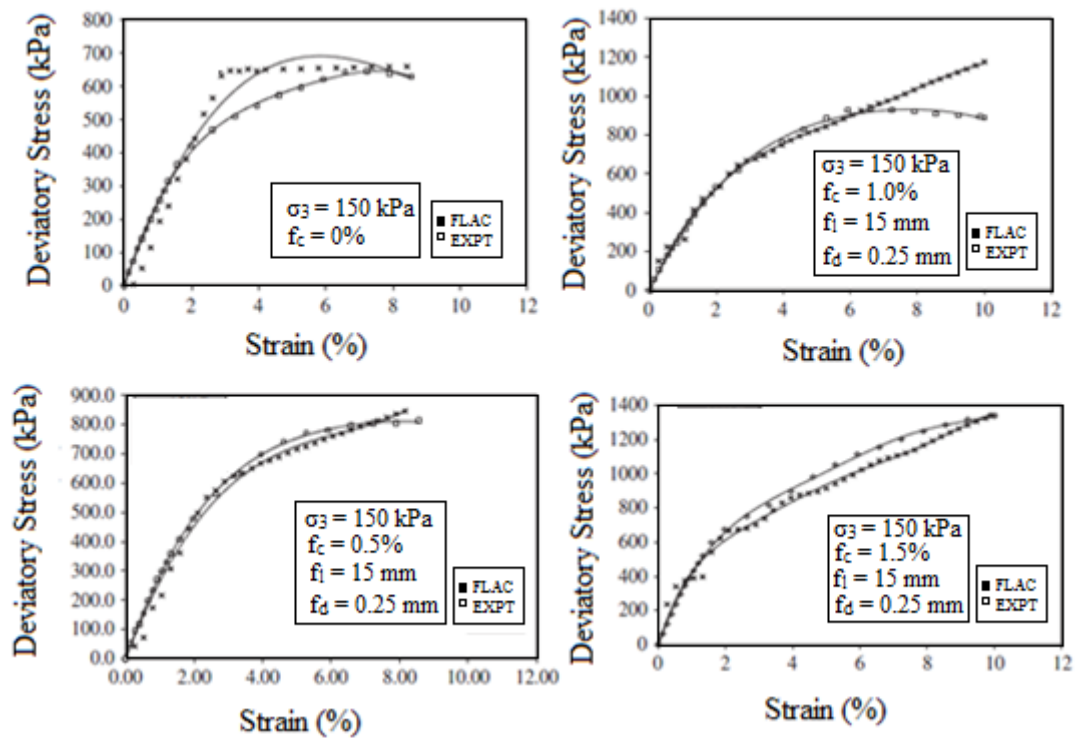
Figure 3.6 : Experimental and numerical stress-strain plots (Babu et. al, 2007)

Ranjan et al. (1994) performed triaxial compression tests to investigate the stress deformation behavior of plastic-fiber reinforced fine sand and the effect of confining stress on the failure envelope of reinforced sand. Generally the effects of fiber content, aspect ratio and confining stresses are searched. In this study poorly graded fine sand was mixed with the plastic fibers. For sample preparation, a standard Proctor test was performed on unreinforced soil and the optimum moisture content at the maximum dry unit weight was determined. Fiber contents of 1%, 2%, 3% and 4% of the weight of the soil solids were mixed with soil at the optimum moisture

content. Samples were tested at a confining stress of 50-400 kPa with varying fiber contents and aspect ratios in order to obtain the effect of fiber parameters, such as the fiber content and aspect ratio, on the shear strength.

Figure 3.7 indicates that the addition of fibers affected the behaviour of sand. Results indicate that while the unreinforced sand reaches a peak stress at around 10 %, fiber reinforced sand samples do not exhibit any peak stress. In this analysis, the failure condition was defined as the stress corresponding to the peak stress condition or at 20% axial strain whichever was earlier.
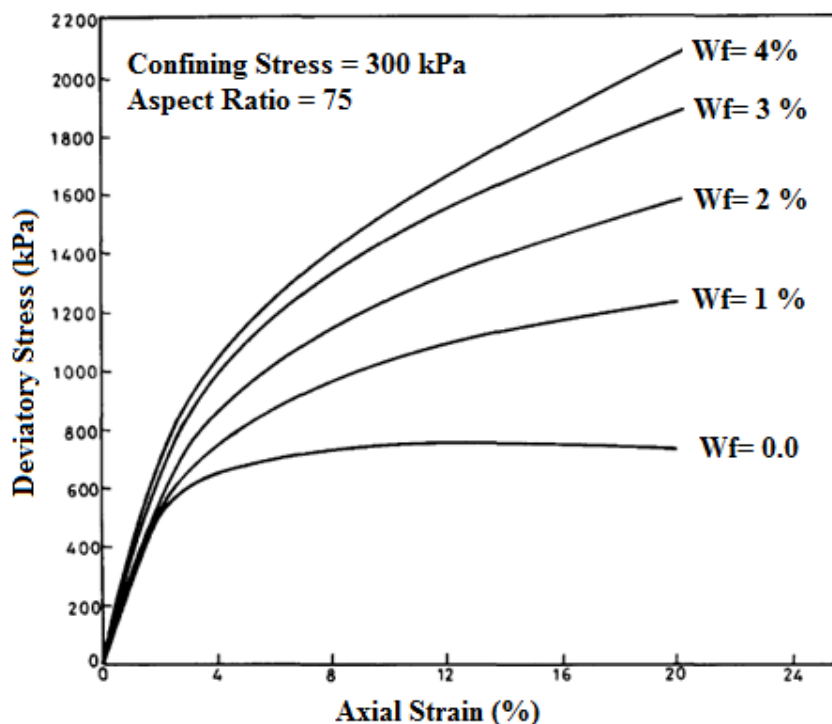
Figure 3.7 : Stress-strain behaviour of fiber-reinforced sand (Ranjan et al. 1994)

The term "critical confining stress" was used to describe the critical stress corresponding to the break in failure envelope. It is stated that at confining stresses below the critical confining stress value, the fibers slip during deformation and at confining stresses above the critical confining stress value, fibers strech or yield. In this research, the effect of fiber aspect ratio was determined by performing triaxial tests with soil samples that has same amount of fibers with different aspect ratios.

As it is shown in Figure 3.8, the aspect ratio of fibers in a soil sample affects the level of critical confining stress in a considerable amount. This process is described by stating that as the length of fiber available to mobilize surface resistance is small

in lower aspect ratios, high confining stresses are required for the mobilization of frictional resistance (Ranjan et. al., 1994).
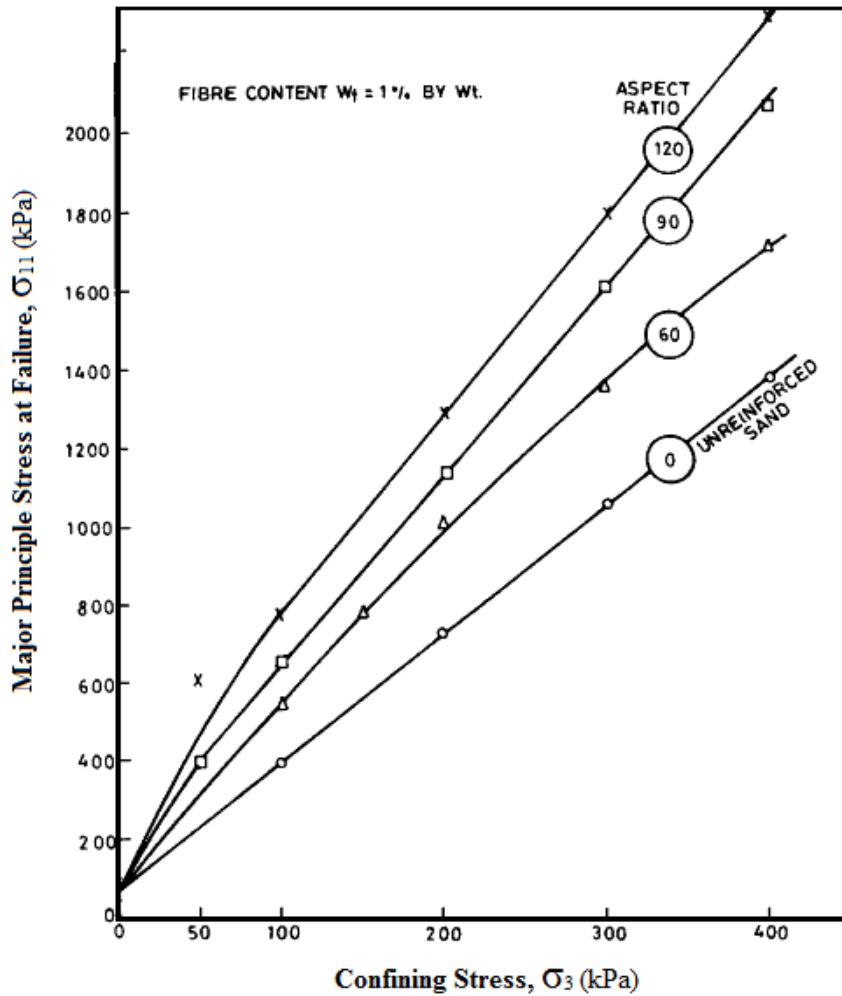
Figure 3.8 : Effect of aspect ratio on critical confining stress (Ranjan et al. 1994)

In this study, it is mentioned that at lower fiber contents, the strength of reinforced sand increases more rapidly. As the specific gravity of fibers was relatively small, they occupied large volume in the composite. Besides, it was observed that for fiber content beyond 2%, as the amount of fibers increased, it became more difficult to create a fairly uniform distribution of fibers inside the soil because fibers tend to ball up. It is concluded that the fibers increased peak shear stress as they reduced the loss of post-peak stress (Ranjan et. al., 1994).

Diambra et al. (2009) performed triaxial compression and extension tests on sand samples reinforced with short polypropylene. The moist tamping technique is used for the preparation of specimens. The fiber concentration is defined as a percentage

of dry weight of sand and fiber concentrations of 0.3%, 0.6% and 0.9% were used alongside with the unreinforced sand. Drained triaxial compression and extension test were performed on isotropically consolidated specimens. The failure condition was defined as 20 % axial strain for compressive loading. According to the results it is noted that fiber addition increased the friction angle and cohesion intercept significantly. Dense specimens have more tendencies to dilate and it results in greater potential tensile stresses in the fibers therefore larger strength increases can be observed compared to loose specimens. In triaxial compression tests, 0.6% fiber content provided a net deviatoric stress increase up to 180-200%. On the other hand, the contribution of fibers to the deviatoric response in triaxial extension tests was limited, only 8% to 10% net strength increase was recorded for the extension tests.

Diambra et al. (2009) developed the theoretical model based on the rule of mixtures. The results of experimental tests are compared with the proposed model based on the rule of mixtures. This model considered the fiber orientation distribution function. It is stated that the excursions between experimental test results and modeling approach can be compensated by a more complex model that also considers the non-linear behavior.

Michalowski and Zhao (1996) presented a mathematical description of a failure criterion for fiber-reinforced soil in a macroscopic stress space. A series of triaxial tests were conducted on sand specimens reinforced with stainless steel or polyamide monofilament fibers. According to experimental test results, it is stated that steel fiber inclusions increased the peak shear stress and the stiffness prior to reaching failure. Polyamide fiber addition also increased the peak shear stress for large confining pressures but a loss of stiffness and an increase of the strain prior to failure was observed. Mohr Coulomb model was used as the matrix failure criterion and it was independent of the intermediate principal stress. The limit condition for the reinforced sand is represented in terms of the maximum shear stress and the mean maximum-minimum principal stress. The internal friction angles calculated from the axisymmetrical triaxial compression tests were used to demonstrate the internal friction angle of the theoretical prediction. In the theoretical model, the fiber failure is defined related to the volumetric concentration, aspect ratio, yield point, fiber-soil interface friction angle and the internal friction angle of the granular matrix. As it can be seen in Figure 3.9 (a)-(b), the predictions of the theoretical model were consistent

with the results of experimental tests conducted on both steel fiber reinforced sand and polyamide fiber reinforced sand.
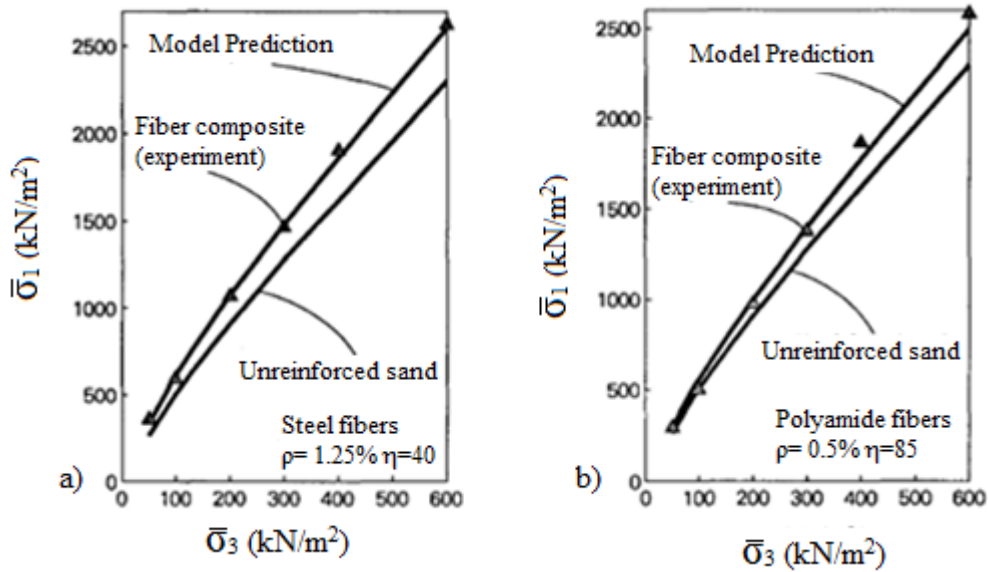
Figure 3.9 : Comparison of theoretical and experimental failure criteria
(Michalowski and Zhao, 1996)

Maher and Gray (1990) performed laboratory triaxial compression tests on sands reinforced with discrete, randomly distributed fibers to determine the effect of sand granulometry and fiber properties on the strength-deformation process of the composites. The assumptions for the theoretical model are stated below.

1. Fibers have a constant length and diameter.

2. The smaller portion of a fiber length on either side of a failure plane is uniformly distributed between zero and half of the fiber length.

3. All the fibers have the same probability of making all possible angles with any arbitrarily chosen fixed axis.

4. Fibers and their points of intersection with any failure plane are randomly distributed in the soil mass.

5. When the confining stress is less than the critical confining stress, fibers slip during deformation. At confining stresses higher than the critical confining stress, fibers yield according to the Mohr-Coulomb yield criterion.

Also the Poisson-Distribution assumption is valid for this theoretical model. Thus, it is stated that the number of fibers in a volume is equal to the known average number

of fibers randomly distributed in the matrix and it is directly related to the volume fraction β_f, length L and diameter d of the fibers (Maher and Gray, 1990).

According to the theoretical study, the shear strength increase due to fiber inclusion is calculated as:

$$\Delta S_R = t_R \left[\sin w + \cos w \tan \phi \right]$$ **(3.6)**

where

ΔS_R=shear strength increase due to fiber inclusion

t_R=mobilized tensile strength of fiber per unit area of soil

ϕ=internal friction angle of sand

ω=angle of distortion

x=shear displacement parallel to the shear zone

z=thickness of shear zone.

The angle of distortion is calculated as;

$$w = tg^{-1} \left(\frac{x}{z} \right)$$ **(3.7)**

and the t_R is calculated as;

$$t_R = \frac{A_R}{A} \sigma_R$$ **(3.8)**

where

$$A_R = N_S \left(\pi \frac{d^2}{4} \right) A$$ **(3.9)**

A_R= cross sectional area of all fibers crossing the shear plane

A= total cross-sectional area of the failure plane

Ns=average number of fibers intersecting a unit area

d=fiber diameter

σ_R=tensile stress developed in the fiber at the shear failure.

Maher and Gray (1990) developed the theoretical model for calculating the shear strength increase in sand due to fiber inclusion considering the bilinearity of failure envelopes and the existence of critical confining stress. According to the model, for $0 < \sigma_{conf} < \sigma_{crit}$;

$$\Delta S_R = N_S\left(\pi\frac{d^2}{4}\right)\left(2\sigma_{conf}\,tg\,\delta\right)\left(\sin w + \cos w\tan\phi\right)\zeta \qquad\qquad \textbf{(3.10)}$$

and for $0\ \sigma_{conf} > \sigma_{crit}$

$$\Delta S_R = N_S\left(\pi\frac{d^2}{4}\right)\left(2\sigma_{crit}\,tg\,\delta\right)\left(\sin w + \cos w\tan\phi\right)\zeta \qquad\qquad \textbf{(3.11)}$$

where

σ_{crit} = critical confining stress

σ_{conf} = average confining stress in triaxial chamber

ζ = an empirical coefficient depending on sand granulometry and fiber parameters.

Maher and Gray (1990) performed 180 triaxial compression tests on randomly distributed fiber reinforced sand within the scope of experimental program. The sand samples were mixed with fibers at a moisture content of 10% to prevent fiber sunder. Different types of sands were mixed with natural and synthetic fibers to determine the effect of sand granulometry and fiber types on the behavior of composites under static loading conditions. According to the results, it is stated that rounded sands exhibited curved-linear behavior while angular sands exhibit bilinear behavior as it is shown in Figure 3.10 (a)-(b).
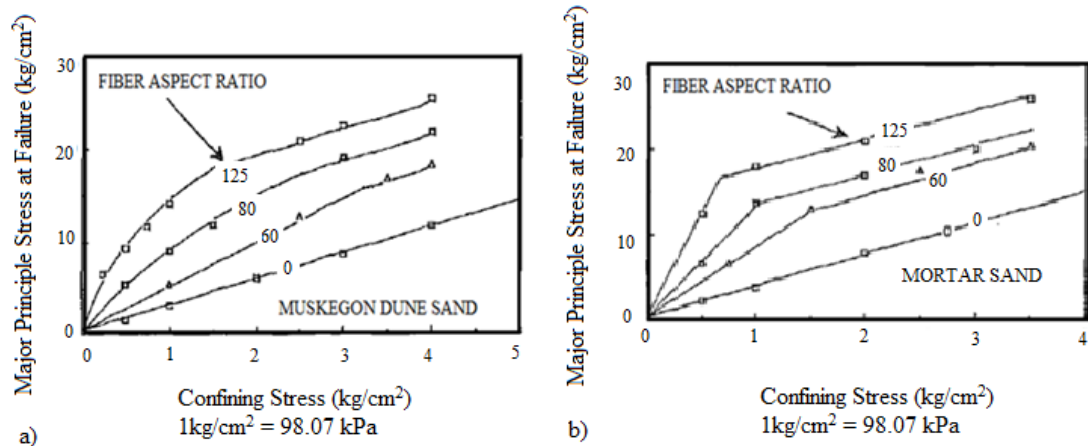
Figure 3.10 : Principal stress envelopes from triaxial tests on reinforced sand:
(a) Muskegon Dune Sand; (b) Mortar Sand (Maher and Gray, 1990)
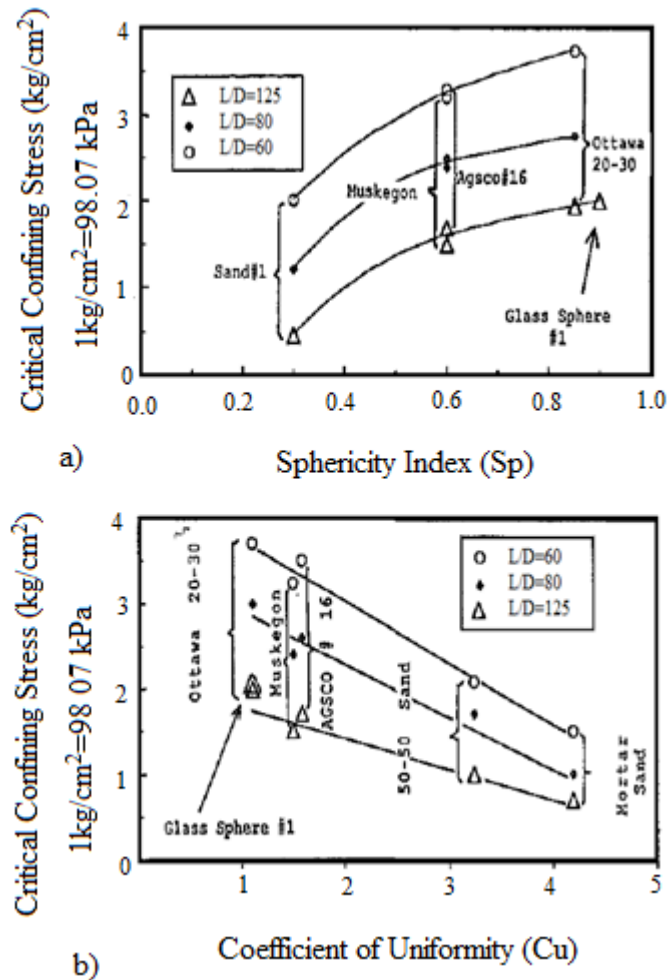
Figure 3.11 : Influence of (a) sand particle and shape; (b) gradation on critical confining stress (Maher & Gray, 1990)

The results indicated that the strength increase provided by fiber addition depends on the soil-fiber parameters such as fiber aspect ratio and modulus, fiber content, grain size, gradation and shape. According to the experimental results it is stated that an increase in fiber aspect ratio (L/D) results in a decrease in σ_{crit} and an increase in shear strength. As it is shown in Figure 3.11 (a)-(b), increase of coefficient of uniformity or a better gradation of sand results in lower σ_{crit} and higher shear strength (Maher and Gray, 1990).

Maher and Gray (1990) stated that at high confining stresses or fiber aspect ratios, the fiber addition causes a linear increase in strength but when those parameters have low values the strength increase reaches an asymptotic upper limit. This behavior can be seen in Figure 3.12.
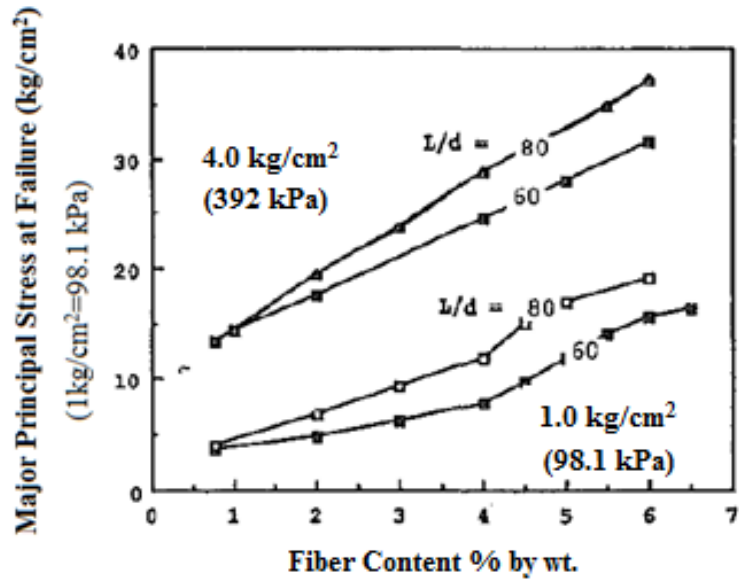
Figure 3.12 : Influence of fiber content and aspect ratio on strength increase in Muskegon Dune Sand (Maher and Gray, 1990)

Functional relationships derived from experimental results in order to estimate σ_{crit} and ζ values, to be used in the theoretical model for the calculations of the effects of fiber inclusions. Maher and Gray (1990) stated that experimental results and the model predictions were in agreement. In Figure 3.13 the Principal Stress Enveloped show this agreement clearly.
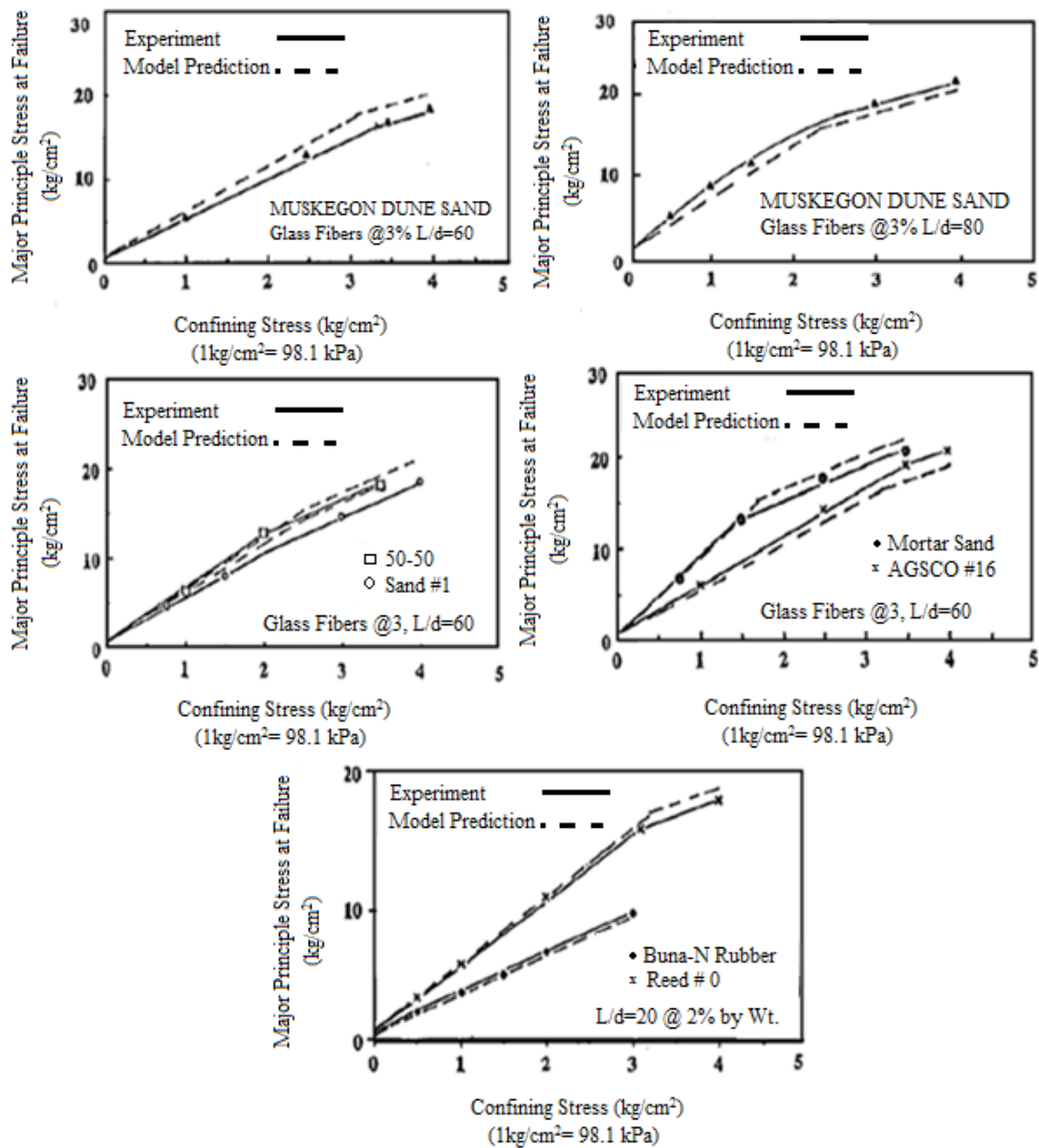
Figure 3.13 : Theoretical versus Experimental Principal Stress Envelopes
(Maher and Gray, 1990)

Santoni et al. (2001) investigated the suitability of randomly oriented discrete fiber reinforced sands for the pavement applications. Six sand types, four fiber types, five fiber lengths, six fiber deniers and five different fiber dosages were used during the laboratory tests. The compressive strengths of specimens were used to determine the performance. The unconfined compression tests were performed with a displacement rate of 0.0423 mm/s. It is decided that the suitable vertical deformation limit is 25mm for pavement applications. Sand types ranged from fine sand to coarse sand. The fiber types were synthetic monofilament, fibrillated, tape and mesh fibers made of polypropylene. For sample preparation, moisture was fundamental to mix and

mold the specimen so moisture control study was performed. The water content of the specimens were arranged to be equal to 8%. Water was added to sand-fiber composites to obtain target moisture content and ensure a uniform mixture. Each specimen was compacted in five layers with modified Proctor tests. The effects of test variables were evaluated by comparing the unconfined compression test results of unreinforced sand and fiber-reinforced sand specimens. According to Figure 3.14, when fiber content of 1% by dry weight of sand was used, it was observed that all fiber types improved the unconfined compressive strength of all sand types.
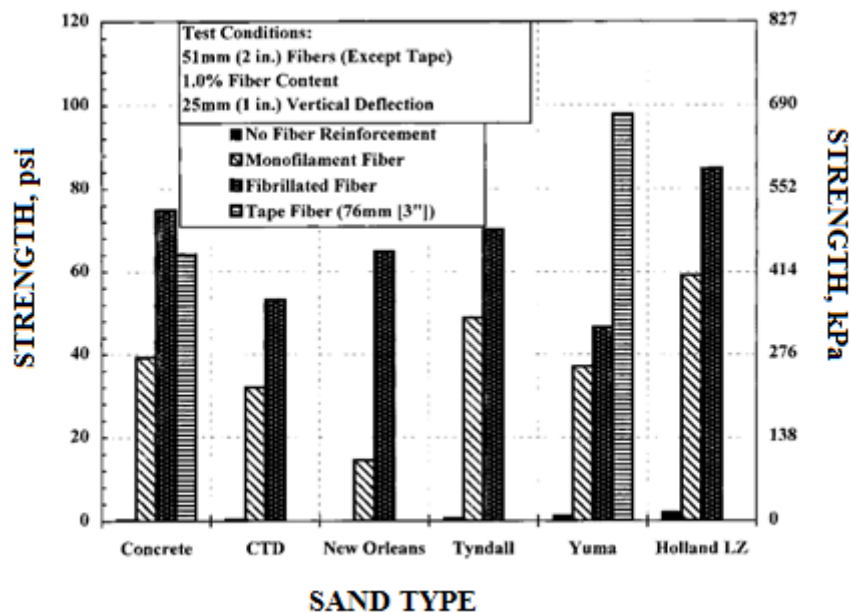
Figure 3.14 : Performance of fiber types by sand type (Santoni et al., 2001)

The effect of fiber length was evaluated by mixing monofilament fibers of different lengths at different deniers. The results are presented in Figure 3.15 and it is stated that while 51 mm (2 in.) monofilament fibers increased the unconfined strength significantly at three deniers, the fiber lengths up to 25 mm (1in.) did not create any significant effect. The control specimen represents the unreinforced sand at the moisture content of 8%. When the effect of fiber denier was evaluated it is concluded that the unconfined compressive strength increases with the decreasing fiber denier. The term "denier" used in this study represents the fiber thickness. As it is shown in Figure 3.15, when the monofilament specimens increased from 4 denier specimens to 20 denier specimens, the unconfined compressive strength of specimens decreased approximately by 13.5%. The decrease in the specimen performance of 12.5% was

29

recorded for fibrillated specimens from the 360 denier to the 1000 denier (Santoni et al., 2001).
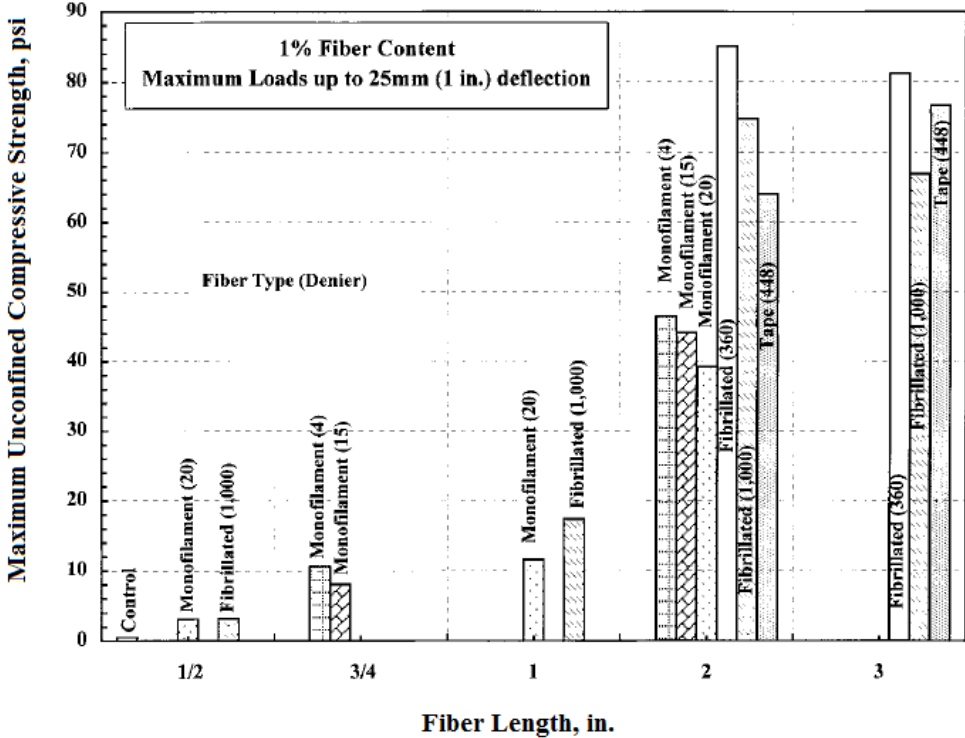
Figure 3.15 : Comparison of fiber type, length and denier in Vicksburg Concrete Sand (Santoni et al., 2001)

Santoni et al. (2001) performed unconfined compression tests with different fiber contents of 0.2, 0.4, 0.6, 0.8 and 1.0 %. It is informed that fiber contents over 1.0% requires excessive deformation in order to initiate the specimen's load support capabilities. According to the test results, the strain softening characteristics, described as decreasing unconfined compressive strength with a corresponding increase in strength, was observed for specimens with fiber contents below 0.6%. On the other hand fiber contents of 0.6-1.0% resulted in strain hardening characteristics, the expected behavior, that are exhibited as an increase in unconfined compressive strength with a corresponding increase in strain. Figure 3.16 shows that the optimum fiber content is between 0.6-1.0% dry weights of sand to obtain optimum unconfined compressive strength. The effect of sand type was determined by using six different types of sand. The experimental results showed that synthetic fiber inclusions improved the unconfined compressive strength of all sand types and there was no considerable difference between the performance of coarse sands and fine sands. Another parameter searched was the silt content and the results showed that silt

contents higher than 12% may degrade the performance of sand reinforced with fibers. According to the test results, it is concluded that dirty sand can also be reinforced with synthetic fibers.
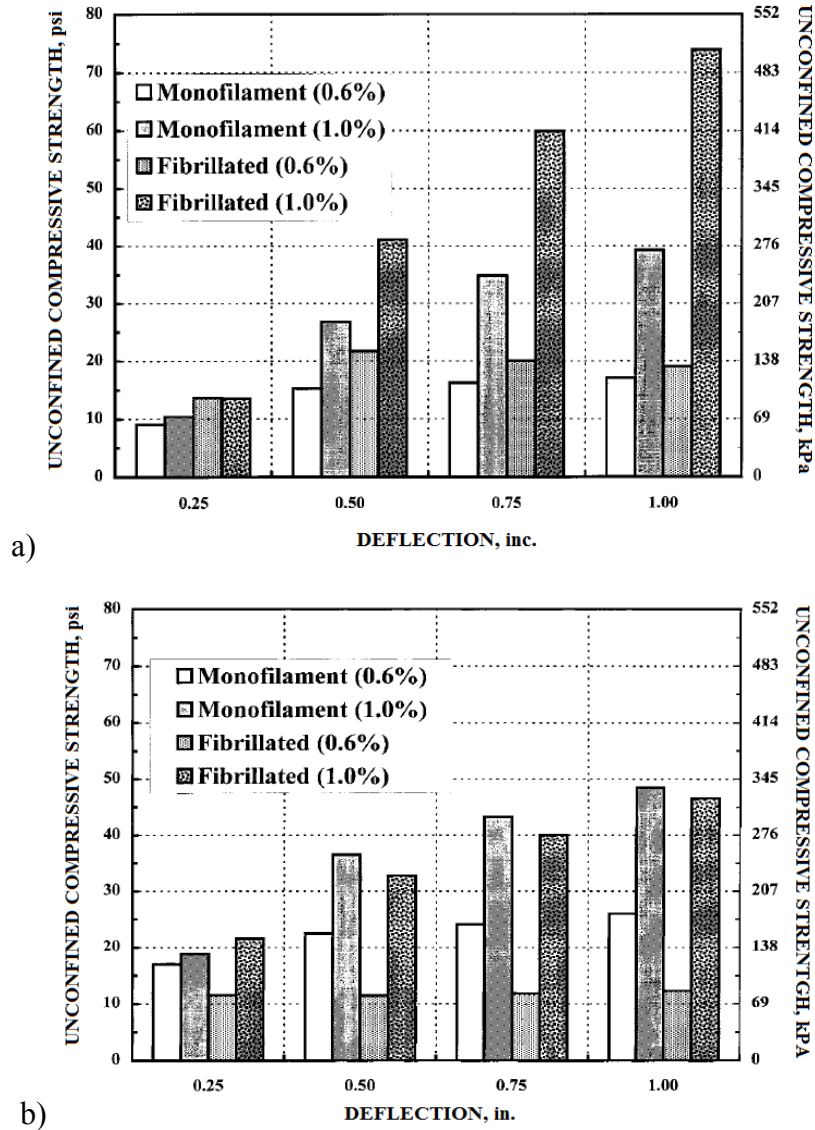
Figure 3.16 : Typical performance of 51mm (2 in.) Monofilament (20 Denier) and Fibrillated (1000 Denier) Fiber in (a) Vicksburg Concrete (b) Yuma Sand (Santoni et al., 2001)

The effect of moisture content was determined by performing the unconfined compression tests at different moisture contents. The specimens were tested just after they were compacted. The fiber content of 0.6% was chosen and 51mm (2in.) monofilament (20 denier) fibers were mixed with sand at different moisture contents. As the results shown in Figure 3.17 exhibits, the moisture contents between the base moisture content of 2.6 % and 14.0%, increased the performance of fiber-sand mixtures. On the other hand when the moisture content reached up to 14.0%, it is

observed that the specimen was saturated and due to drainage, the specimen showed a similar performance as it showed at the base moisture content.
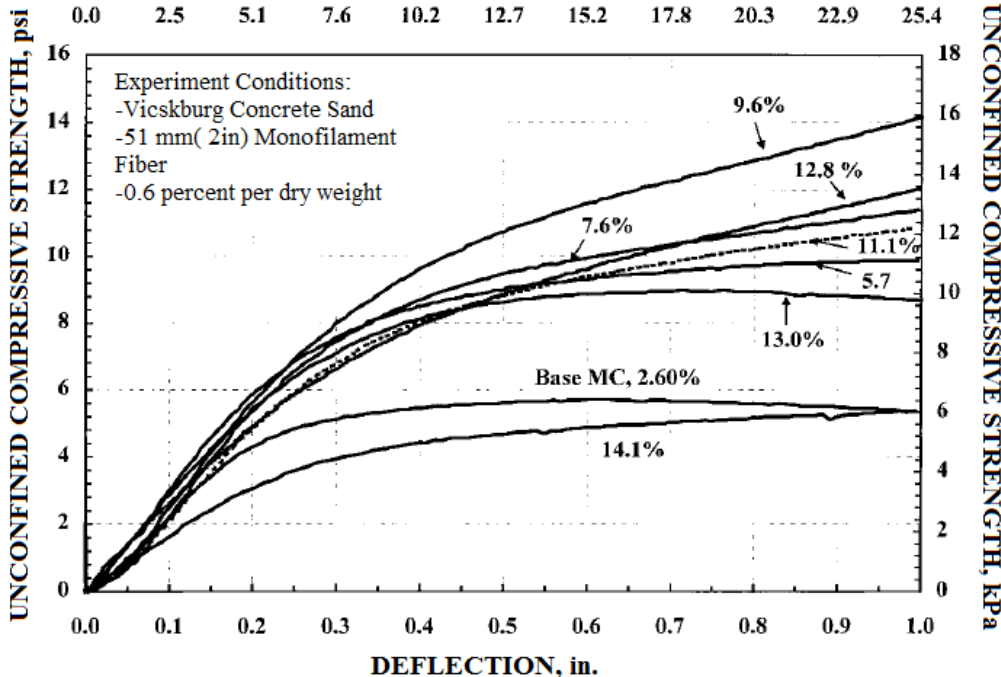
Figure 3.17 : Specimen performance at varying moisture contents
(Santoni et al., 2001)

Ibraim et al. (2009) performed a series of laboratory experiments to determine the liquefaction potential of loose clean sand reinforced with short flexible fibers. The experimental program focused on the undrained behavior in both triaxial compression and triaxial extension. The Houston RF sand is mixed with Loksand™ flexible polypropylene crimped fibers. It is stated that these fibers act predominately in tension. The moist tamping technique is used for preparing unreinforced and reinforced sand specimens at the optimum moisture content, which is determined from the compaction tests as 10%. For sample preparation, the weight of sand was kept constant and the fiber contents used for compressions tests were 0.3%, 0.6% and 0.9% while the fiber contents used for extension tests were 0.3% and 0.6%.The experimental program included drained and undrained triaxial compression and extension tests on isotropically consolidated samples. The consolidation pressures of 30, 100 and 200 kPa were used for the tests. The specimens were saturated by water backpressure up to 300 kPa and CO_2 method. The shape of the homogeneous specimen was preserved well beyond the 20% axial strain in compression and around 10%-12% axial strain in extension. For interpreting the test results, axisymmetric

triaxial conditions were used. It is stated that p and q are respectively the total mean and deviatoric stresses action on the composite where

$$p = p* + u \tag{3.12}$$

where p* is the effective mean stress and u is the pore water pressure. The deviator stress on the sample is denoted as q*. The strain variables are the volumetric strain ε_v and shear strain ε_q. The relations between these quantities and the axial and radial stresses are:

$$p = \frac{\sigma_a + 2\sigma_r}{3} \tag{3.13}$$

$$q = \sigma_a - \sigma_r \tag{3.14}$$

$$\varepsilon_v = \varepsilon_a + 2\varepsilon_r \tag{3.15}$$

$$\varepsilon_q = \frac{2}{3}\left(\varepsilon_a - \varepsilon_r\right) \tag{3.16}$$

the subscripts of a and r represent the axial and radial components respectively. If q*/p*=M, the Mohr-Coulomb mobilized angle of friction $\phi_m{}^*$ is defined as:

$$\sin\phi_m{}^* = \frac{3M_c}{6 + M_c} \tag{3.17}$$

$$\sin\phi_m{}^* = \frac{-3M_c}{6 + M_c} \tag{3.18}$$

The drained triaxial compression and extension tests were performed on isotropically consolidated unreinforced and reinforced specimens at a consolidation pressure of 100 kPa and the results are shown in

Figure **3.18**. As is it shown, at 20% axial strain and with a fiber content of 0.9%, the deviator stress increase was almost 300% compared to that of unreinforced sand. It is stated that fibers ability to withstand tension without plastic deformations provided a significant strength increase for the fiber-sand mixture (Ibraim et al., 2009).
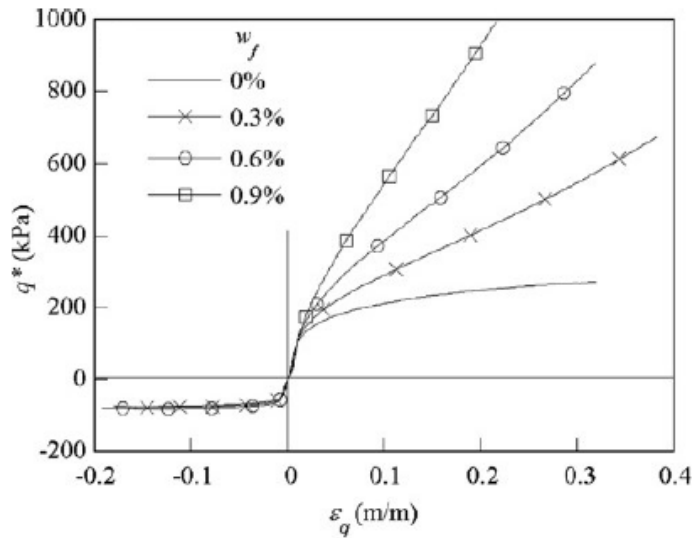
Figure 3.18 : Deviator stress-strain results for drained compression and extension triaxial tests (Ibraim et al.,2009)

According to the results of triaxial extension tests, it can be seen from the Figure 3.26 that the stress-strain relationships for reinforced specimens were similar to that of unreinforced sand. It is stated that sand matrix controls the strength response of the composite in extension. Test results presented in Figure 3.19 also showed that the volumetric response of the composite is affected by the presence of fibers that cause an apparent densification mechanism of the sand matrix. It is stated that the potential of static liquefaction can be affected by the change of the volumetric response from contractive for the unreinforced sand to dilative for the reinforced sand (Ibraim et al., 2009).
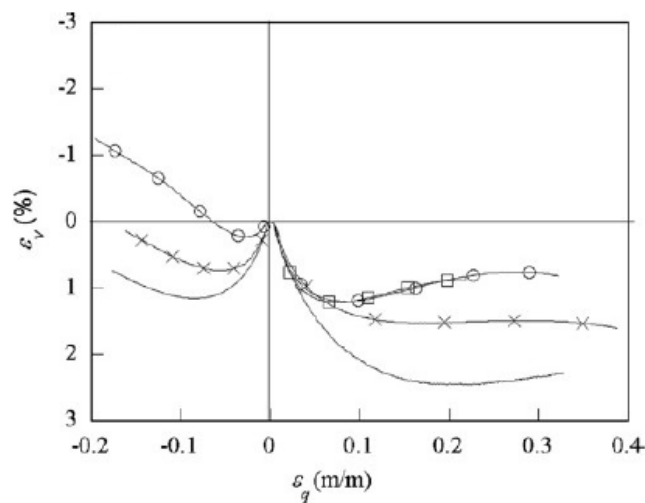

Figure 3.19 : The volumetric behavior for drained compression and extension triaxial tests (Ibraim et al.,2009)

Ibraim et al. (2009) also performed undrained monotonic compression and extension triaxial tests on unreinforced and reinforced sand specimens. For the unreinforced specimens, both in compression and extension tests, a typical behavior of static liquefaction was observed. The generation of pore pressure and a continuous decrease of effective mean stress was followed by a reaching the peak value rapidly, a sharp drop of the deviator stress and steady state as deformation continues. Results showed that fibers converted a strain softening response (typical for loose unreinforced sand) into a strain hardening response both for the compression and the extension tests and thus the monotonic liquefaction is prevented. It is also noted that higher amount of fibers were required to prevent liquefaction in extension. The mobilized angle of friction ϕ^*_m, increased monotonically with the shearing for the specimens reinforced with fiber content between 0.3-0.9% in triaxial compression tests. Also at the end of the experiments, the reinforced sand specimen maintained some stability even after its membrane was removed. It shows that fiber inclusions limit the lateral spreading of the soil, which is accepted as one of the results of liquefaction.

Michalowski and Cermak (2003) performed drained triaxial compression tests on fiber-reinforced sand specimens. Fine and coarse sands were mixed with three types of fibers: polyamide monofilament, steel galvanized wire and polypropylene fibrillated fibers. The amount of fiber added is described by its volumetric content:

$$\rho = \frac{V_r}{V} \quad\quad\quad (3.19)$$

where

ρ = fiber content

V_r = volume of fibers in a specimen

V = total volume of the specimen.

Unreinforced and reinforced specimens were prepared with void ratios of e = 0.58 and e = 0.66. The first step of drained triaxial compression tests was the application of confining stress, σ_3. Than controlled increasing stress, σ_1 was applied. The displacement rate was chosen to be 0.16 mm/min. The axial strain ε_1 and the volumetric strain ε_v were plotted along with the deviatoric stress $\sigma_1 - \sigma_3$. The results of sand reinforced with polyamide fibers show that large failure stresses were recorded

at large strains at the failure. As it is shown in Figure 3.20 (a)-(b), the initial stiffness is affected by the addition of fibers. There is a drop in the initial stiffness for the sand reinforced with large fiber contents. It is stated that the changes in the fabric of the sand produced by the synthetic fibers may be the reason for the loss of initial stiffness. This statement was also supported by the results of sand reinforced with steel fibers as there was no stiffness reduction recorded. The interaction of fibers to the sand grains is searched by performing triaxial tests with different fiber aspect ratios for the same amount of fiber concentrations. As it is shown in Figure 3.21, the recorded strengths increase with the increasing aspect ratio. It is also stated that fiber inclusions caused similar effects for both fine and coarse sand specimens (Michalowski and Cermak, 2003).
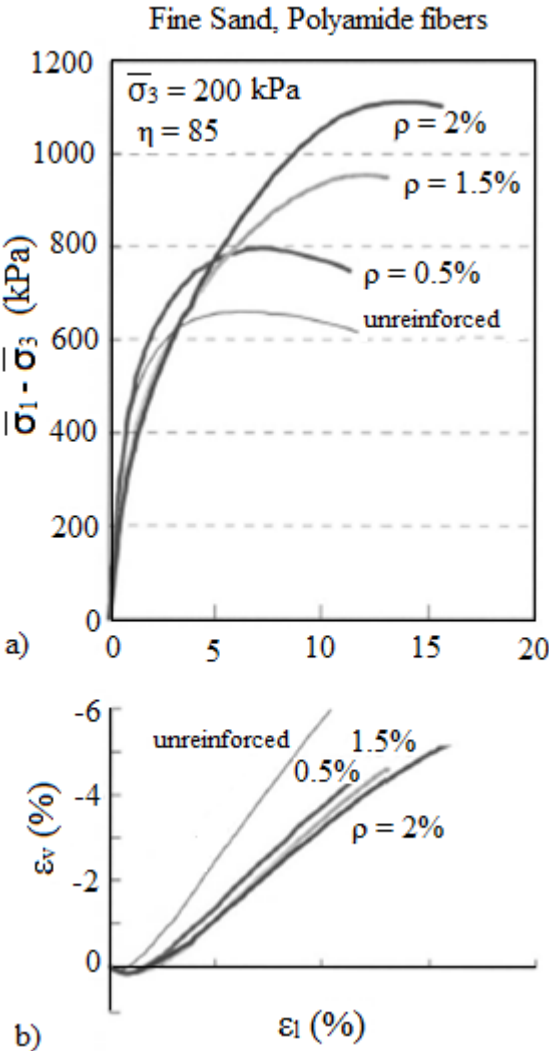

Figure 3.20 : Stress strain and volumetric curves of fine sand reinforced with polyamide fibers (Michalowski and Cermak, 2003)
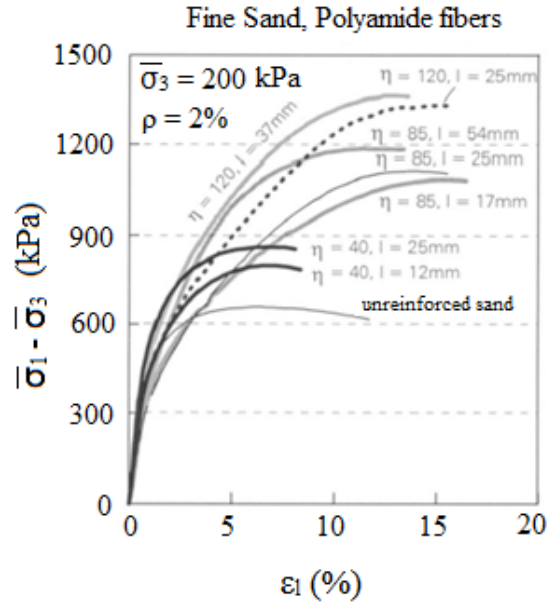
Figure 3.21 : Stress-strain behavior of sand reinforced with polyamide fibers of different aspect ratios and different lengths (Michalowski and Cermak, 2003)

Chen and Loehr (2008) performed consolidated-undrained and consolidated drained type of triaxial compression tests on unreinforced and fiber reinforced sand specimens. The poorly graded Ottawa sand is mixed with fibrillated polypropyene fibers that have a specific gravity of 0.91 gr/cm^3. The test specimens are prepared at loose (D$_r$ ≈ 10%) and medium-dense (D$_r$ ≈ 55%) conditions. The specimens were saturated until B values are measured at least 0.96 before consolidation and shear. The deformation rate preferred was 12.5 mm/hour to eliminate the concerns due to strain rate when comparing the undrained and drained test results. The specimens were sheared up to a maximum axial strain of 30 percent. All the tests were conducted on specimens having diameter of 63.5 mm and height of 124.5 mm. The specimens were isotropically consolidated to the effective stresses of 35, 140, 280 and 415 kPa. Figure 3.22 presents the deviatoric stress (q) versus shear strain (ε_q) of loose and medium dense specimens consolidated to 140kPa effective stress where;

$$q = \sigma_1 - \sigma_3 \tag{3.20}$$

in which σ_1 is the maximum principle stress and σ_3 is the minimum principal stress and

$$\varepsilon_q = \varepsilon_a - \frac{1}{3}\varepsilon_v \tag{3.21}$$

in which ε_a is the axial strain and ε_v is the volumetric strain.

37

It is stated that the loose unreinforced sand reached a peak deviatoric stress at approximately 2% strain and decreased with additional strain. On the other hand, medium dense unreinforced sand specimens reached the peak deviatoric stresses at strains of approximately 5% and decreased slightly at additional strains. The reinforced specimens showed a strain hardening behavior (Chen and Loehr, 2008).

a)

Loose state (Dr ≈ 10%)

b)

Medium-dense state (Dr ≈ 55%)

Figure 3.22 : Deviatoric stress versus triaxial shear strain curves for CU tests for specimens consolidated to 140 kPa effective stress (Chen and Loehr, 2008)

The test results of consolidated undrained tests are presented in Figure 3.23. It is shown that the unreinforced specimens tended to reach peak deviatoric stress levels at axial strain of 1% and maintained stresses until large strains. On the other hand,

reinforced specimens exhibited peak stresses at strains of 20% or greater (Chen and Loehr, 2008).

Figure 3.23 : Deviatoric stress versus triaxial shear strain curves for CD tests for specimens consolidated to 140 kPa effective stress (Chen and Loehr, 2008)

The pore water pressure changes observed in the CU tests are presented in Figure 3.24. The unreinforced specimens at the loose state exhibited the typical "loose sand" behavior with pore pressures increasing throughout the end of the test. For the loose reinforced specimens, the increase in pore pressure at small strains is followed by decrease with additional strains. The medium-dense unreinforced specimens showed that the pore pressure increased at strains up to 1% and and decreased significantly

and it is equal to or less than zero before 10% strains. On the other hand, the medium dense fiber reinforced specimens showed that pore pressure increased at small strains (2%) and that is followed by significant decrease at absolute pore pressures equal to or less than zero before 10% strains (Chen and Loehr, 2008).

a)

Loose state (Dr ≈ 10%)

b)

Medium-dense state (Dr ≈ 55%)

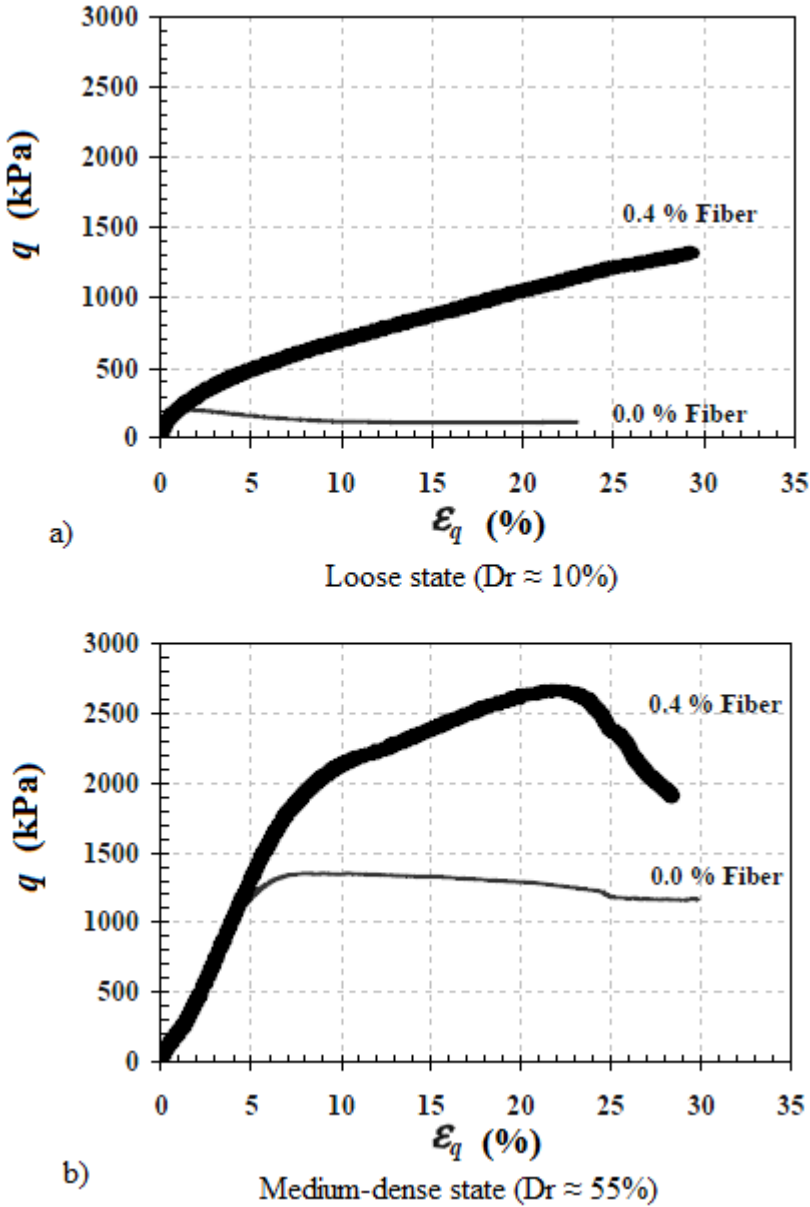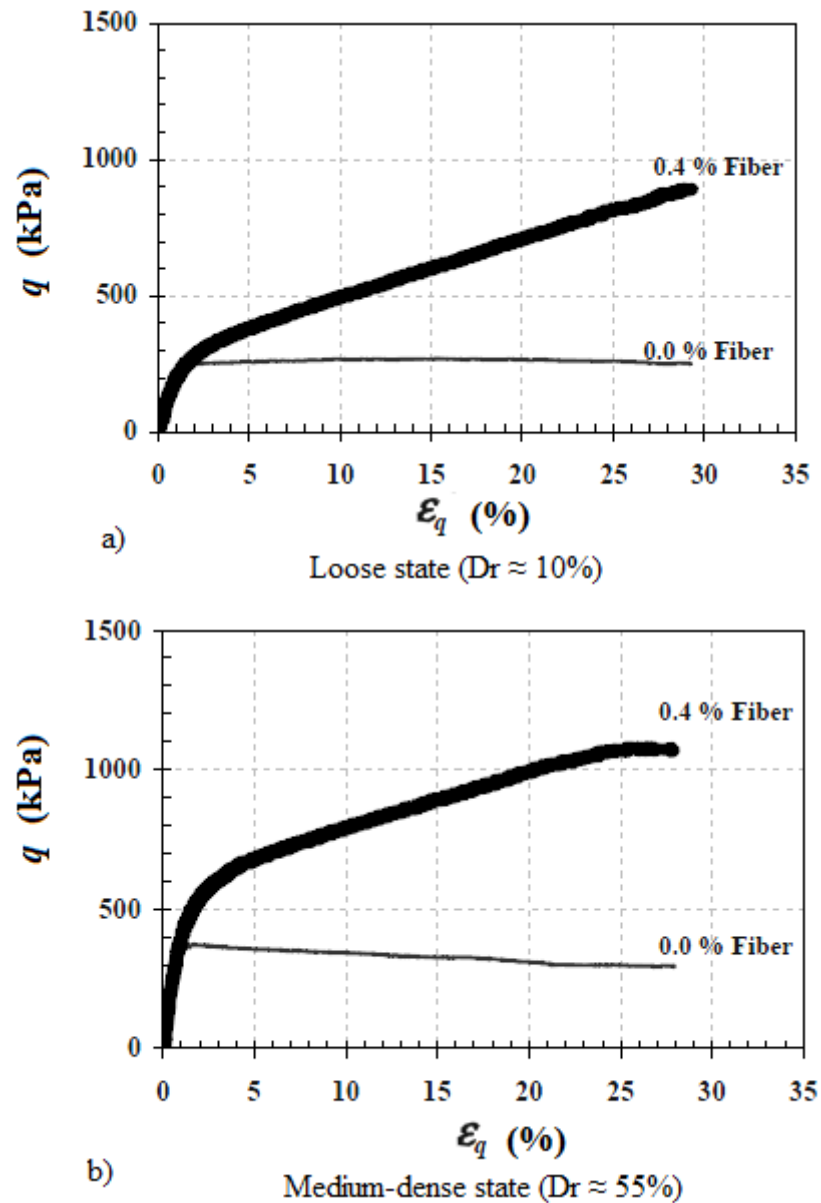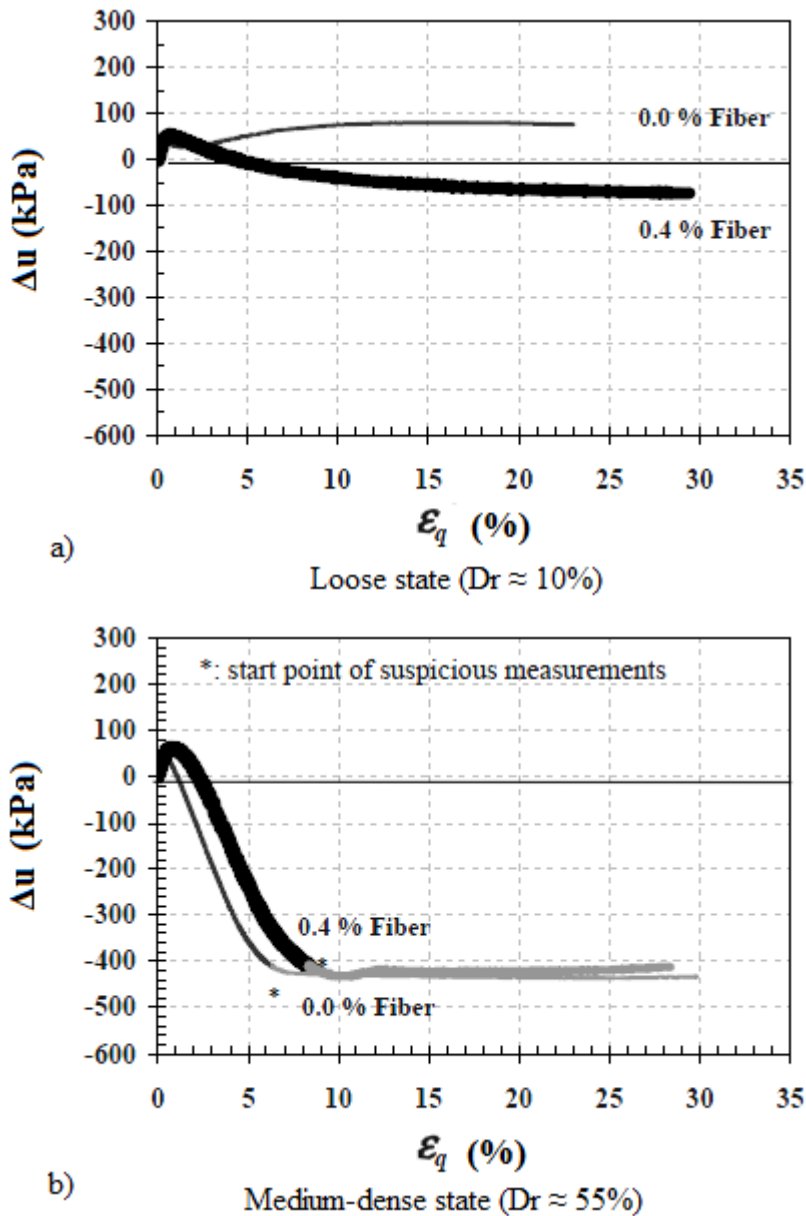**Figure 3.24 :** Change in pore pressure versus triaxial shear strain curves from CU tests for specimens consolidated to 140 kPa effective stress (Chen and Loehr, 2008)

The tests results are also used for determining the Mohr-Coulomb strength parameters, effective cohesion intercept (c') and effective internal friction angle (ϕ'). Failure enveloped were determined from peak effective principal stress ratio failure criterion. The results are shown in Table 3.1. It is presented that fiber inclusion

improved the effective stress friction angles and the effective stress cohesion intercepts significantly.

Table 3.1 : Mohr-Coulomb Strength Parameters (Chen and Loehr, 2008)

Test Type	Relative Density, D_r (%)	0.0% Fiber Content		0.4% Fiber Content	
		c' (kPa)	ϕ' (deg)	c' (kPa)	ϕ' (deg)
CU	10	0.0	30.4	87	43.1
	55	0.0	33.7	0*	43.5*
CD	10	0.0	29.8	21	45.3
	55	0.0	34.2	34	47.9
*Suspicious result due to equipment limitation for pore pressure measurement					

3.5 Direct Shear Tests on Sands Reinforced with Randomly Distributed Fibers

Gray and Ohashi (1983) performed direct shear tests on dry sand specimens reinforced with different types of fibers. They developed theoretical predictions based on a force equilibrium model and they compared their test results to the theoretical predictions. The sand used in the direct shears tests was clean, quartz beach sand. Different types of fibers were used in order to provide a range of elastic moduli. Fibers diameters were from 1mm-2mm and the lengths were in a range between 2-25 cm. The standard direct shear tests were conducted on sand samples that have relative densities of 20% and 100% for both reinforced and unreinforced conditions. Metal wires, natural and synthetic fibers were used as reinforcement. While most of the tests were conducted on fiber area ratios of 0.25 % or 0.50 %, the maximum amount fiber area ratio used was 1.67%. Direct shear tests were conducted as strain controlled and the test continued until a total displacement of 5mm or an average shear strain of 8% was recorded. The fibers were placed with various

orientation angles. Tests were performed with different confining stresses up to 144 kN/m^2.

The theoretical model in this study was developed for two different fiber orientations. Fibers that are perpendicular to the shear place can be seen in Figure 3.25 and fibers that are oriented at an arbitrary angle to the shear plane can be seen in Figure 3.26.
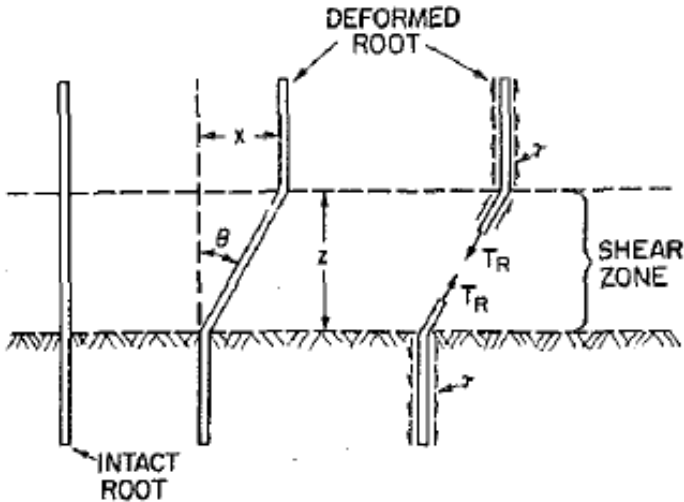
Figure 3.25 : Fiber Reinforcement Model for Perpendicular Orientation to Shear Surface (Gray and Ohashi, 1983)
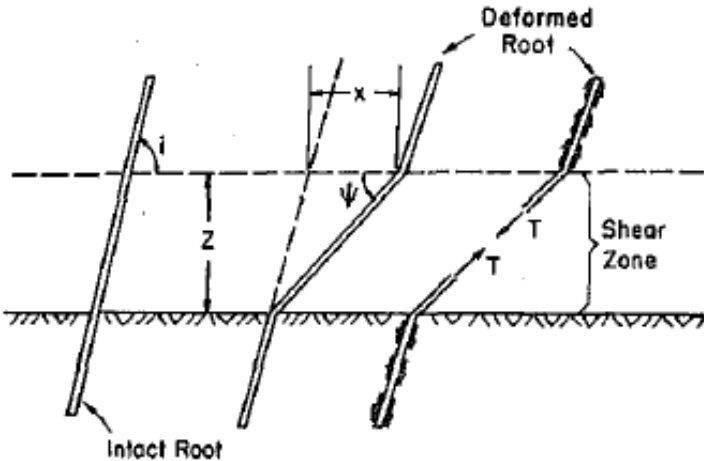
Figure 3.26 : Fiber Reinforcement Model for Fiber Oriented at Angle to Shear Surface (Gray and Ohashi, 1983)

The tensile force, formed as a result of shearing, has two components normal and tangential to the shear plane. It is stated that while tangential component resists shear directly, the normal component mobilizes shear resistance by increasing the confining stress. The shear strength increase caused by the addition of fibers is estimated as:

For perpendicular fibers:

$$\Delta S_R = t_R \left[\sin \theta + \cos \theta \tan \phi \right] \tag{3.22}$$

For oriented fibers:

$$\Delta S_R = t_R \left[\sin(90 - \psi) + \cos(90 - \psi) \tan \phi \right] \tag{3.23}$$

$$\psi = \tan^{-1} \left[\frac{1}{k + (\tan^{-1} i)^{-1}} \right] \tag{3.24}$$

as the shear strength increase due to fiber reinforcement is represented by ΔS_R; the mobilized tensile strength of fibers per unit area of soil is represented by t_R; angle of internal friction angle of sand is represented by φ; the angle of shear distortion is represented by θ; the initial orientation angle of fiber with respect to shear surface is represented by i; the horizontal of shear displacement is represented by x; the thickness of shear zone is represented by z and the shear distortion ratio is represented by k. The mobilized tensile strength per unit area of soil (t_R) is defined as the product of tensile stress developed in the fiber at the shear plane and the fiber area ratio (Gray and Ohashi, 1983).

The possible tensile stress distributions along the length of the fiber are considered as linear or parabolic distributions. The resulting tensile stress at the shear plane for corresponding tensile stress distributions are calculated as given:

For linear distribution:

$$\sigma_R = \left(\frac{4 E_R \tau_R}{D_R} \right)^{1/2} \left\{ z \left(\sec \theta - 1 \right) \right\}^{1/2} \tag{3.25}$$

For parabolic distribution:

$$\sigma_R = \left(\frac{8 E_R \tau_R}{3 D_R} \right)^{1/2} \left\{ z \left(\sec \theta - 1 \right) \right\}^{1/2} \tag{3.26}$$

where E_R is the modulus of the fiber, τ_R is the skin friction stress along the fiber, D_R is the diameter of fiber and z is the thickness of the shear zone.

According to the experimental test results and theoretical predictions, it is stated that fiber reinforcement increased the ultimate shear strength. Figure 3.27 presents that, as the number of fibers increased the shear strength increased alongside with the limited reductions in the post peak shearing resistance. It is stated that the initial orientation angle of fibers did not affect the stress-strain relations in a considerable amount but it affected the peak shear resistance. According to the test results, an initial fiber orientation of 60° is calculated as the optimum orientation for maximum shear strength increase. The average strength increases recorded for loose and dense sand specimens were similar. On the other hand, in loose sand specimens larger strains were necessary for reaching the peak shear resistance. The effect of fiber length was to increase the shear strength of the reinforced sand until reaching a limit. It is stated that the predictions made based on force equilibrium theory were consistent with the experimental test results (Gray and Ohashi, 1983).
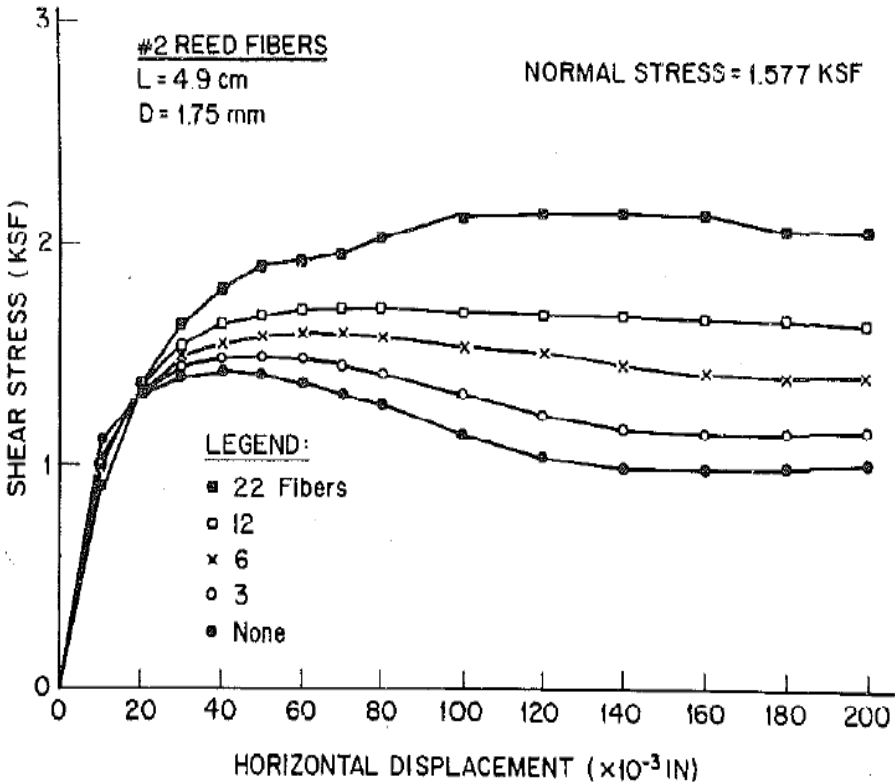

Figure 3.27 : Influence of Number of Fibers on Stress-Deformation Behavior of a Dense Sand (Gray and Ohashi, 1983)

Yetimoglu and Salbas (2003), performed direct shear tests to investigate the shear strength of randomly reinforced sand specimens. The experimental study consists of

direct shear tests performed at the vertical normal stresses of σ_n= 100, 200 and 300kPa. The loading rate was chosen to be 0.002 mm/s and shear stresses were recorded until a total displacement of 16 mm. The sand used in experiments was the uniform quartz river sand. It was sieved through ASTM 10 and washed through ASTM 20. The sand properties are shown in Table 3.2 :.

Table 3.2 : Properties of sand (Yetimoglu and Salbas, 2003)

Property	Value
Specific Gravity	2.64
Maximum dry unit weight (kN/m^3)	17.48
Minimum dry unit weight (kN/m^3)	14.92
Maximum void ratio	0.77
Minimum void ratio	0.51
Coarse sand fraction (%)	2
Medium sand fraction (%)	53
Fine sand fraction (%)	45
Effective grain size D_{10} (mm)	0.20
D_{60} (mm)	0.33
$D3_0$ (mm)	0.26
Coefficient of uniformity C_u	1.65
Coefficient of curvature C_c	1.02
c (kPa) *	0
ϕ (deg) *	42
*Obtained from direct shear tests at D_r = 70 %	

Sand samples were reinforced with polypropylene fibers with the contents (ρ) of 0.10%, 0.25%, 0.50% and 1.00% of the dry weight of sand. The composite was mixed thoroughly by hand to prepare a uniform mixture. Figure 3.28, Figure 3.29, Figure 3.30 and Figure 3.31 show the shear stress-horizontal displacement curves obtained from the reinforced sands including fiber contents of 0.1%, 0.25%, 0.5% and 1.0% respectively. The peak shear strength angle and cohesion values are calculated. As the fiber content increased up to 1%, the shear strength angle decreased slightly from 42.3° to 40.4°. On the other hand, the cohesion value stayed constant as 0kPa. The results show that fiber inclusion affected the peak shear stresses and horizontal displacements at which peak shear stresses mobilized significantly. A smaller loss of post-peak strength was observed for fiber reinforced samples. It is concluded that fiber reinforcement can change the brittle behavior of sand to a more ductile behavior (Yetimoglu and Salbas, 2003).
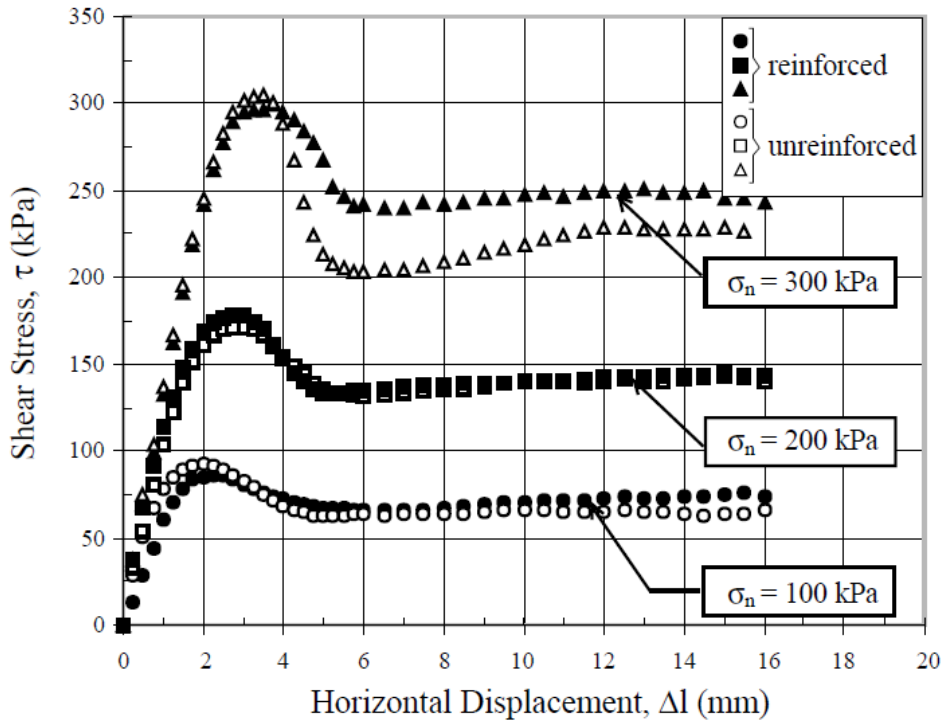
Figure 3.28 : Shear stress-horizontal displacement response for unreinforced sand and reinforced sand with fiber content of $\rho = 0.10\%$ (Yetimoglu and Salbas, 2003)

Figure 3.29 : Shear stress-horizontal displacement response for unreinforced sand and reinforced sand with fiber content of $\rho = 0.25\%$ (Yetimoglu and Salbas, 2003)

Figure 3.30 : Shear stress-horizontal displacement response for unreinforced sand and reinforced sand with fiber content of $\rho = 0.50\%$ (Yetimoglu and Salbas, 2003)
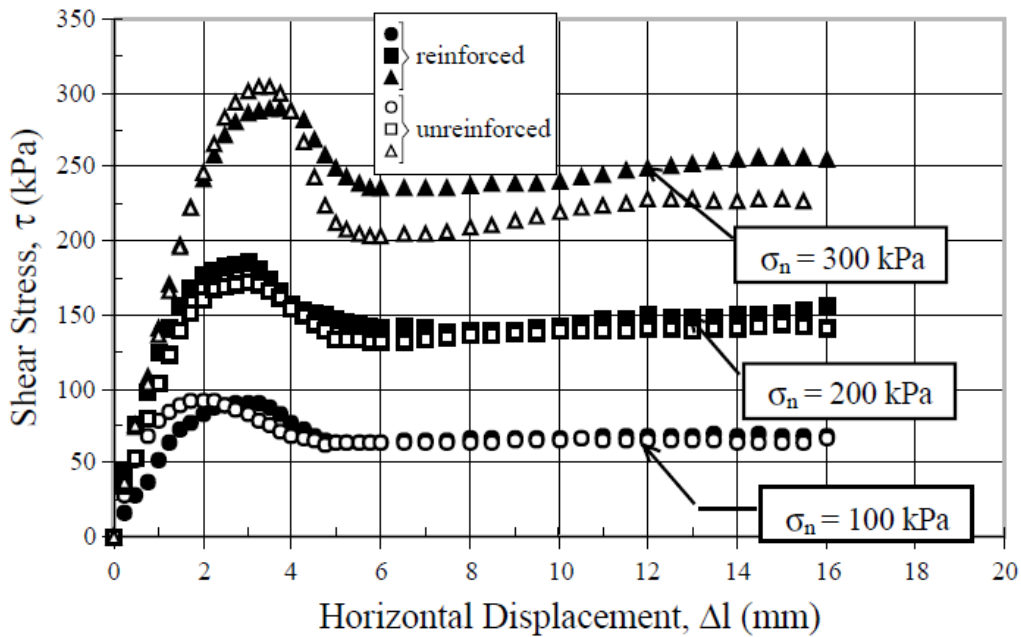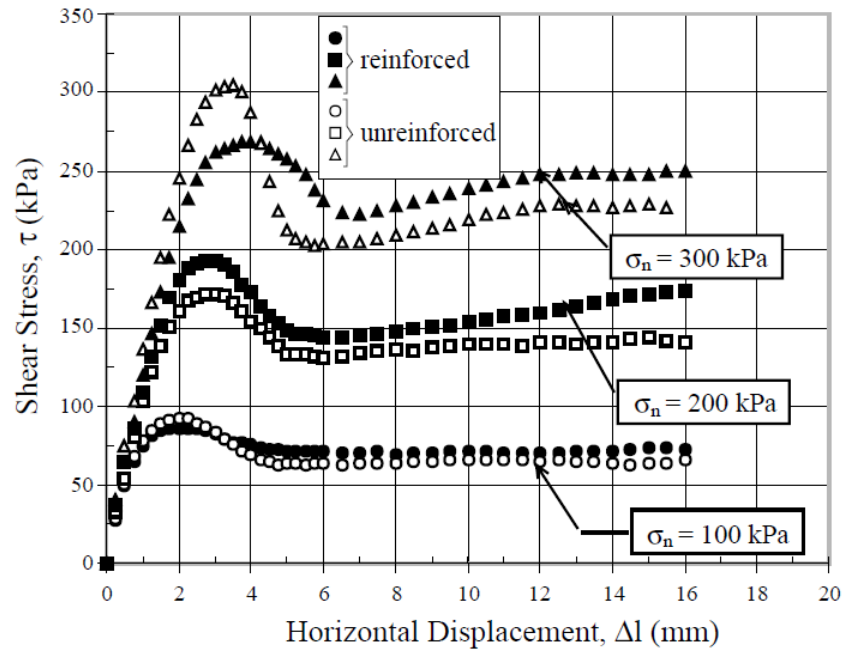

Figure 3.31 : Shear stress-horizontal displacement response for unreinforced sand and reinforced sand with fiber content of $\rho = 1.0\%$ (Yetimoglu and Salbas, 2003)

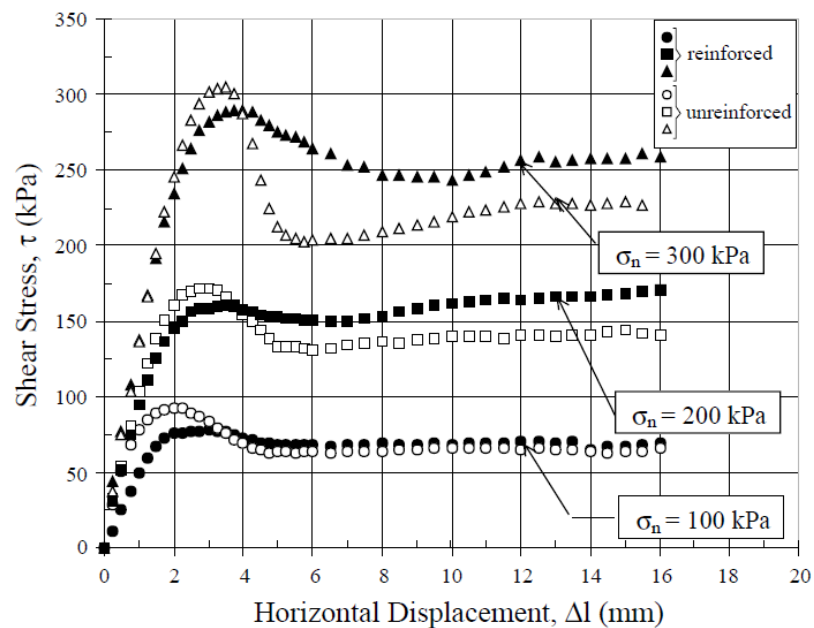Michalowski and Cermak (2003) also performed fiber pull through tests in a modified shear box to determine the behavior of the composite. The results of fine grained sand reinforced with polyamide are shown in Figure 3.32 (a) and the results of fine grained sand reinforced with steel wires are shown in Figure 3.32 (b). The

results for pull through tests conducted on fine and coarse sands were similar. Additional direct shear tests were performed when it is considered that a uniform stress distribution may not be available through a fiber. The friction angles calculated are shown in Figure 3.32 (Michalowski and Cermak, 2003).
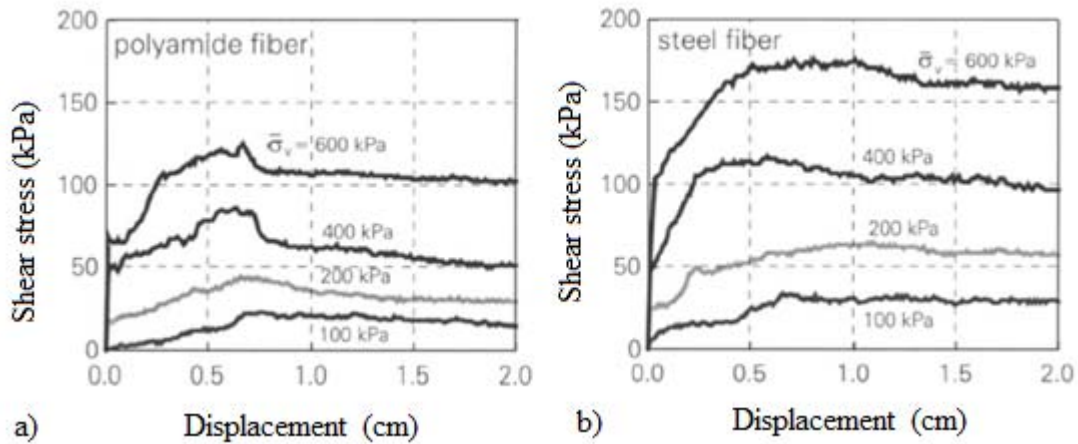

Figure 3.32 : Fiber pullthrough tests in fine sand (a) polyamide and (b) steel (Michalowski and Cermak, 2003)
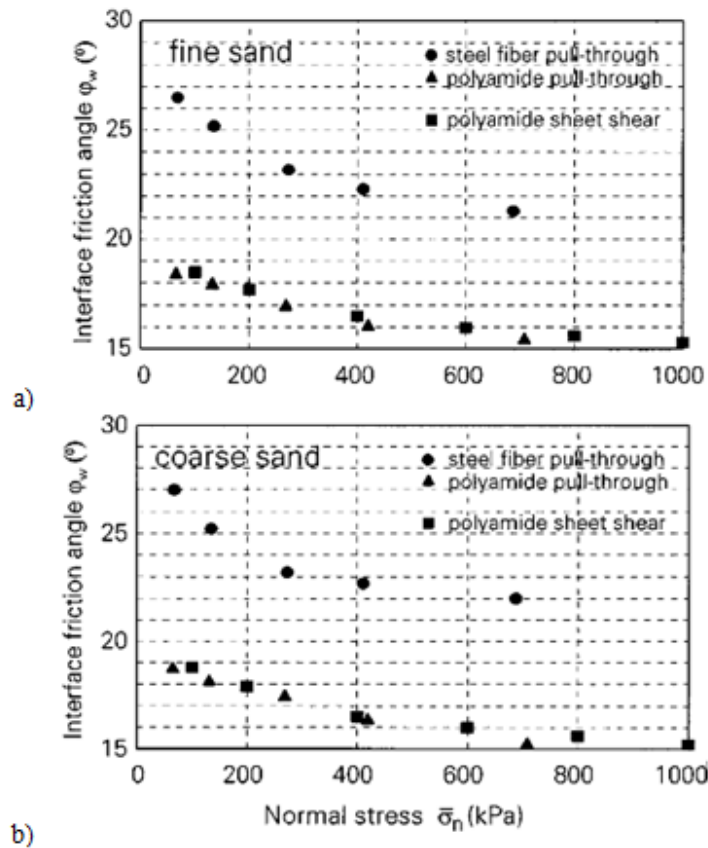

Figure 3.33 : Friction angles for reinforced (a) fine sand and (b) coarse sand(Michalowski and Cermak, 2003)

48

The results of the experimental study done by Michalowski and Cermak (2003) showed that fiber addition of 2% of volume increased the shear strength in a considerable amount. For small fiber contents, the reinforcing effect is more prominent compared to coarse sand. On the other hand, large fiber inclusion resulted in greater strength increases in coarse sand. The reinforced sand behavior was modeled using an energy-based homogenization technique to calculate the macroscopic plastic stress state of the composite. The frictional interaction of fibers and sand was mainly considered in this technique. According to this technique, the calculations were based on the equation of the work rate of the macroscopic stress to the work dissipation rate in a deformation process. The failure stress of fiber reinforced sand was calculated with the model. Figure 3.34 shows the macroscopic internal friction angles predicted from the model and it is concluded that they were consistent with the experimental results. It is also noted that this model was sensitive to the fiber contents and fiber aspect ratios.
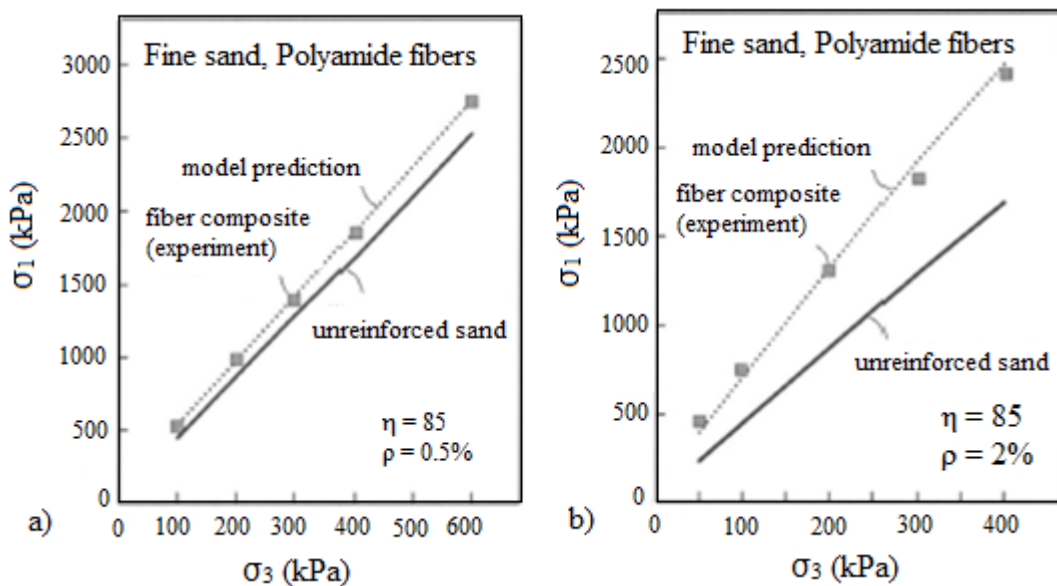

Figure 3.34 : Model predictions and experimental results steel (Michalowski and Cermak, 2003)

Ibraim and Fourmont (2006) performed compaction and direct shear tests on unreinforced and reinforced sand specimens of different densities. In this study very fine sand, Houston RF sand is reinforced with randomly distributed discrete crimped polypropylene fibers. Compaction tests were performed with a Proctor compaction apparatus on unreinforced sand and sand samples that are reinforced at fiber contents of 0.1%, 0.3% and 0.5%. The optimum moisture content is calculated as 10% and it

is stated that fibers up to 0.5 % of dry weight has no significant effect on the optimum moisture content. For sample preparation, the amount of water for the optimum moisture content is used for the mixing of soil and fibers. The maximum dosage of fibers that can be mixed with the sand is determined as 2% after applying compaction to four different densities of fiber-sand mixtures. A series of preliminary direct shears tests were performed on fully saturated sand specimens and unsaturated sand specimens at the optimum moisture content. Considering the results, researchers decided to perform direct shear tests on unsaturated sand specimens, which have optimum moisture content. The specimen void ratios were chosen as 0.8, 0.9 and 1.0 for the experimental direct shear tests. The applied normal stress was in a range of 55.3 to 310.6 kPa. Test results indicated that the peak shear stress of unreinforced sand is smaller than the peak shear stress of reinforced sand. The randomly oriented fibers increase the failure peak shear strength and corresponding horizontal displacements. At low effective normal stress values, the increase of the peak shear strength was almost linear for all specimen densities. On the other hand, higher normal stress values enable the peak shear stress to approach a limiting value. A limit of 0.4% of fibers provides 15-20% increase in shear strength. An increase of 30-40% was obtained for 0.8% and the highest fiber content of 1.0% resulted in a 60 % in the shear stress increase (Ibraim and Fourmont, 2006).

Sadek et al. (2010) conducted a series of direct shear tests to determine the effect of various parameters on the shear strength of the fiber-sand composite. Two types of sands (Ottawa sand and BGL sand) were mixed with three types of nylon fibers with different diameters and aspect ratios. For sample preparation the void ratios of 0.6 and 0.71, which correspond to a relative density of approximately 55%, were used for unreinforced specimens. For test specimens, the volumetric fiber content ranged between 0 to 1.5%. Minimum three specimens were tested with the normal stress levels of 100, 150 and 200kN/m^2 to determine the effects of each parameter. According to the results of tests conducted on fine Ottawa sand, it is determined that similar stress-displacement curves were obtained for the unreinforced specimens and fiber-reinforced specimens except for an increase in the slope at small displacements. For the coarse sand, fiber inclusions improved both shear strength and ductility. The experiments on the coarse BGL sand and fine Ottawa sand indicated that the dimensions of sand grains and the diameters of fibers effect the shear strength of

composites significantly. While the reinforcing effect in fines significant for small fiber concentrations, the strength increase of coarse sand reinforced with larger fiber concentrations was greater. The effect of grain size is presented in Figure 3.35. For the fiber content of 1.5%, a maximum increase in shear strength was 17%. On the other hand, the maximum shear strength increase was 37% for coarse sand reinforced with 1% fibers. It is stated that an increase in the fiber aspect ratio increases the strength of low-fiber-content composites compared to high-fiber-content composites. It is stated that the maximum shear strength value increased with the increasing fiber content, resulting in an increase of the friction angle of the composite.
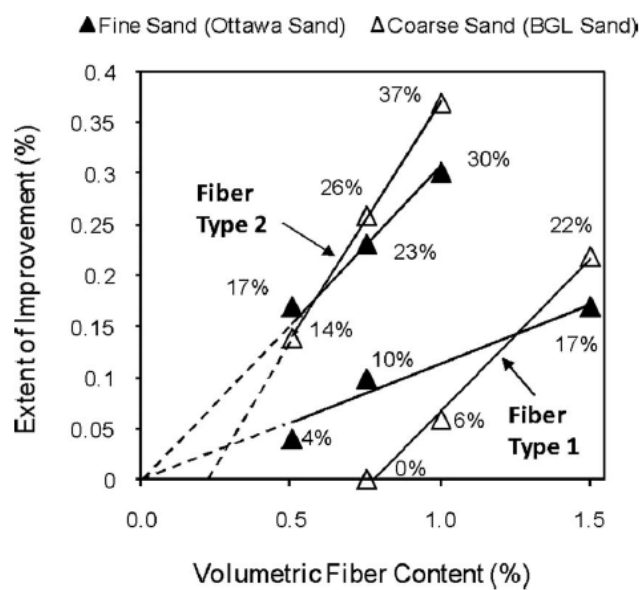

Figure 3.35 : Extend of improvement in shear strength of fiber reinforced Ottawa sand and BGL sand (Sadek et al., 2010)

3.6 Results

In this part of the thesis, firstly brief information about the dynamic properties and static behavior of sand is presented. Secondly, previous studies on fiber reinforced sand are presented. In the previous studies, fiber reinforced sand samples are subjected to triaxial tests and direct shear tests. In these studies, the effect of several parameters on the static behavior of fiber reinforced sand is investigated. The experiments were conducted on different sand types, fiber types, fiber contents, fiber aspect ratios, confining pressures, strain rates, sample preparation and testing methods. The previous studies showed that, fiber reinforcement improves the static behavior of sand. On the other hand, the degree of improvement obtained at the studies depends on the tested parameters.

4. EXPERIMENTAL STUDY

The experimental study consists of static and dynamic laboratory tests on unreinforced and reinforced sand specimens. First the grain size distribution of the sand that will be used in the experiments is determined. As it is stated in the previous studies on fiber reinforced sands, an optimum moisture content is required to produce fairly uniform distirubiton of fibers in sand solids. The Modified Proctor Test is performed to decide the optimum water content that is required for sample preparation. After the Modified Proctor Test, sieve analysis is performed again to confirm that performing the Modified Proctor Test has not effected the grain size distribution of the sand.

The experimental study mainly consists of two parts. At the first part, the maximum initial Elasicity Modulus is determined for confining pressures of 30kPa and 100kPa. The same samples were subjected to static triaxial compression test. The consolidated undrained and consolidated drained triaxial compression tests were performed on the randomly distributed fiber reinforced sand samples to determine the the effect of fiber inclusions on the static behavior of sand. Unreinforced samples and sampled reinforced with different fiber contents are tested in order to determine the effect of fiber inclusions and strain rate. Also triaxial compression tests are performed on unsaturated samples in order to determine the effect of fiber inclusions on the shear strength parameters.

The second part of the experimental study consists of direct shear tests that are conducted on unreinforced and reinforced sand samples prepared at certain water content. Five different fiber contents are tested at the same strain rate. The effect of fiber inclusion on the shear strength parameters are compared using the test results of direct shear tests and triaxial tests on unsaturated samples.

4.1 Triaxial Test Apparatus

The triaxial tests apparatus is used for both monotonic and cyclic loading conditions. The details of a typical triaxial cell are shown in Figure 4.1. The main components of a triaxial test apparatus are cell base, cell body and top, loading piston and loading caps (Head, 1998).

The cyclic triaxial test apparatus Model DTC-311, shown in Figure 4.2, was developed by the Japanese company "Seiken Inc." and was brought to Istanbul Technical University Soil Dynamics Laboratory within the scope of ITU-JICA (Japan International Cooperation Agency) cooperation.
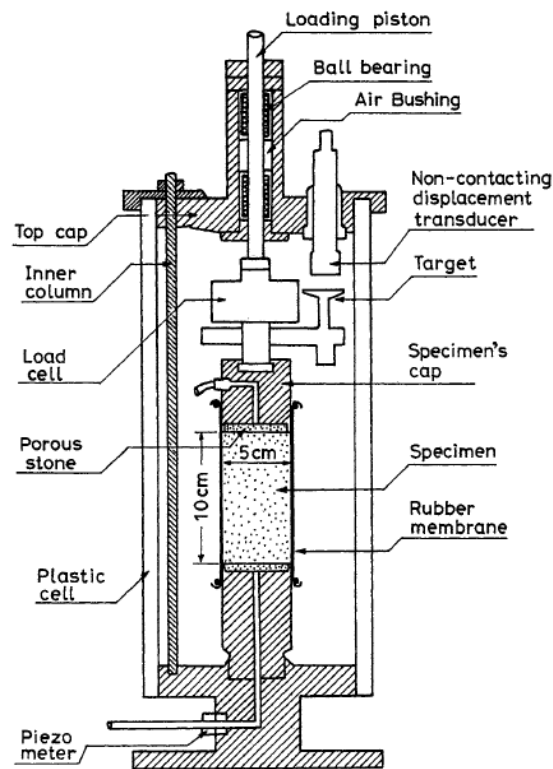
Figure 4.1 : Details of a Triaxial Test Apparatus (Head, 1998)

The device is capable of applying cyclic and monotonic loads. The load cell has a vertical load capacity of 500 kgf and lateral load capacity of 10 kg/cm2. It is possible to form specimens with diameters of 50 mm, 60 mm, 75 mm and heights of 100 mm, 120 mm and 150 mm by changing the top and bottom caps. The vertical loading apparatus is capable of applying 200 kgf dynamic load. For monotonic loading conditions, the loading capacity is 500 kgf and rate of loading is between 0.002mm/min and 2.0mm/min. It is possible to apply pressures between 0-10

kg/cm2. The air pressure is transmitted to water leading to triaxial chamber and the pressure regulator controls its amount. The drainage valves connected to the top and bottom caps are used for supplying water into the specimen and applying the backpressure. The 25ml burette pipe is connected to the drainage valves and it is used for calculating the amount of water drained during consolidation. The test apparatus also includes a water tank and a vacuum tank with volumes of 5 lt.

Figure 4.2 : Triaxial Test Apparatus in ITU Soil Dynamics Laboratory

The cyclic loading is applied to the specimen by uniform sinusoidal load and its frequency ranges between 0.001 Hz and 2.0 Hz. The load, displacement and pore water pressure transducers are used for monitoring the specimen behaviour and the data is directly transferred to the computer. The computer program, Virtuel Bench Logger, is used for transferring the data and also drawing the graphics.

The schematically drawing of the loading unit and triaxial chamber are shown in Figure 4.3.

1 Air Actuator	9 Back Pressure Gauge	17 Manual Jack Handle
2 Master Gage Change Valve	10 Vacuum Gage	18 Lower B. P. Tank
3 Loading Frame	11 Double Tube Burette (25ml)	19 Water Tank
4 Vertical Displacement	12 Switching Valve	20 Air Filter
5 Load Cell Dummy	13 Upper B. P. Tank	21 Speed Control Unit
6 Vertical Pressure Gauge	14 Specimen Manifold System	22 Air Slide Regulator
7 Confining Pressure Gauge	15 Mechanical Jack	23 Vacuum Tank
8 Triaxial Chamber	16 Primary P. Regulator	24 De-Air Water Tank
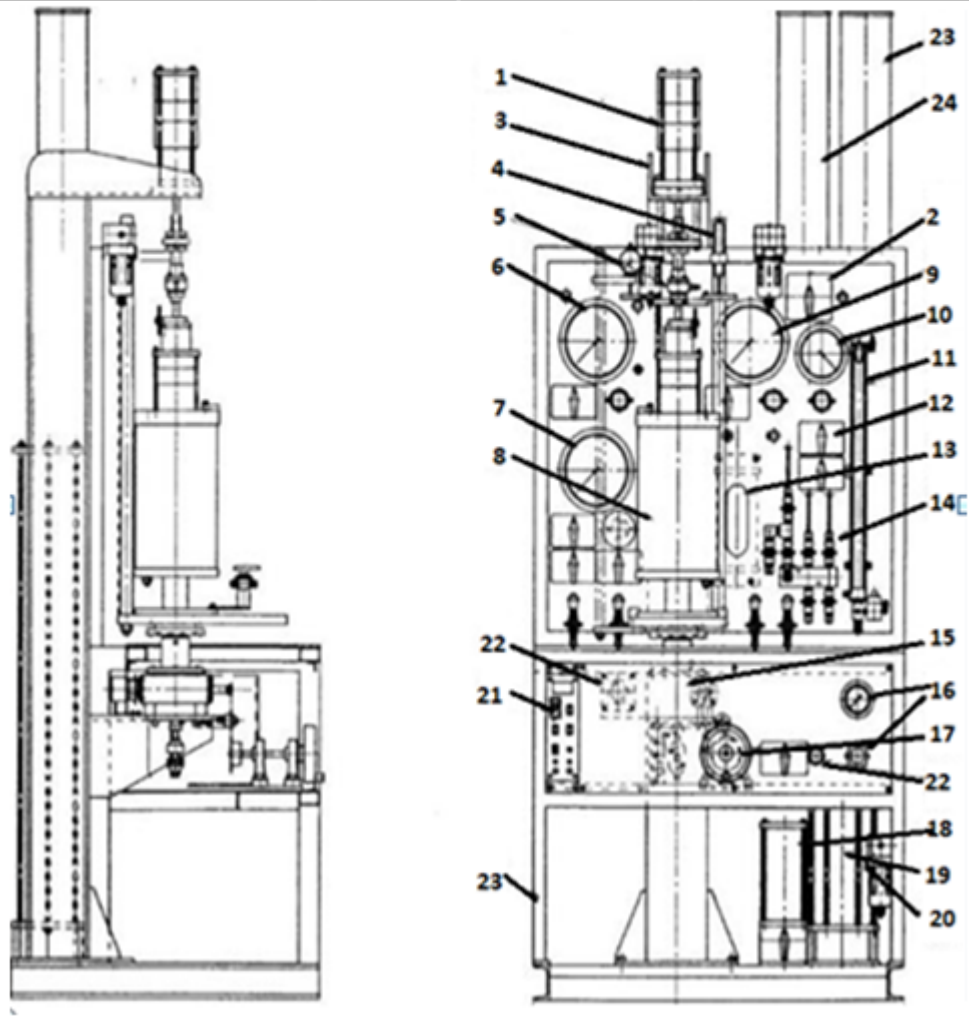
Figure 4.3 : Loading Unit and Triaxial Chamber (Seiken Inc.)

The digital system shown in Figure 4.4 is used for calibrating the data. When the digital system starts to operate, the condition of gain button, ATT5 button and CAL.με button must be controlled. The ATT button controls the sensitivity of measurements. The CAL.με button calibrates the μ ε input. The CAL.με button is switched by pressing the CALL.ON button and it starts the calibration. First the AUTO button is switched and the digital voltmeter should show the value of "0.00". Then CALL.ON button is switched and the value of voltmeter is arranged as "5.00" by using the GAIN control button which controls the sensitivity of the amplifier. The

ZERO-C-BAL button controls the changes in the measurement and after it is switched to zero, the ZERO CONTROLLER is used for setting the voltmeter value shown on digital indicator (DV) to "0.00". The ZERO-C-BAL button is kept constant at the C-BAL position and the voltmeter value is set to "0.00" by using C-BAL button. At the same time, for calibrating the sensitivity of the measurements, ATT 1, 2 or 5 button is calibrated. The MEANS button is pushed for adjusting the indicator to the rated value of the sensor. After that, CAL.ON is switched and DV value is set to "10.00" with turning MEAS controller. At the end CAL button is switched off and so the device will be ready to record experimental data. The mechanical gauges are also placed to be used for experimental calculations.

Figure 4.4 : Digital System of the Triaxial Apparatus

4.2 Test Materials

The Akpınar Sand is used in the experimental study. The sand is first washed through ASTM #200 sieve and then sieved through ASTM #10 sieve. According to the Unified Soil Classification System the sand is classified as SP. The constant head permeability test is conducted on sand samples at relative densities of 30%, 50% and 80%. The microscopic analysis of the Akpınar Sand has been conducted by the Istanbul Technical University, Civil Engineering Faculty, Construction Materials Laboratory. The results obtained from the binocular microscope showed that sand particles are clean and semi-circular, semi-angular shaped. The composition mainly consists of quartz and it includes magnetite in small amounts. The grain size

distribution curve of Akpınar Sand is shown in Figure 4.5 . The parameters of the sand are shown in Table 4.1.

Table 4.1 : Properties of Sand

Property	Value
Specific Gravity	2.69
Maximum void ratio	0.85
Minimum void ratio	0.54
Permeability (m/s)	4×10^{-4}
Sand fraction (%)	99
Fine materials (%)	1
Effective grain size D_{10} (mm)	0.22
D_{60} (mm)	0.35
D_{30} (mm)	0.27
Coefficient of uniformity C_u	1.60
Coefficient of curvature C_c	0.95
c (kPa)	0
ϕ (deg)	40
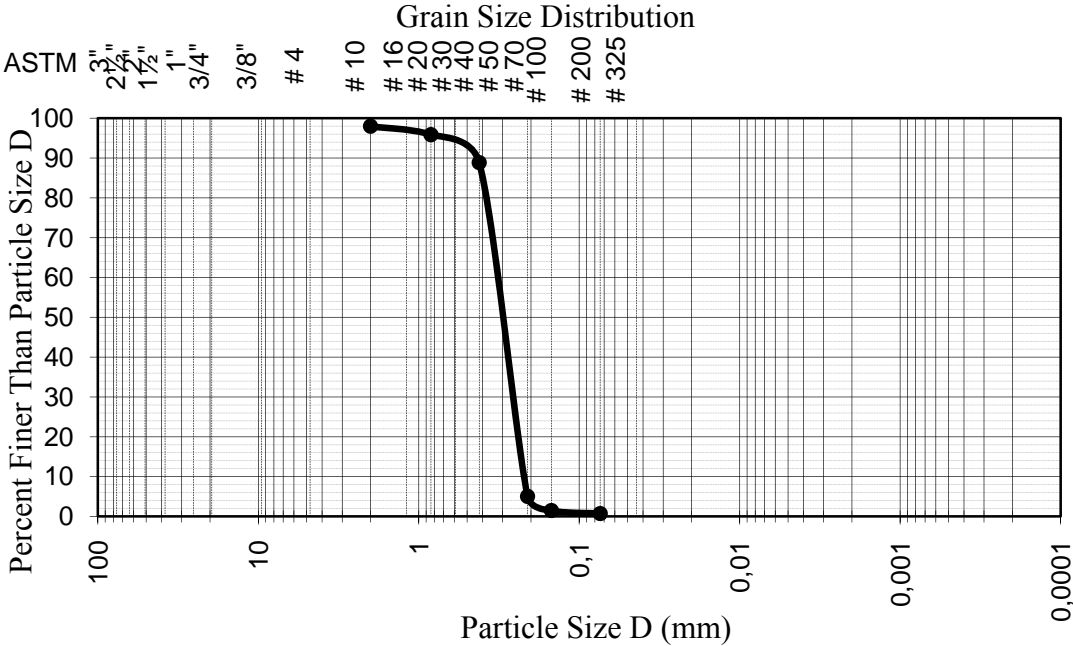
Figure 4.5 : Grain Size Distribution Curve of Akpınar Sand

The fiber used as the reinforcement is called FORTA MIGHTY-MONO fiber. It is made of pure homopolymer polypropylene. The photo of fibers is shown in Figure 4.6 are produced according to ASTM C1116. The fiber parameters are presented in Table 4.2.

Table 4.2 : Fiber Properties

Color	White
Structure	Single Fiber
Specific Weight (g/cm^3)	0.91
Length	19 mm
Water Absorption	0
Tensile Stress	570-660 MPa

Figure 4.6: Fibers

4.3 Compaction Test

The first step for sample preparation was to determine the required amount of water for mixing the fiber into the sand uniformly. According to the previous studies on fiber-reinforced sand, water is required for obtaining an efficient mixture and preventing fiber-sand segregation (Ibraim and Fourmont, 2006). For determining the amount of water that will be added to the fiber-sand mixture, compaction test is performed on unreinforced sand to determine the optimum water content.

The optimum water content is determined by performing Modified Proctor Test. For conducting Modified Proctor Test, a mold with a volume of 2304cm^3 was used. The rammer weighting 4.54 kg was dropped from a height of 45 cm. The soil was compacted in five layers with applying 56 blows to each layer. Figure 4.7 shows the compaction curves obtained. Despite the deviations, it is clearly obtained that an optimum water content of 10 % will be used for sample preparation. Considering this information, the randomly distributed fiber reinforced sand samples were prepared at this water content.
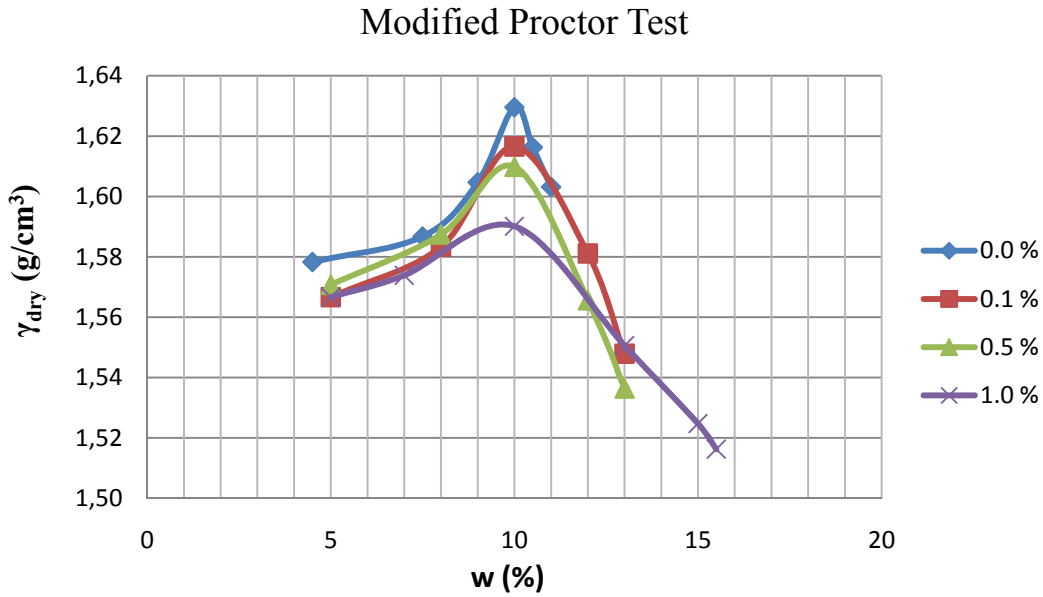
Figure 4.7 : Modified Proctor Test Results

Also the sieve analysis is performed after the modified Proctor Test to confirm that compaction has not effected the grain size distribution curve. The grain size distribution curves before and after the Modied Proctor Test are presented in Figure 4.8 to show the exact match of the curves.
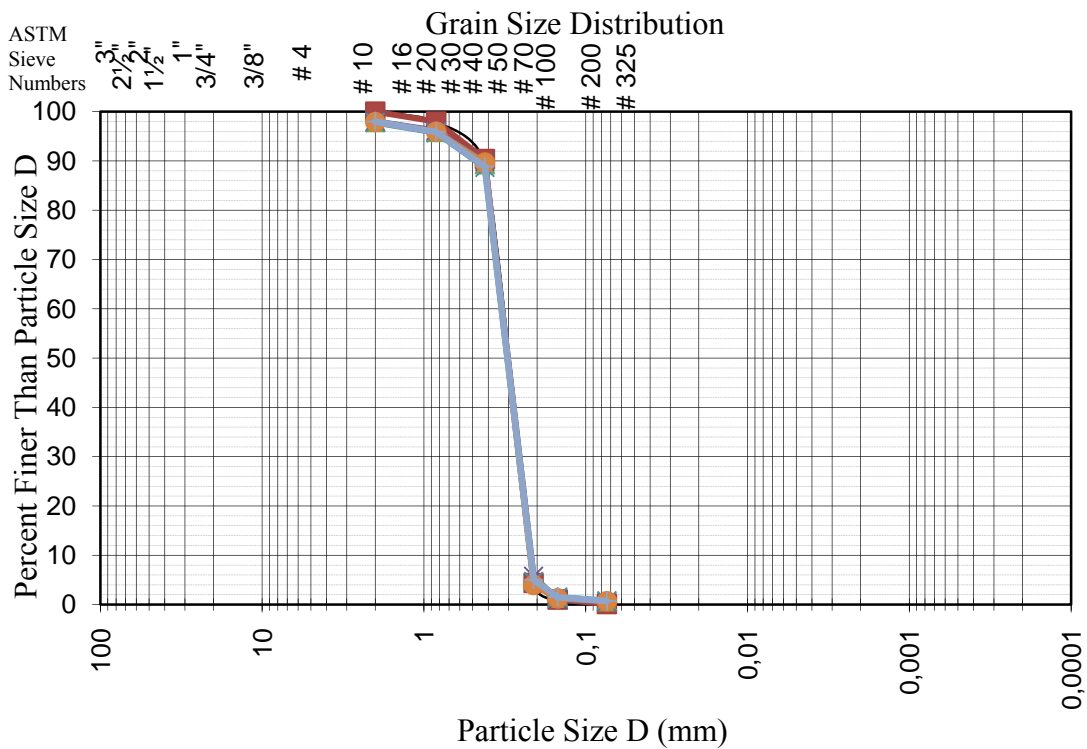
Figure 4.8 : Comparision of Grain Size Distribution Curves before and after compaction

4.4 Sample Preparation

The triaxial test apparatus is used for performing static triaxial compression tests and cyclic triaxial tests. The tests were conducted on samples of 50 mm diameter and 100 mm height, having a relative density around 55 %. The amount of fibers added to the sand was taken as a percentage of the dry weight of the sand. The fibers are accepted as a part of the sand skeleton. The fiber contents tested are 1.0%, 0.5% and 0.1%. The results are compared with the results of unreinforced sand. For sample preparation, fibers were separated to enable a uniform mixture. The fibers, sand and water are mixed thoroughly by hand until a uniform mixture is obtained. It is observed that fibers disperse in the sand easily. Before the mixture is placed in the test apparatus, the burette is filled with water. The air bubbles inside the top and bottom drainage pipes must be expelled by applying a backpressure of 10-20kPa. After that, porous stones at the top and bottom caps are saturated. The rubber membrane, having a thickness of 0.15mm is placed and O rings are used to fasten the membrane. The split mold is placed around the membrane and the mold is fixed with an apparatus holding the parts of the mold together. A small amount of vacuum is applied inside the mold to stick the membrane to the inner wall of the mold. The porous paper is placed on the porous stone at the bottom cap. The fiber reinforced sand sample is transferred to the mould with a spoon in five layers and compacted lightly by wet tamping method to achieve a uniform sample. The sample is placed in 5 layer and 30 blows are applied on each layer. The second porous paper is placed on the sample. After placing the sample, the loading device with three bases is placed and they are fixed. The membrane is rolled over the top cap and O-rings are used to fasten the membrane to the loading device. They are required for avoiding the transfer of water and air into the sample during the experiment. At this stage, 30kPa vacuum is applied inside the sample to prevent any deformation and then the split mold is removed as the sample can stand still due to vacuum. When the specimen is standing with the help of vacuum, its dimensions are measured to determine the volume. The loading piston on the top cap is lowered until it touches the porous paper smoothly. The cell chamber and chamber cap are placed and they are fixed with three screws on the top. Air pressure between 30kPa is applied to the water tank that enables water transfer into the chamber and so the chamber is filled with water until the level marked on the chamber. The loading piston is lowered and after it is

completely loose, gauges are calibrated. Carbondioxyde gas is transferred inside the specimen for 30 minutes. For samples that are going to be tested in unsaturated conditions, CO_2 method is not used and back pressure is not applied inside the sample. The vertical deformation changes are recorded to be used in final volume calculations. The water level of the burette is recorded. After that, vacuum is turned off and distilled water is transferred into the soil from the bottom cap due to the head difference between the water supply tank and the triaxial chamber. At this stage, the external pressure holds the sample together. This process is continued until all the air inside the water pipe is removed. It takes approximately 15 minutes but the air bubbles inside the pipe must be carefully observed.

The backpressure of 270kPa and confining pressure of 300kPa is applied to the specimen and after waiting for 4 hours, the degree of saturation is determined. The degree of saturation can be increased by increasing the backpressure and cell pressure simultaneously, in order to maintain the confining stress acting to the sample. The B coefficient is calculated for determining the saturation and it is calculated as:

$$B = \frac{\Delta u}{\Delta \sigma_3}$$ (4.1)

where Δu is the resulting change in pore pressure and $\Delta \sigma_3$ is the pressure increase for determining the saturation. At this stage the cell pressure is increased to 330kPa and the back pressure is increased to 300 kPa for determining the saturation. When the B coefficient is greater or equal to 97%, the specimen is accepted as saturated. After the first cyclic triaxial test, the cell pressure is increased up to 400 kPa while the back pressure is constant. The drainage valves are opened and the water level of the burette is controlled in order to determine if the consolidation phase is complete. The change of water level in the burette shows the volume change of the specimen. When the water level is constants, the specimen is ready for the experiment. After waiting for 30 minutes the cell pressure is increased up to 500 kPa and the back pressure is increased to 400 kPa in order to confirm the saturation level. At this stage, the sample is ready for the static triaxial test. For the undrained test, the drainage valves are kept close during the test and for the drained test, the drainage valves are kept open during the test.

For the unsaturated test specimens, the sample is not subjected to CO_2 gas or backpressure. The cell pressure confined at the desired confining pressure value and subjected to undrained test.

4.5 Test Procedure

When the specimen is ready for the experiment, the maximum initial Elasticity Modulus values for unreinforced and reinforced sand specimens were determined by using cyclic triaxial apparatus in accordance with ASTM D3999-91. The load controlled test type was preferred. First, the cyclic loading is applied while the confining pressure of 30kPa is applied on the specimen. The cyclic loading is applied at very small values. The load is applied as staged loading with the frequency of 0.1Hz. Small strains, between 10^{-4} and 10^{-6} are determined by the gap-sensors. The Elasticity Modulus values are calculated as:

$$E = \frac{\Delta\sigma}{\Delta\varepsilon} \tag{4.2}$$

where $\Delta\sigma$ is the deviatory stress and $\Delta\varepsilon$ is the small axial strains.

After the maximum initial Elasticity Modulus under the confining pressure of 30kPa is determined, the experiment is stopped. It is necessary to wait for 15 minutes until the consolidation phase is completed. At the end of this time interval, water level in the burette is recorded in order to be used for estimating the volume change in the specimen. In scope of this research, the initial maximum Elasticity Modulus values are also determined under the cell pressure of 500kPa and backpressure of 400kPa.

The triaxial compression test under monotonic loading is carried out after completing the cyclic loading tests in undrained conditions. The conditions are kept constant and kinematically controlled increasing stress is applied under a confining stress of 100kPa during the undrained conditions. The tests were conducted at strain rates of 1.00 mm/min, 1.25 mm/min, 1.50 mm/min for saturated specimens and the strain rate of 1.0 mm/min is applied for unsaturated specimens. The drained tests are performed on unreinforced sand samples and sand samples reinforced with fiber contents of 0.5 and 1.0% fiber contents at the strain rate of 1.00 mm/min. For the unreinforced sand samples the effect of strain rates of 0.5 mm/min, 1.0 mm/min and 2.0 mm/min are determined by conducting consolidated drained test. Deviator load was applied until the specimen failed or up to a strain of 20%, whichever was earlier.

The photos of unreinforced sand and fiber-sand mixtures before and after the triaxial test application are taken by using a digital microscope. They are presented in Figure 4.9.
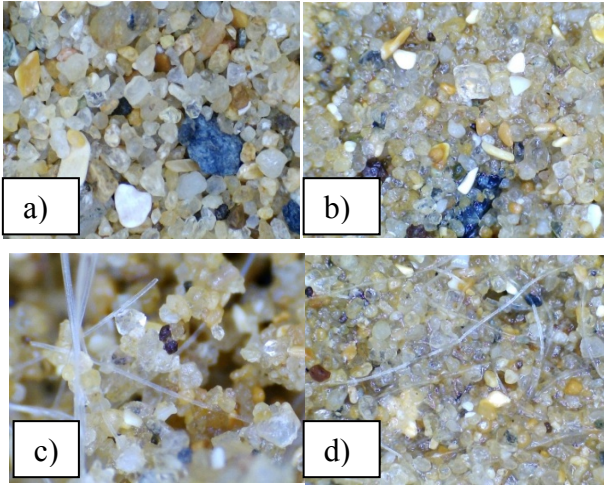
Figure 4.9: Microscopic images a) unreinforced sand before (a) and after (b) the experiment, reinforced sand before (c) and after (d) the experiment

4.6 Direct Shear Tests

Direct Shear Tests are performed to determine the effect of fibers on the shear strength parameters of sand. The sand used in direct shear tests is the same as the sand used in triaxial tests. The sand is washed through ASTM #200 sieve and then sieved through ASTM #10 sieve. The tests are conducted in a shear box with the dimensions of 60 mm x 60 mm in plane and 20 mm in depth. The samples are prepared at relative densities around 55%. The unreinforced and reinforced sand samples are prepared at optimum water content by using the oven dried sand. The tested fiber contents are 0.5 %, 0.75%, 1.0% and 2.0% of the dry weight of sand. The fibers, sand and water are mixed thoroughly by hand. During the sample preparation, the difficulty of obtaining a fairly uniform mixture increases as the amount of fibers that will be mixed into soil increases. Thus, the upper limit of fiber content is decided as 2.0% of dry weight of sand. The sample including 2.0 % fiber is shown in Figure 4.10 and it can be seen that a fairly uniform mixture is obtained with randomly distributed fibers.

Figure 4.10: Fiber reinforced sample

The sample is placed into the direct shear box with tamping lightly. The porous papers are placed before and after the sample is placed. The surface of the sample must be smooth as it is shown in Figure 4.11. The direct shear test apparatus used is showed in Figure 4.12. The normal vertical stresses of σ_n =100, 200 and 300 kPa are applied at unreinforced and reinforced sand samples. The loading rate was 0.12mm/min for all tests. The settlements are recorded for 15 minutes after the sample is loaded. Shear stresses were recorded as a function of horizontal displacement up to a total displacement of 12 mm in order to observe the post failure behavior.

Figure 4.11 : Direct Shear Test Sample

Figure 4.12 : Direct Shear Test Apparatus

5. EXPERIMENTAL RESULTS

In this part of the thesis, the experimental results of the laboratory tests conducted at ITU Soil Mechanics Laboratory are presented.

5.1 Maximum Elasticity Modulus Values

The maximum Elasticity Modulus (E_{max}) values are determined by conducting load controlled cyclic triaxial test on unreinforced and reinforced sand samples. The E_{max} values are calculated for confining pressures of 30 kPa and 100 kPa. Through these experiments, the effect of confining pressure acting on the specimen and the effect of fiber inclusions are determined.

The gap sensors recorded small strains (order of 10^{-4} and 10^{-6}) and the deviator stress-axial strain graphs are used for calculating the E_{max} values. For example, as it is shown in Figure 5.1, the slope of the deviator stress-axial strain graph of unreinforced sand at the confining pressure of 100 kPa is estimated. The maximum modulus, E_{max} is calculated approximately 250MPa.
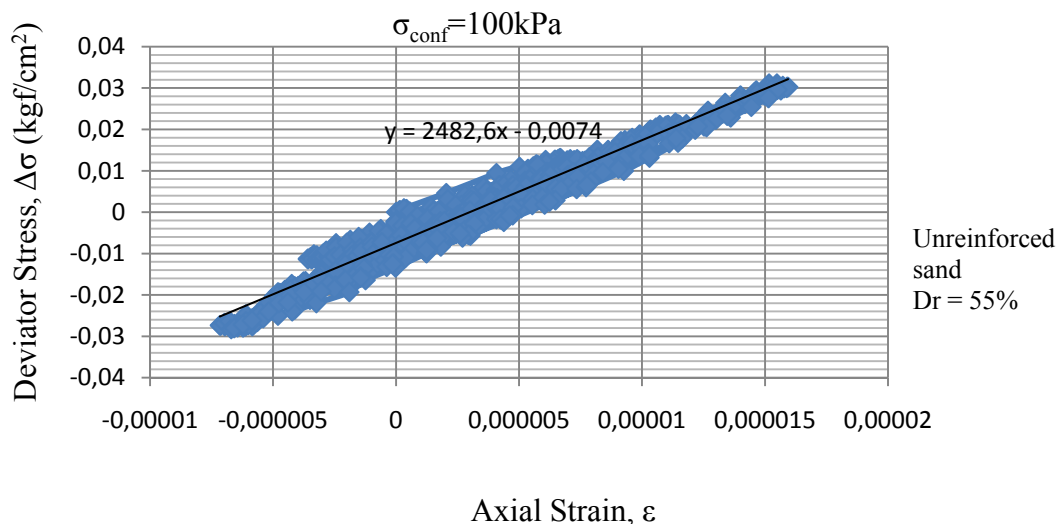
Figure 5.1 : Determination of E_{max} value for unreinforced sand

The effect of fiber inclusions is searched by conducting the experiments on unreinforced sand and reinforced sand with fiber contents of 0.1%, 0.5% and 1.0 %.

The E_{max} values are calculated at strain levels of 10^{-6}-10^{-4}. Properties of the test specimens and test results are presented in the Appendix A. The comparison of E_{max} values obtained for fiber contents of 0.0%, 0.1%, 0.5% and 1.0% are presented in Figure 5.2.
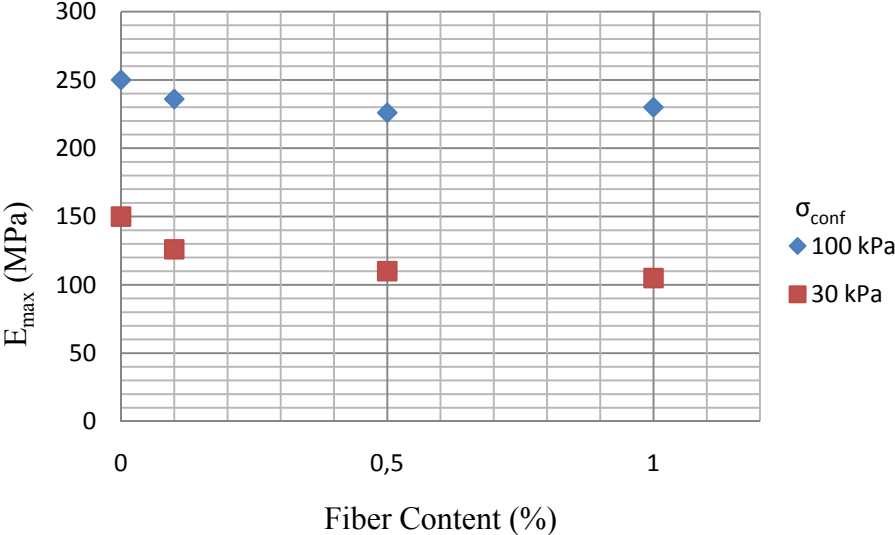
Figure 5.2 : E_{max} values for different fiber contents

According to the results, it is concluded that the E_{max} values calculated for the confining pressure of 100 kPa are higher than the E_{max} values calculated for the confining pressure of 30 kPa. As the fiber content increased, a slight decrease in the E_{max} value is calculated. This decrease is more evident at the confining pressure of 30kPa. Also the E_{max} values calculated for the reinforced sand samples at fiber contents of 0.5% and 1.0% are appoximately the same. It can be concluded that fiber addition did not result in a significant change of the maximum modulus.

5.2 Static Behavior of Fiber Reinforced Sand

Firstly, the consolidated undrained static triaxial compression tests are conducted on sand samples having a relative density around 55 %. Figure 5.3 shows the test sample before and after the test. The static triaxial compression tests are conducted at strain rates of 1.00 mm/min, 1.25 mm/min and 1.50 mm/min to observe the effect of strain rate on the static behaviour of unreinforced and reinforced sand. The triaxial test results of reinforced samples having fiber contents of 0.1%, 0.5% and 1.0% and unreinforced sand samples are compared in order to determine the effect of fiber inclusion. Secondly, unreinforced sand samples are subjected to CD test at strain

rates of 0.50 mm/min, 1.00 mm/min and 2.0 mm/min in order to determine the effect of strain rate. Thirdly, unsaturated samples that are prepared at the water content of 10% are subjected to triaxial test. In the third part of the triaxial testing programme, the consolidated drained tests are performed at the strain rate of 1.00mm/min in order to determine the effect of tested fiber contents. Properties of test samples and the static triaxial test results are presented in the Appendix B.
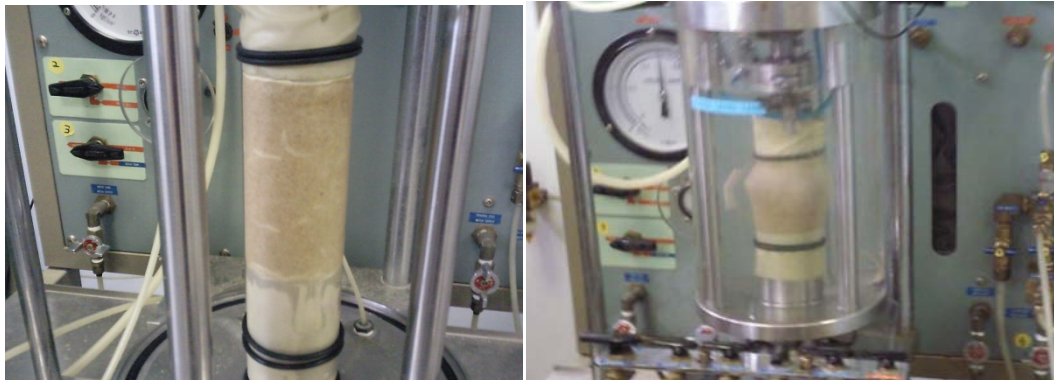
Figure 5.3 : Sand sample before and after the compression test

5.2.1 Effect of Strain Rate on the Static Behavior

In scope of this investigation, for each of the tested fiber content, the monotonic loading was applied at different strain rates to determine whether these strain rates will affect the stress-strain response of unreinforced and randomly distributed fiber reinforced sand samples in a considerable amount.

Firstly, saturated sand specimens are tested in undrained condition. The samples are allowed to saturate until B values are reached at least 0.97. The samples are tested at three different but close strain rates. The test results of unreinforced and reinforced sand samples with fiber contents of 0.1%, 0.5% and 1.0% are presented.

Figure 5.4 (a)-(b) shows the stress-strain behaviour of unreinforced sand at strain rates of 1.00 mm/min, 1.25 mm/min and 1.50 mm/min. The consolidated undrained triaxial compression tests are conducted on samples that have a saturation degree of 97-98%. The peak deviator stress of 1500 kPa is recorded at an axial strain of 10%. As the results show, the effect of strain rate on the stress-strain behaviour of fiber reinforced sand can be considered insignificant. The initial increase of the pore water pressure at small strains is followed by an important decrease at absolute pore pressures at axial strain of approximately 10%. While the results of tests conducted on strain rates of 1.00 mm/min and 1.50 mm/min are very similar, the test results of

the test conducted on 1.25 mm/min showed a slight difference. After the peak deviator stress is recorded, the deviator stress value decreases with the increasing axial strain.
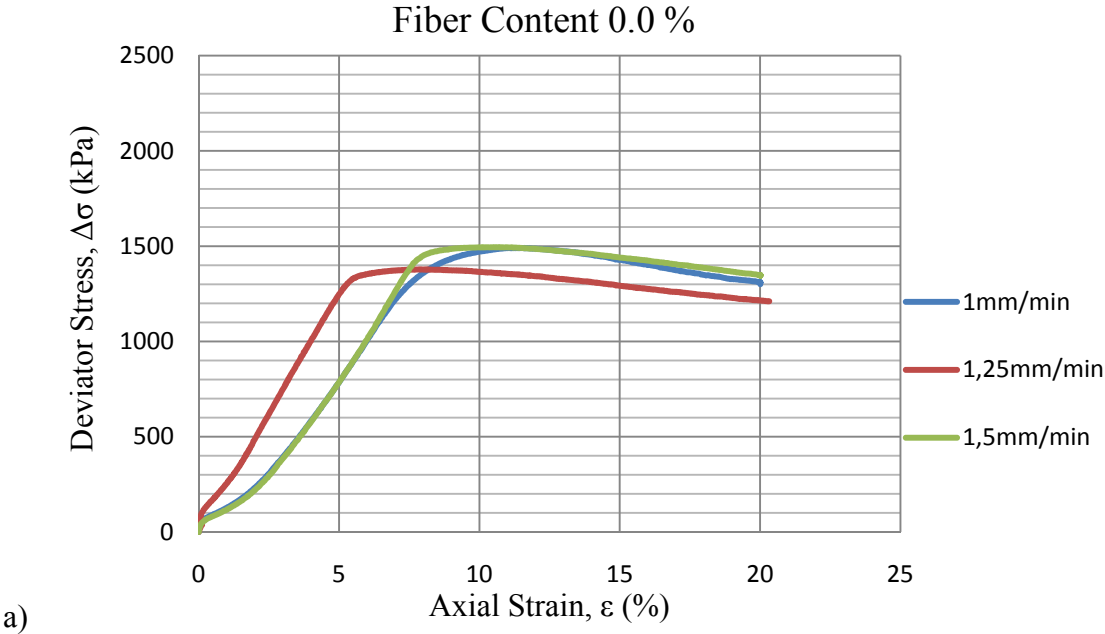
a)
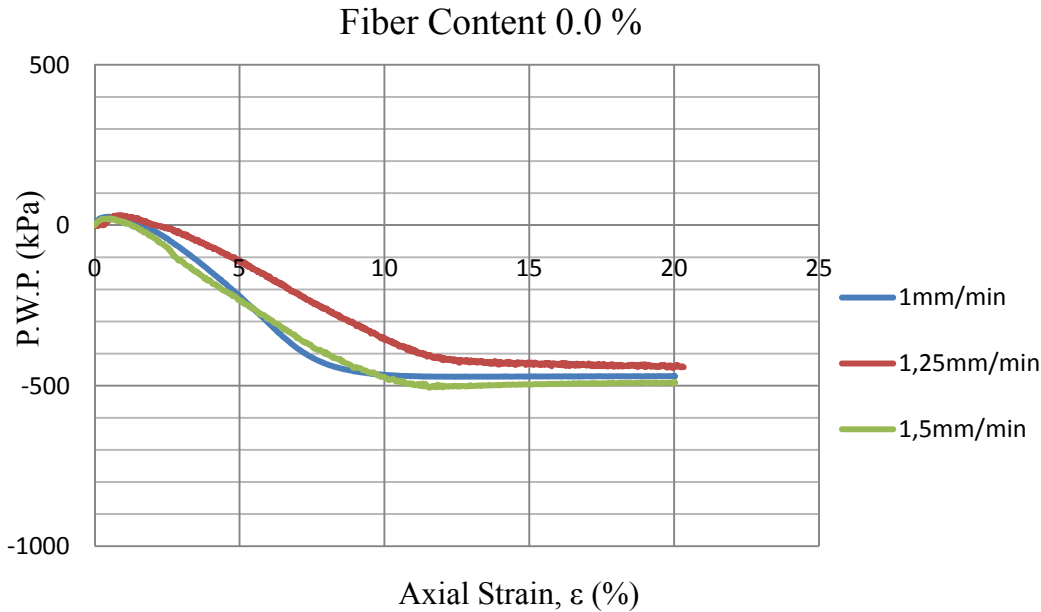
b)

Figure 5.4: Effect of strain rate on the static behavior of unreinforced sand

The effect of strain rate on sand reinforced with 0.1% fiber content is shown in Figure 5.5 (a)-(b). For the triaxial tests conducted with strain rates of 1.00 mm/min, 1.25 mm/min and 1.50 mm/min. According to the results, the tested strain rates showed insignificant differences. Due to fiber addition, the peak value is recorded at

higher strain levels compared to unreinforced sand. It can be seen that the peak deviator stress recorded is 1600 kPa at an axial strain around 12%. After the peak deviator stress is recorded, the deviator stress value decreases in an insignificant amount.

a)

b)
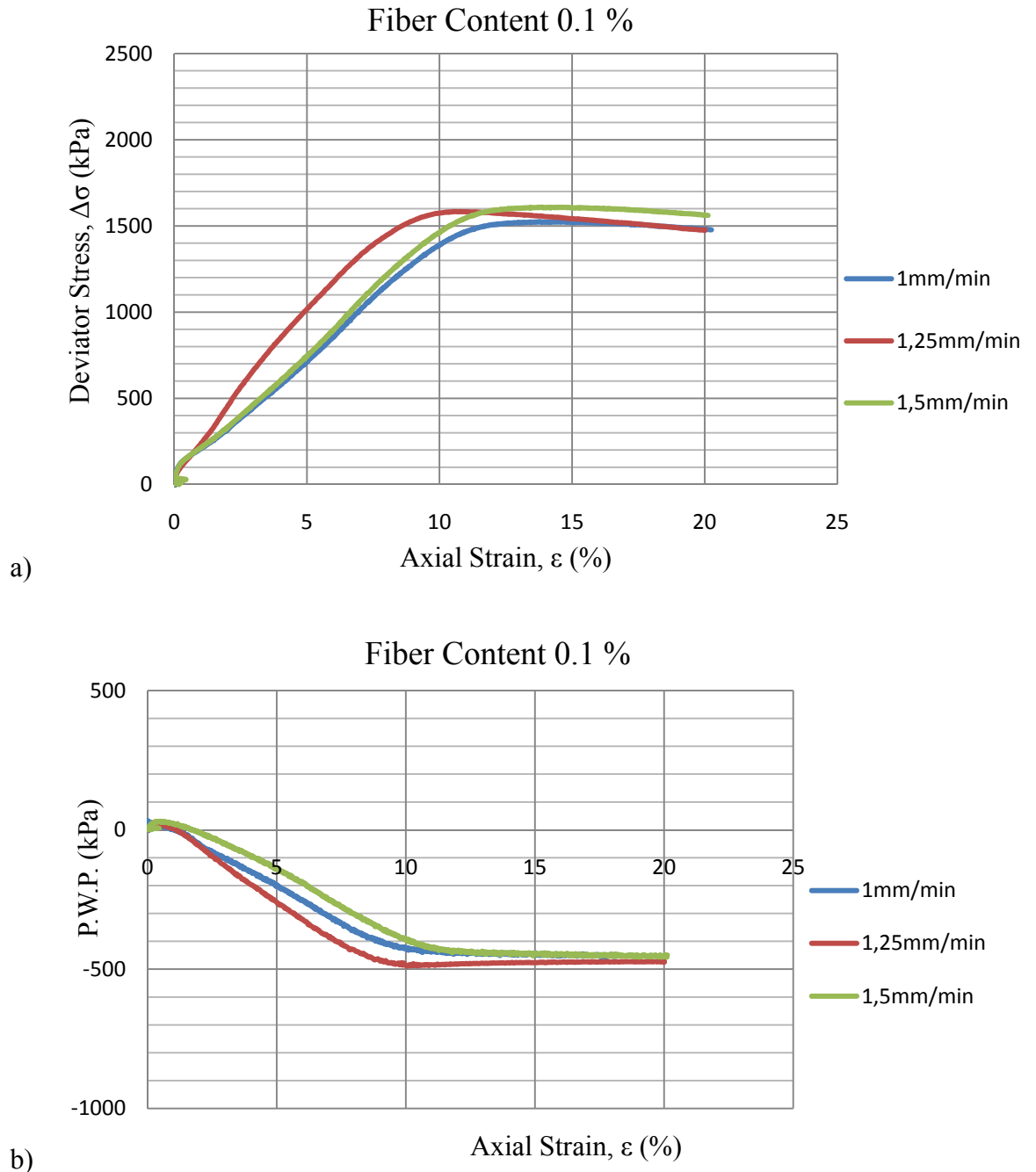
Figure 5.5: Effect of strain rate on the static behavior of 0.1% fiber reinforced sand

For fiber content of 0.5 %, the static response of experiments with the strain rate of 1.0 mm/min, 1.25 mm/min and 1.5 mm/min are presented in Figure 5.6 (a)-(b). The static responses recorded showed insignificant differences. The highest deviator

stress values recorded are around 1700 kPa and they are recorded at axial strains between 10-15%.

Fiber Content 0.5 %

a)

Fiber Content 0.5 %

b)
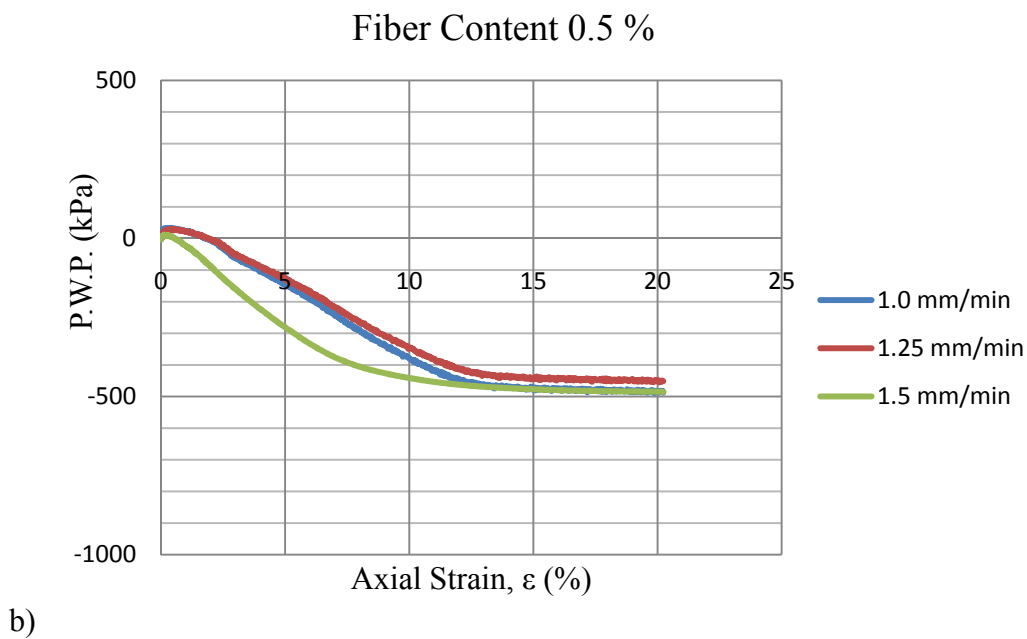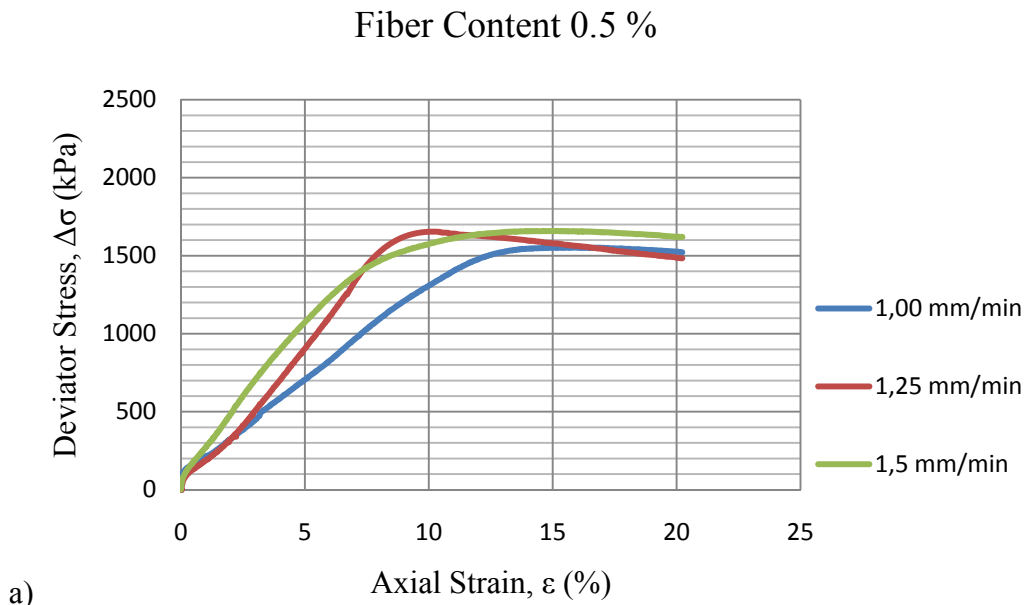
Figure 5.6: Effect of strain rate on the static behavior of 0.5% fiber reinforced sand

The static response of sand reinforced with 1% fiber content is presented in Figure 5.7. As the fiber content increased up to 1.0 %, the static behaviours that are recorded for strain rates of 1.00 mm/min, 1.25 mm/min and 1.50 mm/min are very similar. It can be stated that conducting the experiments at strain rates of 1.00mm/min, 1.25mm/min and 1.50mm/min have no significant effect on the static behavior of sand both for unreinforced and reinforced sand specimens with fiber contents of

0.1%, 0.5% and 1.0%. It either affects the maximum deviator stress value or the axial strain that value was reached in a negligible amount.

a)

b)
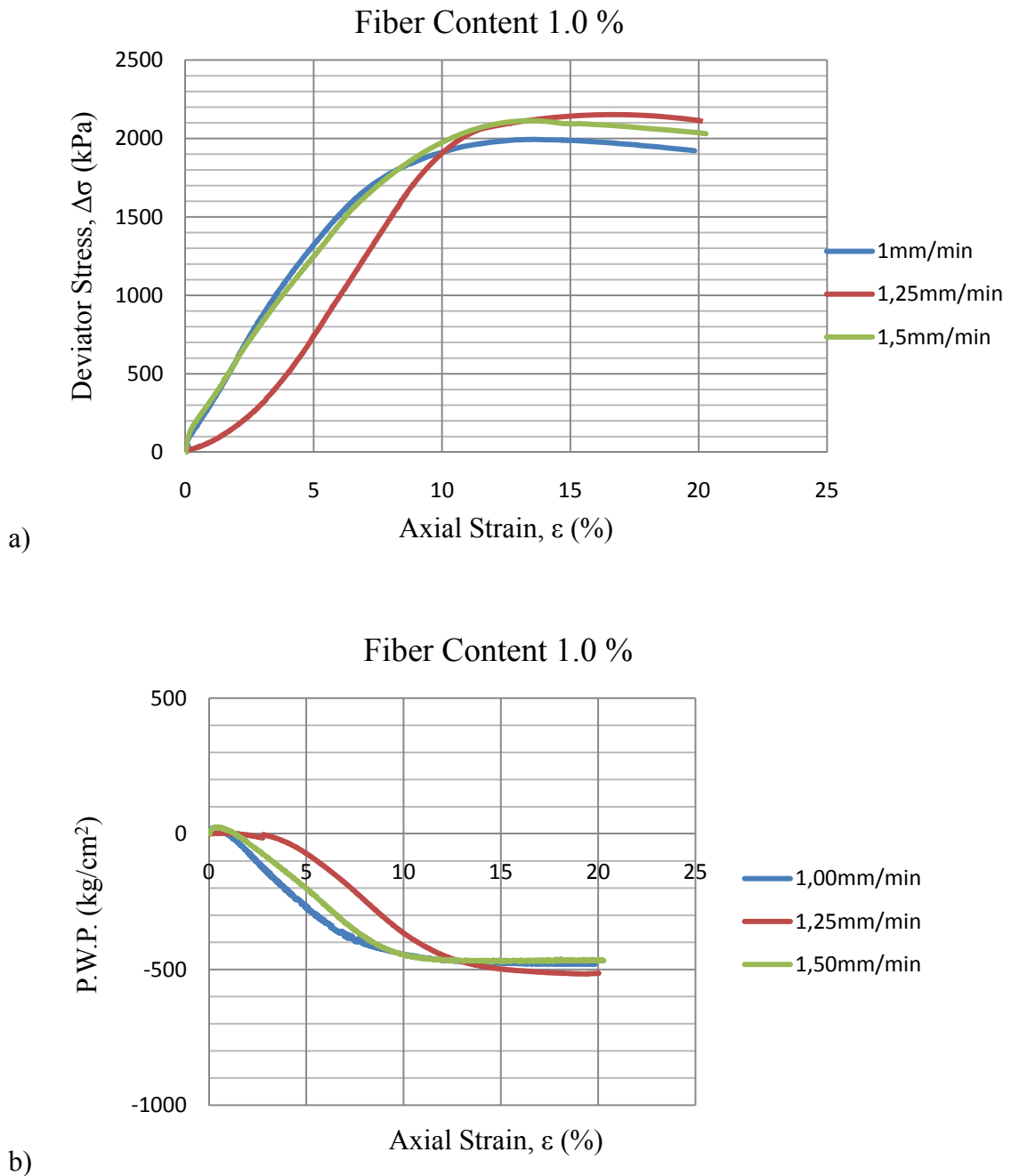
Figure 5.7 : Effect of strain rate on the static behavior of fiber reinforced sand with fiber content of 1.0 %

Secondly, the effect of strain rate is determined by performing consolidated drained tests on unreinforced sand with the relative density of 55%. The samples are tested at the confining pressure of 100kPa and the tested strain rates are 0.50 mm/min, 1.00 mm/min and 2.00 mm/min. The change in the deviator stress, void ratio and the ratio of volume change to the volume after consolidation are presented Figure 5.8.

Fiber Content: 0.0 %

a)

Fiber Content: 0.0 %

b)

Fiber 0.0 %

c)
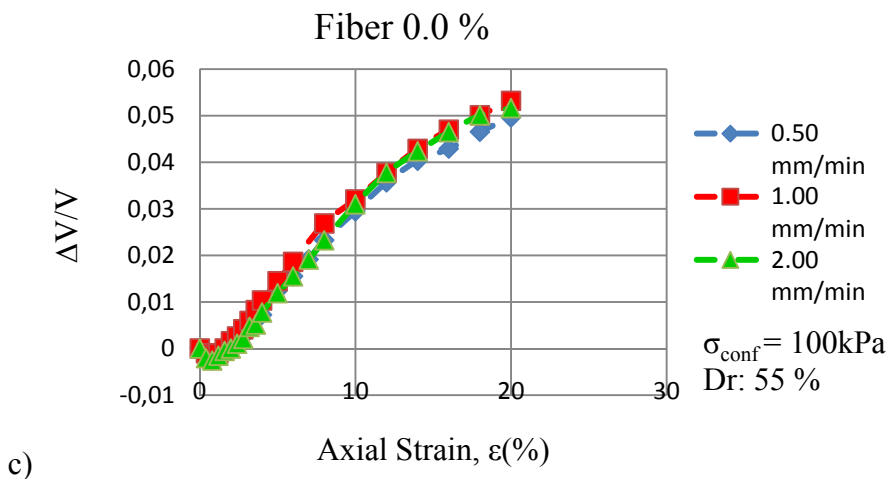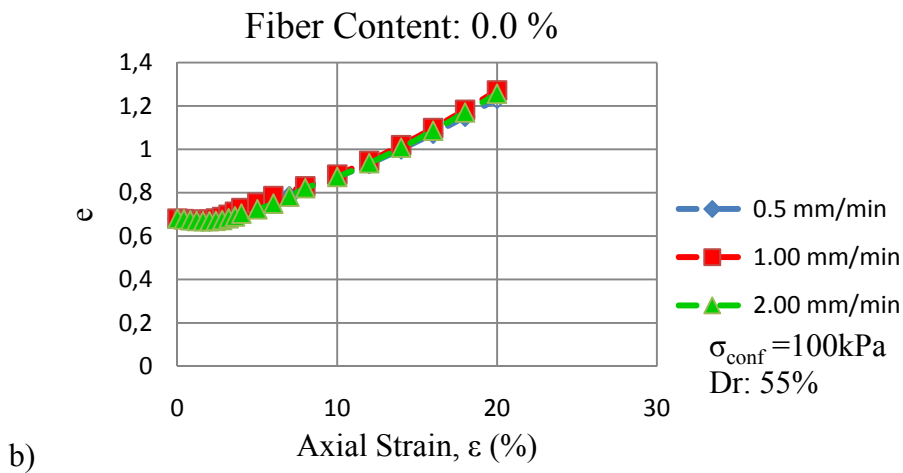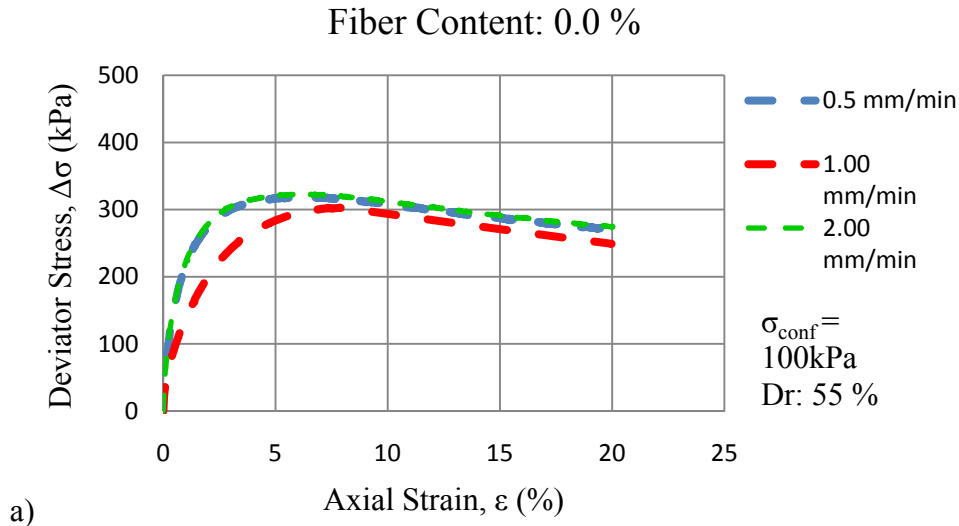
Figure 5.8: Effect of strain rate on the static behavior of unreinforced sand obtained from CD tests

It is presented that the tested strain rates did not effect the stress-strain response or the change in the volume or void ratio considerably.

5.2.2 Effect of Fiber Content on the Static Behavior

In scope of this experimental program, the effect of fiber content on the static behavior of fiber reinforced sand is investigated by conducting a series of triaxial tests. The results are used to compare the effect of fiber inclusion on the static behavior of sand. Consolidated undrained tests are performed on saturated sand specimens reinforced with randomly distributed fibers at fiber contents of 0.0%, 0.1%, 0.5% and 1.0%.

Figure 5.9 presents the static triaxial tests performed at the strain rate of 1.00mm/min. The fiber contents of 0.1 % and 0.5% affected the stress-strain behaviour of sand similarly. On the other hand the fiber content of 1.0% caused a significant improvement. While the unreinforced sand reaches the peak stress value at the axial strain around 10 %, reinforced sand samples reach the peak stress value at axial strains around 12-14 % .

a)

b)
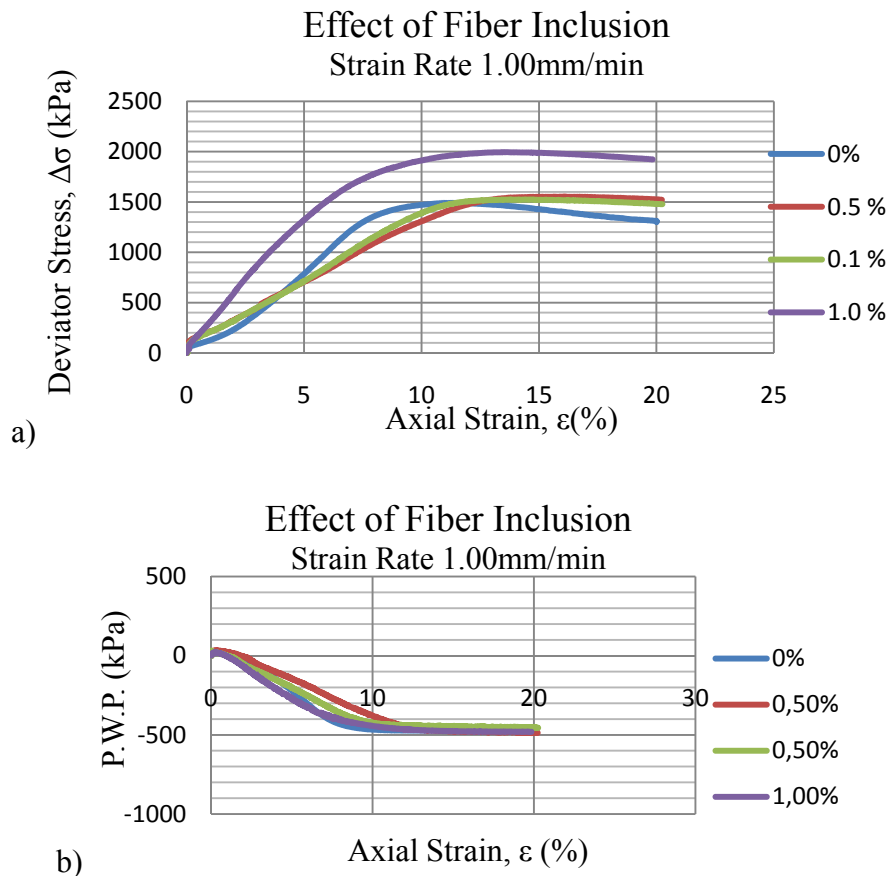
Figure 5.9: Effect of fiber inclusions at the strain rate of 1.00mm/min

Figure 5.10 presents the static triaxial tests performed at the strain rate of 1.25 mm/min. In these set of tests, the effect of fiber inclusion is more apparent. While the

fiber contents of 0.1 % and 0.5 % caused approximately 15 % increase of the peak stress value, the fiber addition of 1.0 % caused approximately 60 % increase of the peak stress value. As the fiber content increased, the peak stresses are observed at greater axial strains.
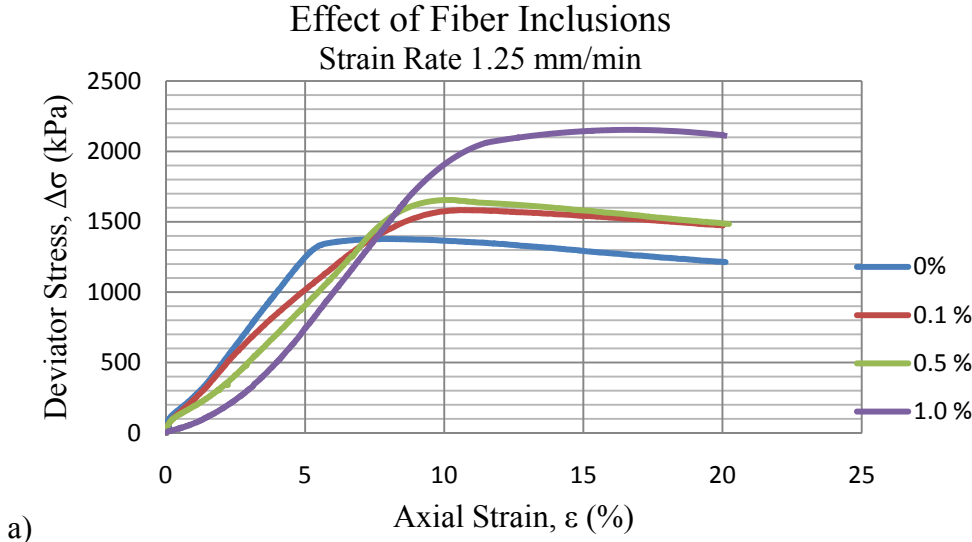
a)
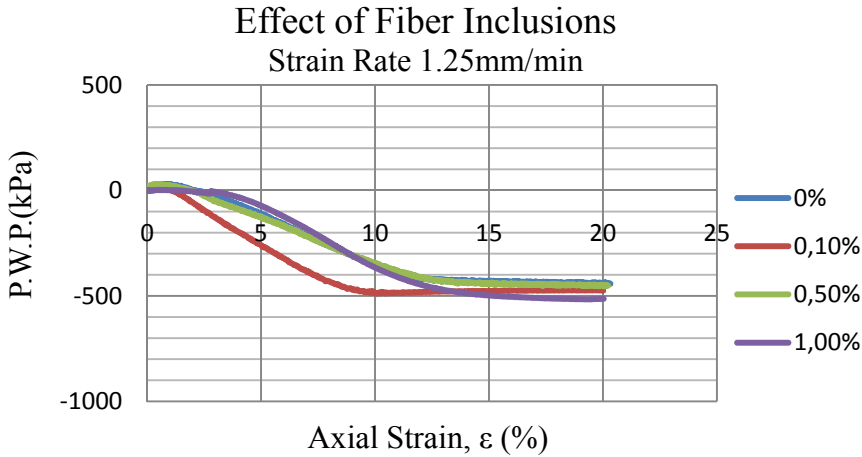
b)

Figure 5.10: Effect of fiber inclusions at the strain rate of 1.25mm/min

The results of triaxial tests performed at a strain rate of 1.50 mm/min are presented in Figure 5.11. Comparing the static triaxial test results presented it can be stated that, the fiber addition improved the static behavior of sand. While the fiber addition of 0.1% and 0.5% caused a slight increase of the peak stress value, the addition of 1.0% resulted in a significant increase. Also, the peak stresses are observed at greater axial strains due to fiber addition.

Effect of Fiber Inclusion
Strain Rate 1.50 mm/min

a)

Effect of Fiber Inclusions
Strain Rate 1.50 mm/min

b)
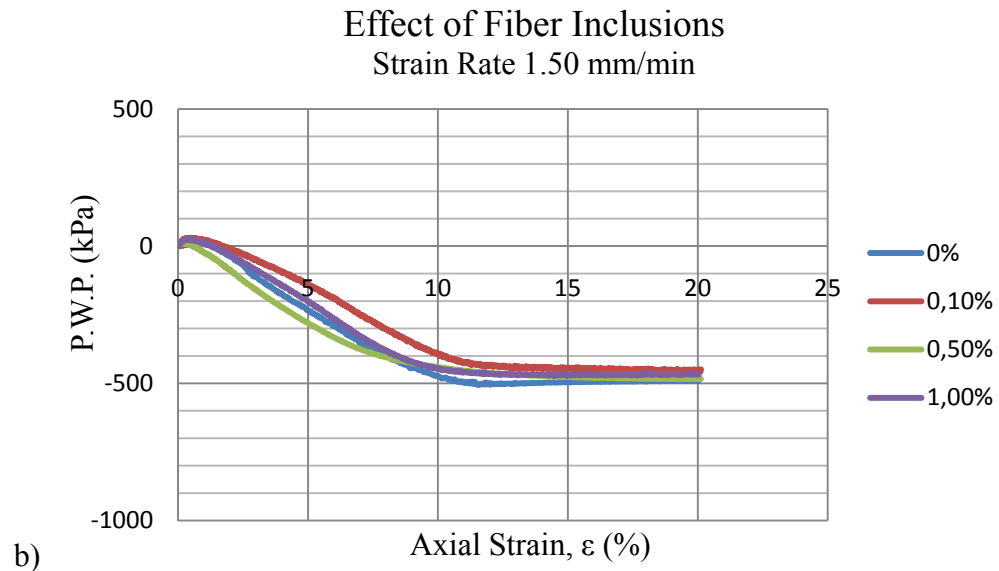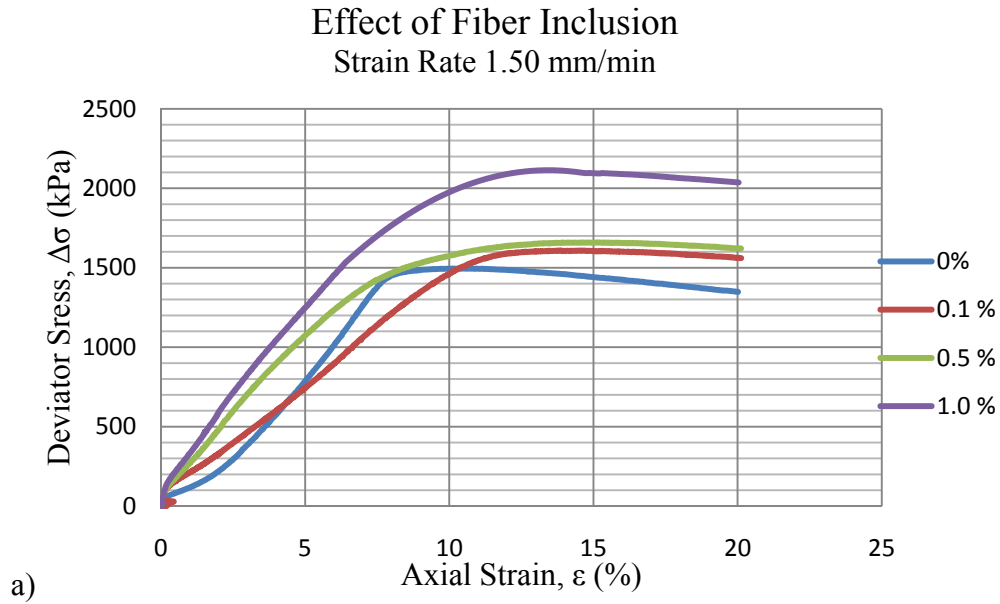
Figure 5.11: Effect of fiber inclusions at the strain rate of 1.50mm/min

In general the results of consolidated undrained triaxial tests showed that while the inclusion of 0.1% and 0.5% fiber contents increased the peak stress values slightly, the inclusion of 1.0% fiber content resulted in a significant improvement of the stress-strain behavior of sand. As shown on the figures, the pore water pressure reached the limit value at axial strain of approximately 10%.

Consolidated drained tests are performed on saturated sand specimens reinforced with randomly distributed fibers at fiber contents of 0.0%, 0.5% and 1.0%. The strain rate is 1.00mm/min in each test and the confining pressure of 100kPa is applied. The stress-strain response is shown in Figure 5.13. Ignoring the slight difference between

relative densities, it can be stated that fiber addition improved the static behavior of sand considerably.
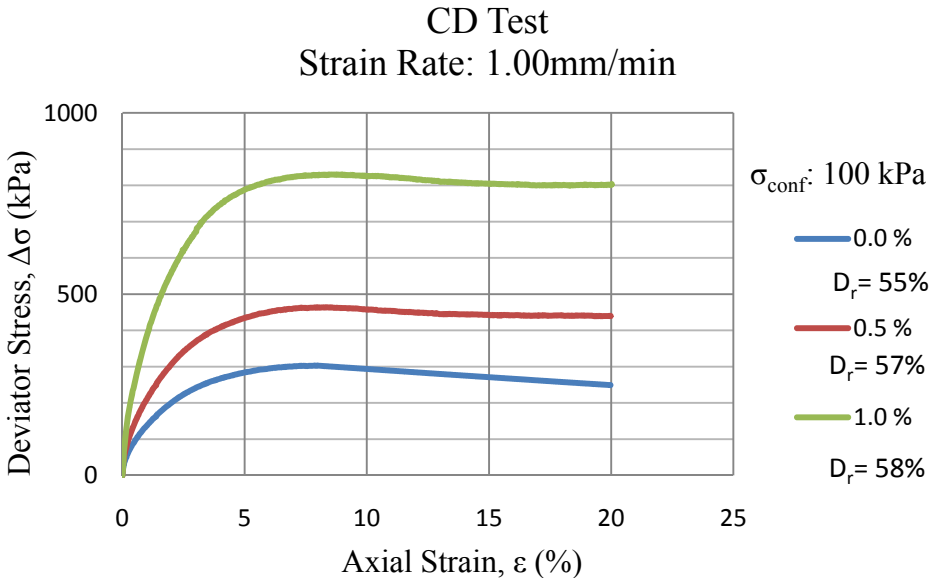
Figure 5.12: Effect of fiber inclusions at the strain rate of 1.00mm/min obtained from CD tests

Also the change in the void ratio and volume are presented in Figure 5.13. It is shown that while addition of 0.5% fiber content decreased the void ratio and volume change, the addition of 1.0% increased these parameters. The details of the test specimens and results of the CU and CD tests are presented in the Attachment B.

CD Test
Strain Rate: 1.00mm/min

a)

CD Test
Strain Rate: 1.00 mm/min

b)
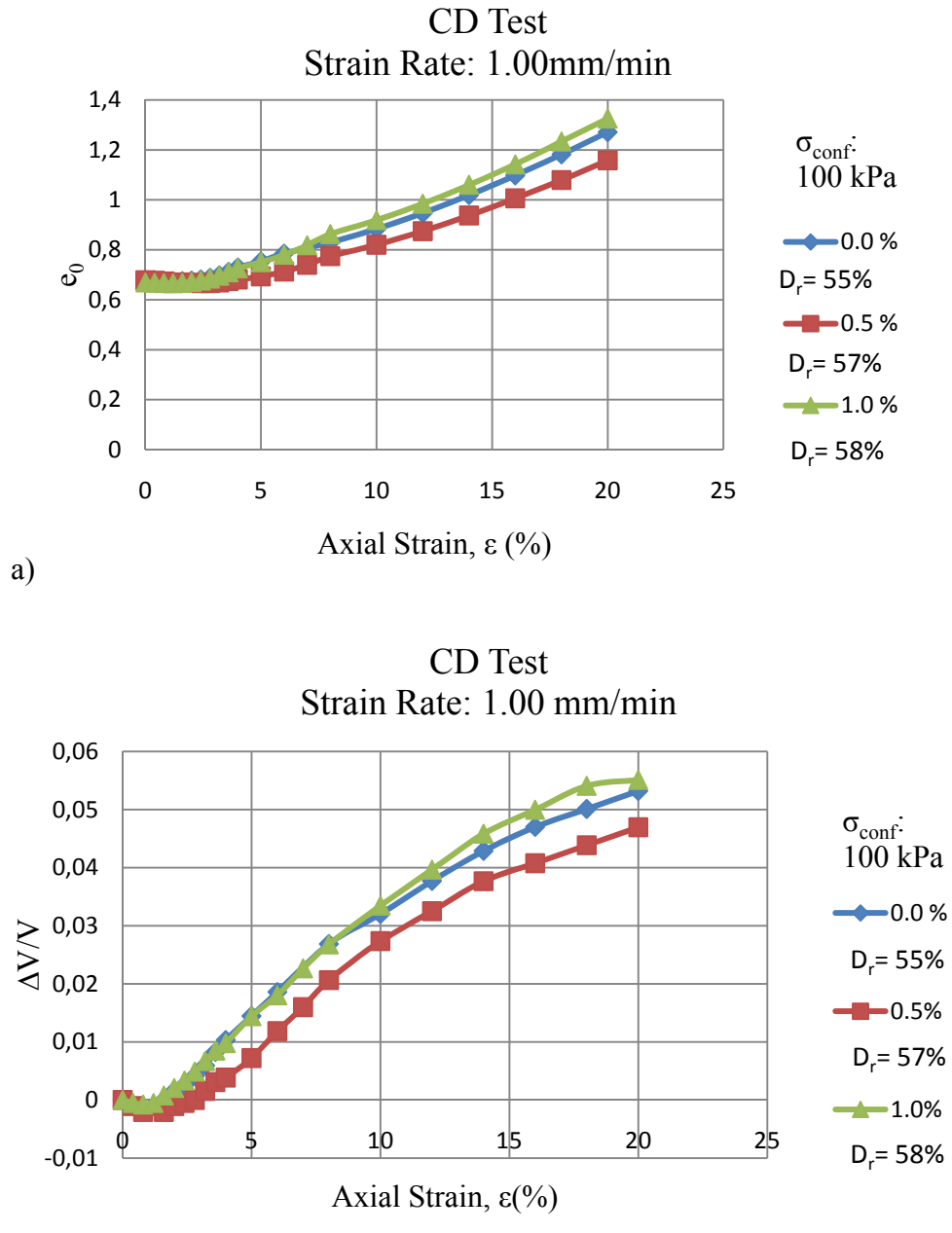
Figure 5.13: Effect of fiber inclusions on the void ratio and volume obtained from CD tests

5.2.3 Triaxial Compression Tests on Unsaturated Samples

At the second part of the triaxial compression test program, unreinforced and reinforced sand specimens are prepared at the water content of 10% and tested on unsaturated condition. As it is essential to add a certain amount of water to prepare a fairly uniform distribution of fibers into the sand, it was not possible to prepare dry samples. Even the unreinforced samples are prepared at the water content of 10% to keep the conditions same as the reinforced samples. During the sample preparation phase, specimens are not exposed to CO_2 gas and back pressure is not applied. The

specimen is confined by the cell pressure. The specimens are subjected to deviator loading right after they are placed in the triaxial system. The unsaturated specimens are tested at the confining pressure of 100kPa and the strain rate of 1.00 mm/min is applied. Figure 5.14 shows the stress-strain response of unreinforced sand and reinforced sand specimens including fiber contents of 0.1%, 0.5% and 1.0%. It can be seen that the fiber addition improved the static behaviour of sand considerably. As the fiber content increased, the recorded peak value is also increased at higher axial strains. Even the addition of fiber amount that is 0.1% of the dry weight of the sand caused increase of the failure deviator stress. Especially for the fiber addition of 1.0%, the peak value is recorded at the axial strain of 20%. On the other hand, the peak stress values recorded for saturated specimens are very high compared to peak stress values of unsaturated specimens.
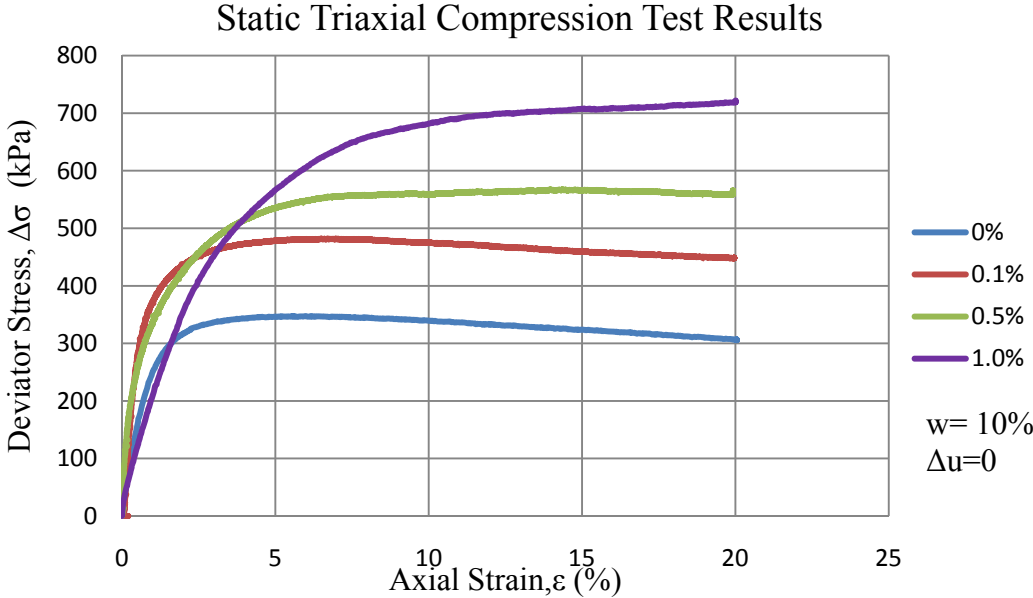
Figure 5.14: Static response of unsaturated samples

In addition to these tests, the triaxial compression tests are performed onunsaturated specimens that are prepared at water content of 10% with confining pressures of 200kPa and 300kPa to determine the effect of fiber inclusions on the shear strength parameters of sand. These triaxial tests are performed on unreinforced samples and reinforced samples that include 1.0 % fiber content. Figure 5.15, Figure 5.16 and Figure 5.17 and shows the static responses of unreinforced sand and sand reinforced with the fiber content of 1.0%.
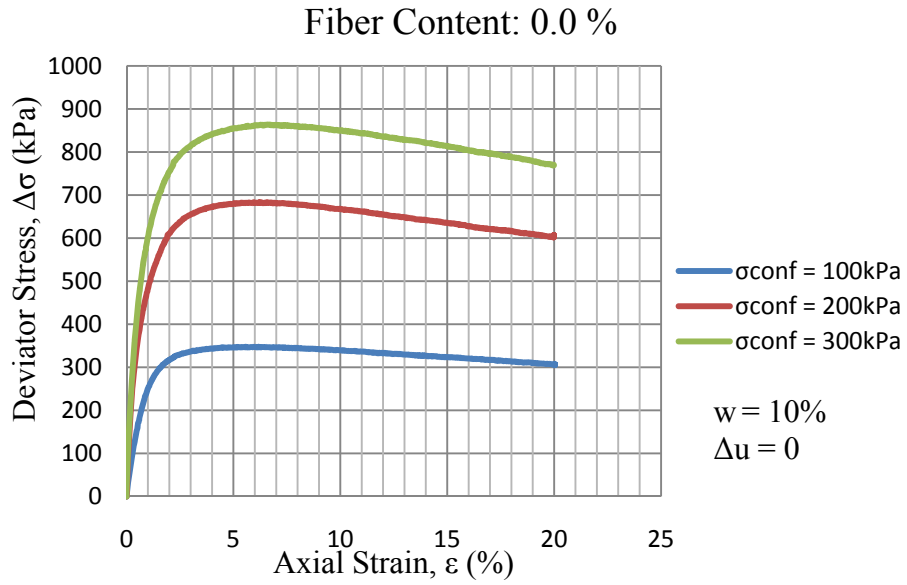
Figure 5.15: Stress-Strain response of unsaturated unreinforced specimens at different confining stresses
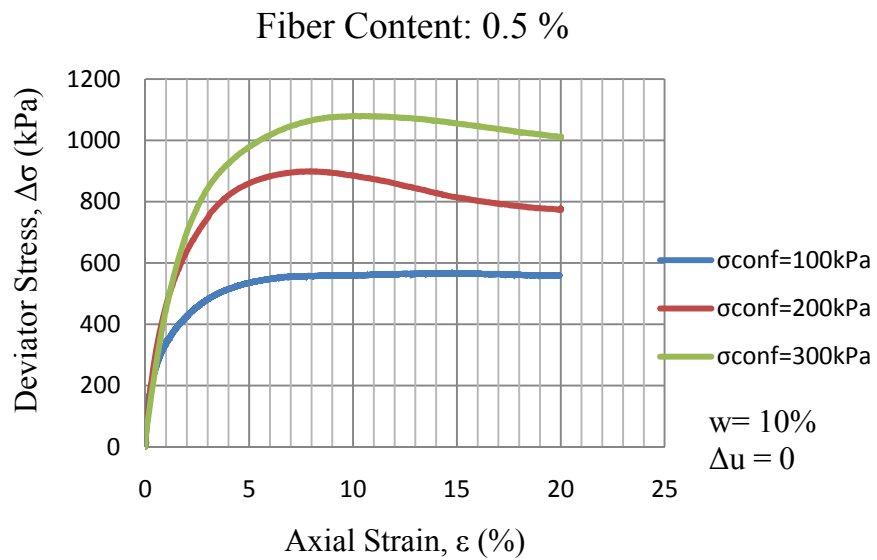
Figure 5.16: Stress-Strain response of unsaturated specimens reinforced with fiber content of 0.5% at different confining stresses
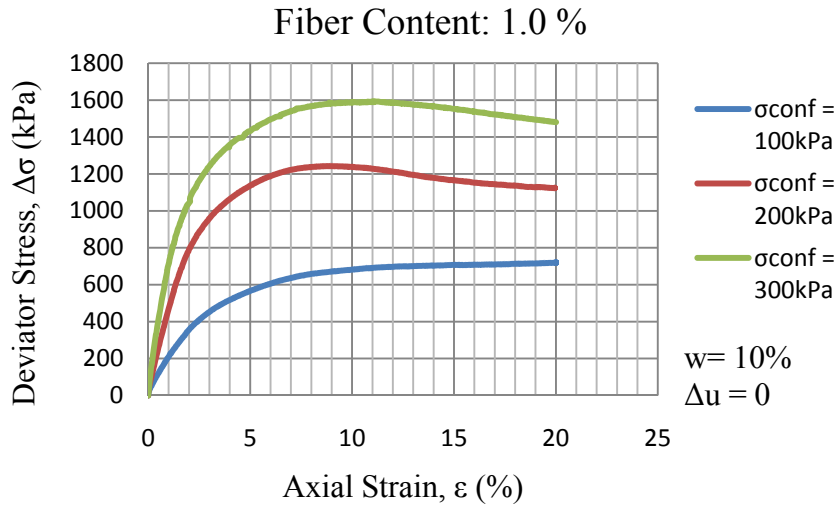
Figure 5.17: Stress-Strain response of unsaturated specimens reinforced with fiber content of 1.0% at different confining stresses

The shear stress-normal stress graph for the unreinforced sand is shown in Figure 5.18. While the cohesion intercept is calculated as zero, the shear strength angle is calculated as 37°.
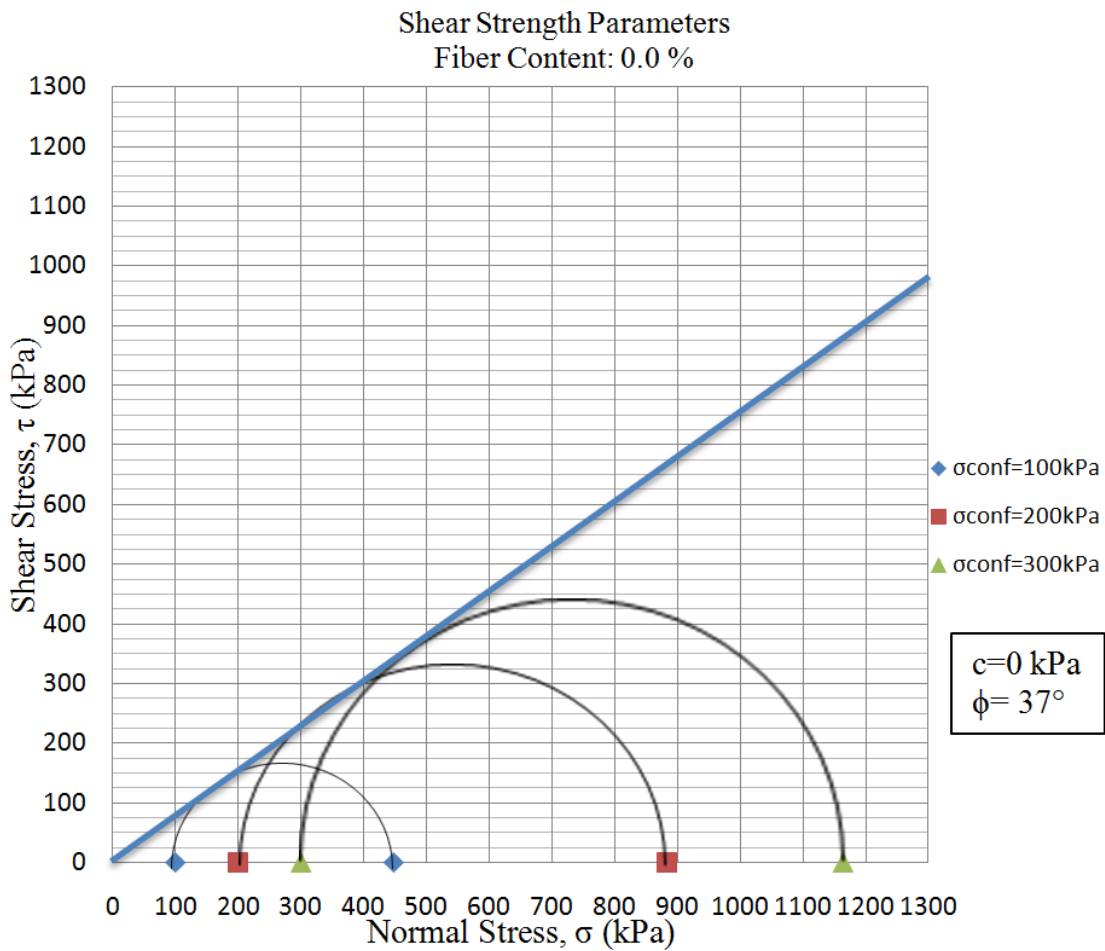
Figure 5.18: Shear stress-Normal stress graph for unreinforced sand

The shear stress-normal stress graph for the sand reinforced with fiber content of 0.5% is shown in Figure 5.19. While the cohesion intercept is calculated as 65kPa the shear strength angle is calculated as 39°. The addition of fiber increased both of the parameters.
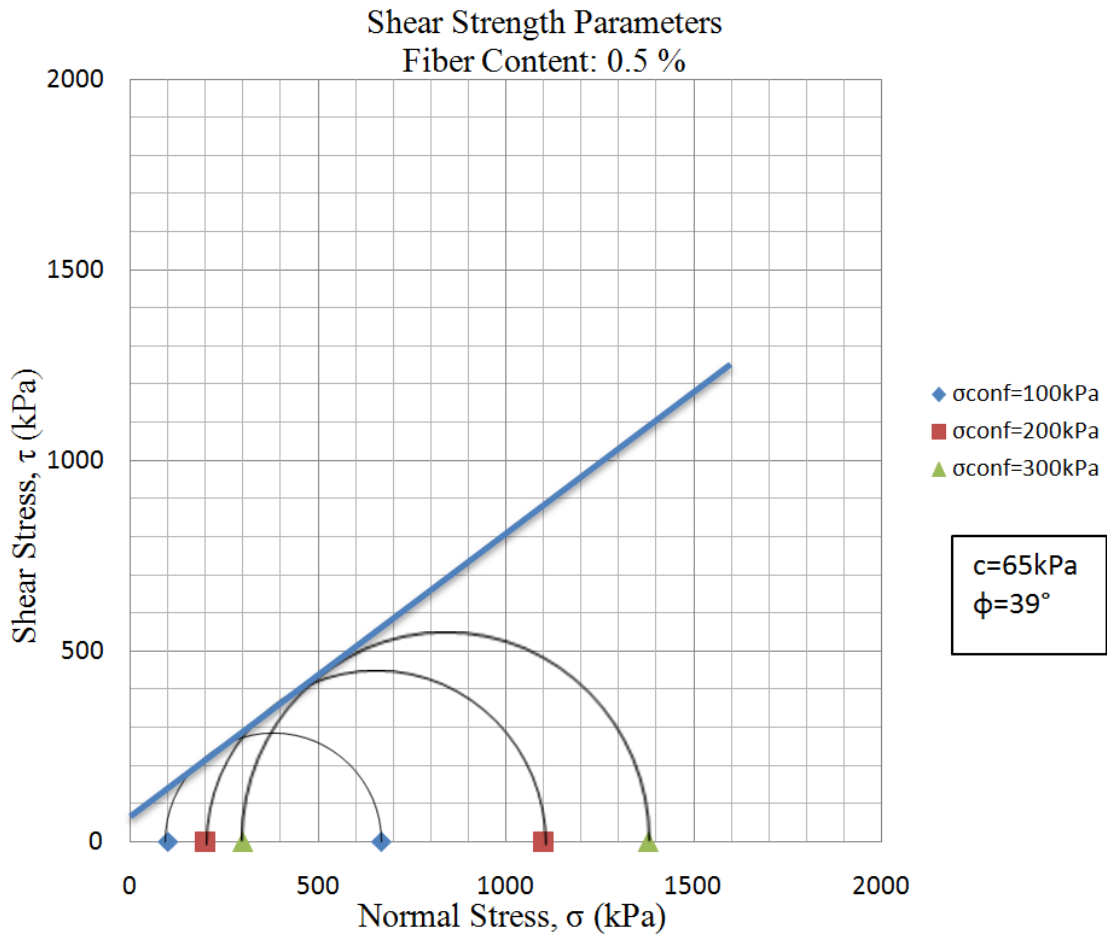
Figure 5.19: Shear stress-Normal stress graph for sand samples reinforced with fiber content of 0.5%

The shear stress-normal stress graph for the sand reinforced with tha fiber content of 1.0% is shown in Figure 5.20. While the cohesion intercept is calculated as 80 kPa, the shear strength angle is calculated as 45°. It is observed that fiber addition of 1.0% of the dry weight of sand at the water content of 10% caused the increase of both the shear strength angle and cohesion intercept. Properties of the samples and test results are presented in the Appendix B.
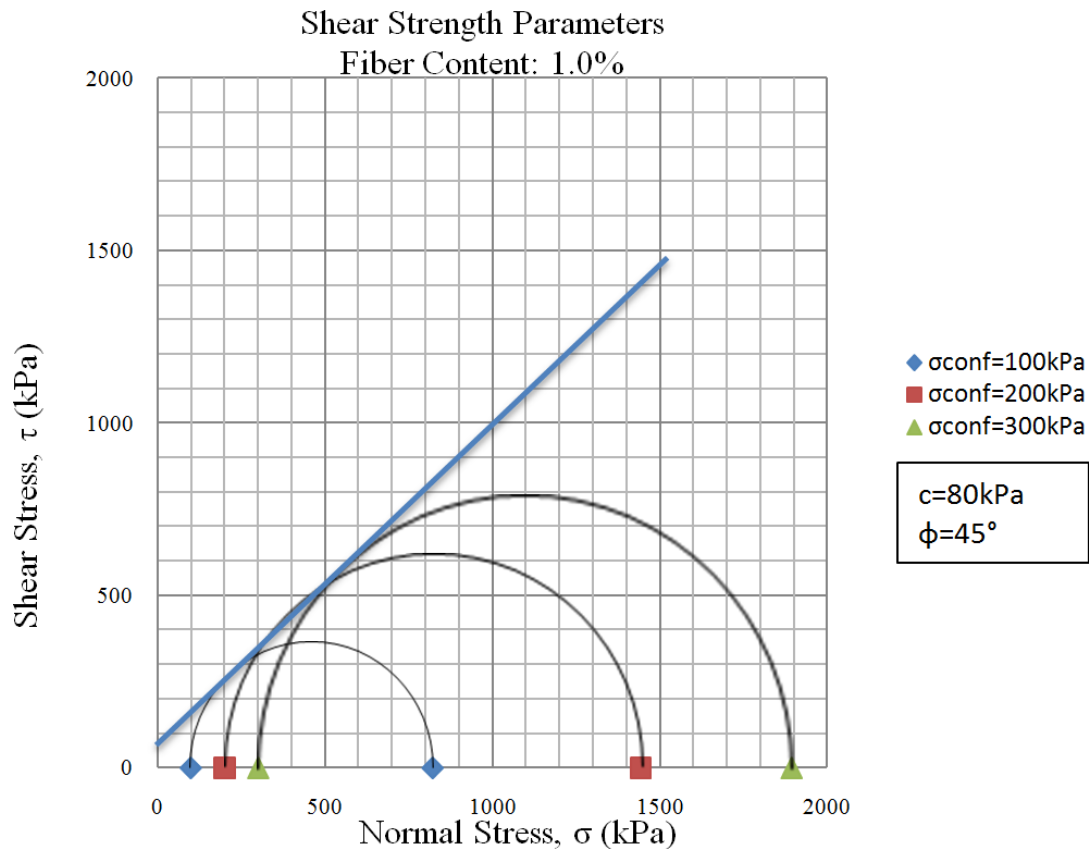
Figure 5.20: Shear stress-Normal stress graph for sand samples reinforced with fiber content of 1.0%

5.3 Direct Shear Test Results

Direct Shear Tests are performed on unreinforced and reinforced sand samples at relative densities around 55 % to determine the effect of fiber inclusions on the shear strength parameters of sand. The samples are prepared at the water content of 10% and fiber contents of 0.5%, 0.75%, 1.0% and 2.0% are tested. Fibers are mixed randomly into the soil. As the fiber content increases, mixing fibers into the sand becomes harder so higher fiber contents are not tested. The strain rate was kept constant at 0.12mm/min for all tests. The shear stress-horizontal displacement curves of unreinforced and reinforced sand specimens are presented in Figure 5.21, Figure 5.22 and Figure 5.23. Under the same normal stress, the peak stress value recorded increases due to fiber addition. In the reinforced specimens, the recorded shear stress values increased with increasing horizonal displacement. Especially under the normal stresses of 200kPa and 300kPa, first the fiber reinforced samples reached a peak value at around horizontal displacement of 5 mm that is followed by a small decrease of the shear stress and a gradual increase due to increace in horizontal stresss. While the effect of fiber inclusions is more apprent for the normal stresses of

100 kPa and 200 kPa, the fiber addition caused an insignificant improvement for the normal stress of 300 kPa.
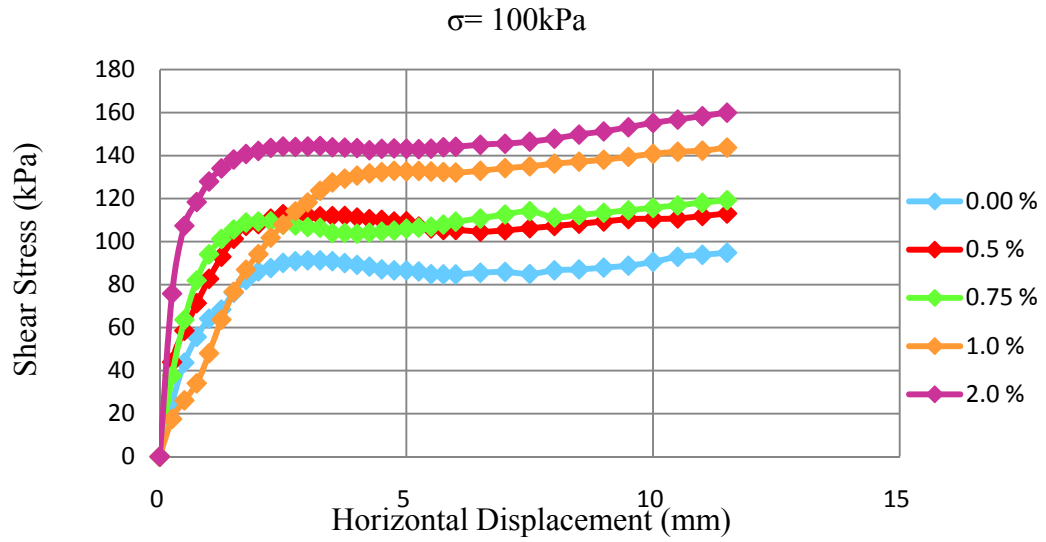
Figure 5.21: Shear stress-horizontal displacement response for unreinforced and reinforced sand samples at the normal stress of σ = 100kPa
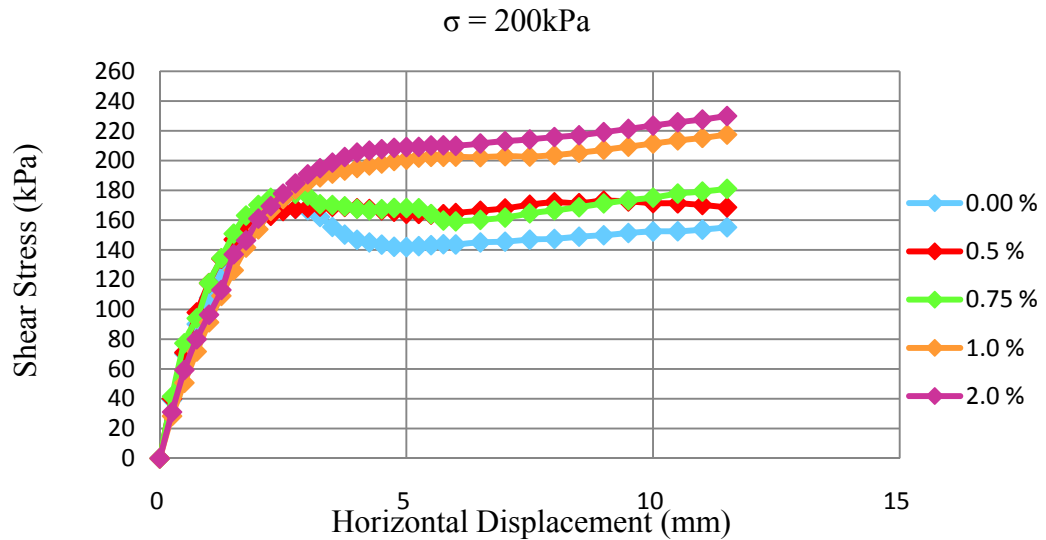
Figure 5.22: Shear stress-horizontal displacement response for unreinforced and reinforced sand samples at the normal stress of σ = 200kPa
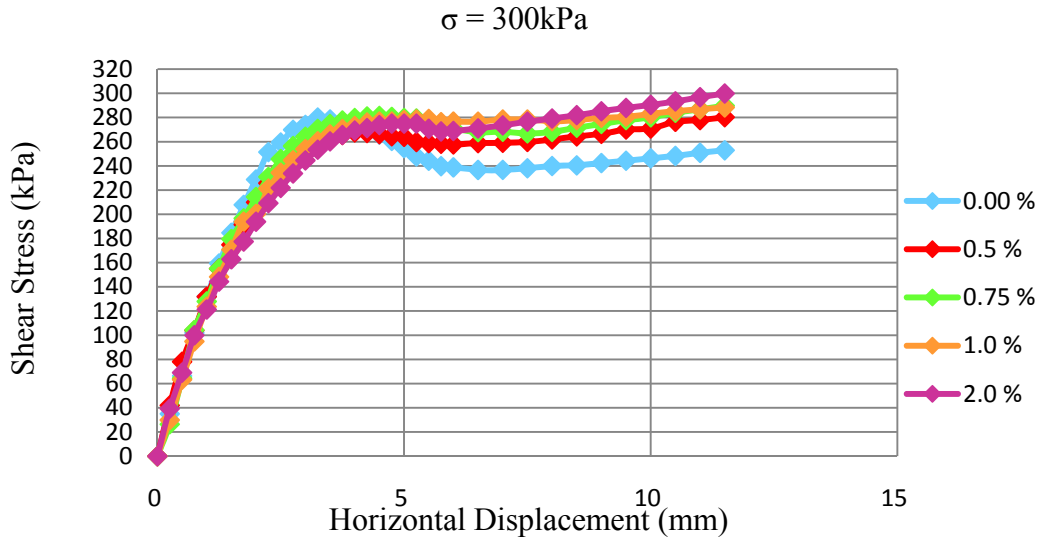
Figure 5.23: Shear stress-horizontal displacement response for unreinforced and reinforced sand samples at the normal stress of σ = 300kPa

In the direct shear test, the peak shear strength angle (ϕ) and cohesion (c) parameters are calculated by linear regression analyses with correlation coefficients that are approximately equal to unity (R^2=0.98-1.00). The summary of the direct shear test results are presented in Table 5.1. It is resulted that the randomly distributed fiber addition affected the shear strength parameters of sand. The shear strength angle decreased, as the fiber content increased from 0.5 % to 2.0%. An apparent cohesion value is calculated for fiber reinforced sand samples. The shear stress-normal stress graphs are presented in Appendix C.

Table 5.1: Direct Shear Test Results for unreinforced and reinforced sand

Fiber Content (%)	σ_{nf} (kPa)	τ_{nf} (kPa)	ϕ (°)	c (kPa)
	123	95		
0.00	209	168	40	0
	317	280		
	104	72		
0.50	235	173	34	24
	371	280		
	12	119		
0.75	247	181	35	25
	371	290		
	124	144		
1.00	247	218	30	70
	371	288		
	124	160		
2.00	247	230	29	90
	371	300		

The peak shear strength angle and cohesion parameters calculated from CU tests that are performed on unsaturated specimens at the water content of 10% (whose results are presented in Figure 5.15-Figure 5.20) are compared with the parameters obtained from direct shear tests. Figure 5.24 shows the shear strength angles calculated for unreinforced and reinforced sand specimens by performing direct shear and CU tests on samples prepared at the water content of 10%. It is presented that the shear strength angle decreases due to fiber addition in direct shear tests.

$y = 12x^2 - 4x + 37$
$R^2 = 1$

$y = 3,1409x^2 - 11,826x + 40,001$
$R^2 = 0,9104$

w= 10%
Direct Shear Test

Static Triaxial Test

Unsaturated Sample
Strain Rate: 1.00mm/min
$\sigma_{conf} = 100kPa$
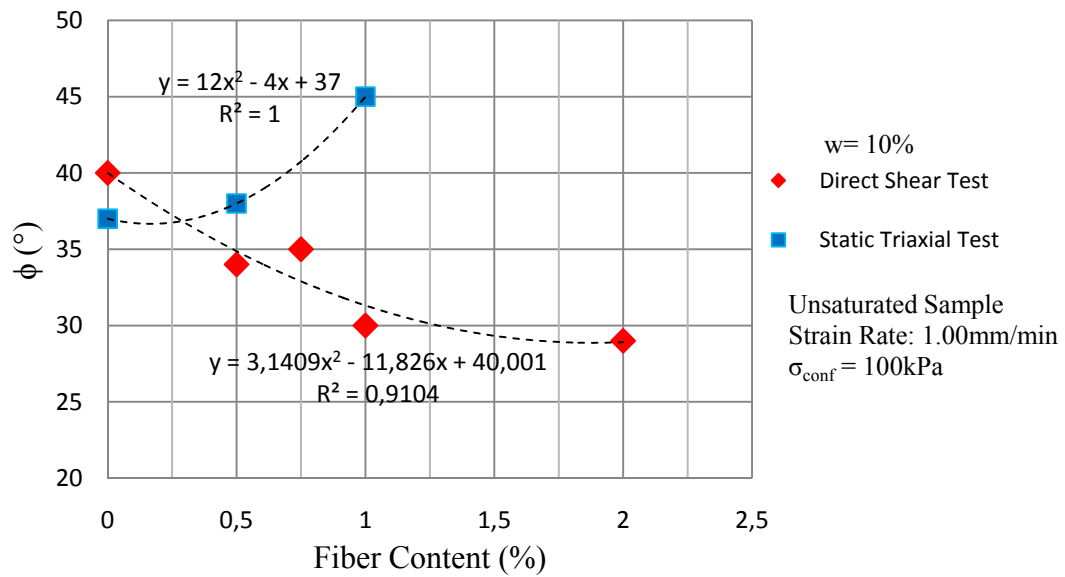
Figure 5.24: Shear strength angles of unreinforced and reinforced sand samples obtained from direct shear tests and CU tests

On the other hand, the shear strength angle values calculated from CU tests increased due to fiber addition. Also the apparent cohesion values are calculated for the unreinforced and reinforced specimens and they are presented in Figure 5.25. For both of the test types, the apparent cohesion value increased significantly due to fiber addition.
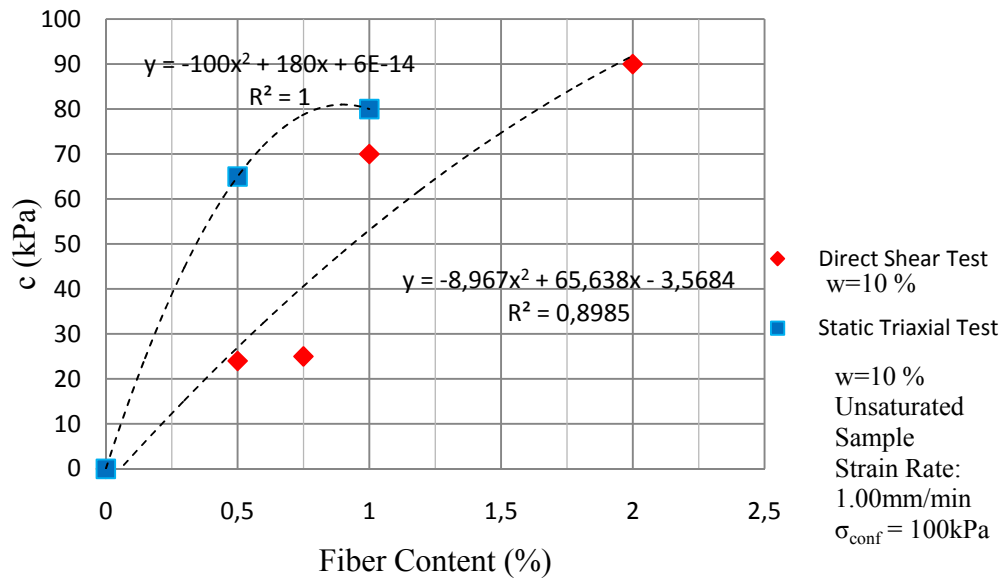
Figure 5.25: Cohesion intercepts of unreinforced and reinforced sand samples obtained from direct shear tests and CU tests

6. CONCLUSION AND RECOMMENDATIONS

Soil improvement with addition of substances is a common ground treatment. According to the additives, the behavior of soil changes significantly. The method of reinforcing soil with fiber inclusions is used for landfills and stabilization of shallow slope failures. Previous studies on randomly distributed fiber reinforced sands show that additions of fibers improves the static behavior of sand and affects the shear strength parameters depending on several factors. These factors are soil type, grain size distribution, gradation, particle shape, fiber type, fiber aspect ratio, fiber content and testing method parameters.

In scope of this thesis, the effects of one type of polypropylene fibers to the dynamic properties and static behavior of sand are searched by performing laboratory tests. The polypropylene fibers are mixed randomly into the poorly graded Akpınar sand at certain water content in order to obtain a fairly uniform mixture. The fibers contents are determined as the percentage of the dry weight of sand. The samples are prepared at relative densities around 55 %.

In the experimental part of the thesis, first triaxial compression test system is used. The saturated specimens are subjected to cyclic triaxial loading and the maximum modulus values (E_{max}) are determined for confining pressure of 30 kPa and 100 kPa. The results of unreinforced sand samples and sand samples that are reinforced with fiber contents of 0.1%, 0.5% and 1.0% are compared. The E_{max} values are calculated from the stress-strain graphs obtained for small strains (order of 10^{-4} and 10^{-6}). The results showed that the Emax value decreased slightly due to fiber addition for both of the confining pressure values. While the E_{max} value decreased from 250MPa to 240MPa for the confining pressure of 100kPa, it decreased from 150MPa to 110MPa for the confining pressure of 30kPa as the fiber content increased up to 1%.

In the second part of the triaxial testing program, undrained static triaxial test is performed on samples confined at 100kPa. The samples are tested at both unsaturated and saturated conditions. For the saturated samples, B coefficient of 0.97 or more is required. The strain controlled static loading is applied at strain rates of

1.00 mm/min, 1.25 mm/min and 1.50 mm/min. The test results of unreinforced samples are compared with the results of sand samples reinforced with fiber contents of 0.1%, 0.5% and 1.0% are compared. According to the results, it is observed that the tested strain rates did not affect the stress-strain graphs in a considerable amount. On the other hand fiber inclusions increased the peak stress value significantly. As the fiber content increased, higher peak stress values are recorded at higher axial strains. The slight increase of the pore water pressure is followed by a significant decrease at higher axial strains. The consolidated drained triaxial test results showed that fiber inclusion improved the stress-strain behavior of sand considerably. On the other hand the strain rates of 0.5 mm/min, 1.0 mm/min and 2.0 mm/min did not show significant effect on the stress-strain response of unreinforced sand. The change in the volume and void ratio is also insignificant.

In addition to these tests, the unsaturated specimens are tested in the triaxial system. The samples are prepared at the water content of 10% and they are not exposed to either CO_2 gas or backpressure. The samples are confined with the cell pressure of 100kPa and tested at the strain rate of 1.00 mm/min. In this case, the peak stress values recorded are very small compared to that of saturated specimens but the peak values are recorded at the same axial stress levels. For determining the shear strength parameters, the unreinforced sand and sand reinforced with fiber content of 1.0% are also tested at confining pressure of 200kPa and 300kPa in unsaturated condition. The unreinforced sand has cohesion intercept (c) of zero and shear strength angle (ϕ) of 37°. For the sand reinforced with the fiber content of 1.0%, the cohesion intercept is calculated as 80kPa and the shear strength angle is calculated as 45°. It shows that fiber addition improved the shear strength parameters of the sand significantly.

In the second part of the experimental study, direct shear tests are performed. The samples are prepared at the relative density around 55% and fiber contents of 0.5%, 0.75%, 1.0% and 2.0% of dry weight of sand is mixed into sand at the water content of 10%. The direct shear tests is performed with a strain rate of 0.12 mm/min. The shear stress-horizontal displacement curves for the normal stresses of 100 kPa, 200 kPa and 300 kPa showed that while the unreinforced samples showed the strain softening behavior, the fiber reinforced samples showed strain hardening behavior. The shear strength parameters are calculated for all samples. As the shear strength

angle decreases due to increasing fiber content, the apparent cohesion value increased in a considerable amount.

Comparing the shear strength parameters calculated from unsaturated triaxial compression tests and direct shear tests, it can be observed that while the apparent cohesion value increases due to fiber addition in both testing methods, the change in the shear strength angle showed differences. Increasing fiber content decreased the shear strength angle calculated from direct shear test results but it increased the shear strength angle calculated from triaxial compression test.

In conclusion, the randomly distributed FORTA MIGHTY-MONO fiber inclusion improved the strength of Akpınar sand considerably. The results obtained from the experimental study are also consistent with the previous researches that are conducted on randomly distributed polypropylene fiber reinforced sands. The method of randomly distributed fiber inclusions can be preferred for landfills, pavements and slope stabilization. The experimental study can also be advanced with an analytical model or additional laboratory tests.

REFERENCES

Babu, G. L. Sivakumar, Vasudevan, A. K., Haldar, S., 2007: Numerical Simulations of Fiber-Reinforced Sand Behavior. *Geotextiles and Geomembranes*, Vol. **26**, No:2, pp. 181-188.

Baker, H., *<http://cee.engr.ucdavis.edu>*, accessed at 10.04.2011

Bathurst, R. J., *< http://www.geosyntheticssociety.org>*, accessed at 12.04.2011

Bowles, J. E., 1997: Foundation Analysis and Design, 5th Edition. Singapore: McGraw-Hill Book Co.

Burke, G. K., 2004:. Jet Grouting Systems: Advantages and Disadvantages. In GeoSupport 2004: Drilled Shafts, Micropiling, Deep Mixing, Remedial Methods, and Special Foundation Systems, American Society of Civil Engineers, pp. 875-886

Chen, C. W., Loehr, J. E, 2008: Undrained and Drained Triaxial Tests of Fiber-Reinforced Sand. Proceedings of the 4th Asian Regional Conference on Geosynthetics, Shangai, pp.114-120

Das, B. M., 2007: Principles of Foundation Engineering. Thomson.

Das, B. M., 2011: Principles of Geotechnical Engineering, 7th Edition. Unites States of America: Cengage Learning.

Das, B. M., 1993: Principles of Soil Dynamics. Boston: PWS-KENT Publishing Company.

Diambra, A., Ibraim, E., Wood, D. Muir, Russell, A. R., 2009: Fibre reinforced sands: experiments and modelling. *Geotextiles and Geomembranes*, Vol. **28**, No.4, pp. 238-250.

Freitag, D. R., 1985: Soil ramdomly reinforced with fibers. *Journal of Geotechnical Engineering* , Vol. **112**, No. 8, pp. 823-826.

Gray, D. H. and Ohashi, H., 1983: Mechanics of fiber reinforced in sand. *Journal of Geotechnical Engineering, ASCE* , Vol. **109**, No. 3, pp. 335-353.

Gunaratme, M., 2006: The Foundation Engineering Handbook. Boca Raton FL: Taylor & Francis Group.

Head, K. H., 1998: Manual of Soil Laboratory Testing. London: Pentech Press.

Ibraim, E., and Fourmont, S., 2006: Behaviour of Sand Reinforced with Fibres. *Soil Stress-Strain Behavior: Measurement, Modeling and Analysis Geotechnical Symposium*, Roma, Italy, pp. 807-818

Ishihara, K., 1996:. Soil Behaviour in Earthquake Geotechnics, Oxford Science Publications.

Karol, R. H., 2003: Chemical Grouting and Soil Stabilization, Revised and Expanded, CRC Press.

Koerner, R. M., 1998: Designing with Goesynthetics. NJ, Prentice Hall.

Kramer, S. L., 1996: Geotechnical Earthquake Engineering. New Jersey, Prentice Hall.

Maher, M. H. and Gray, D. H., 1990: Static response of sands reinforced with randomly distributed fiber. *Journal of Geotechnical Engineering* , Vol. **116**, No. 11, pp. 1661-1677.

Michalowski, R. L. and Cermak, J., 2003: Triaxial Compression of sand reinforced with fibers. *Journal Geotechnical and Geoenvironmental Engineering, ASCE* , Vol. **129**, No. 2, pp. 125-136.

Mitchell, J. K., 1970: In-Place Treatment of Foundation Soils, *Journal of the Soil Mechanics and Foundation Division* , Vol. **96**, No SM1, pp. 73-110.

Pecker, A., 2007: Advanced Earthquake Engineering Analysis. Italy: Springer.

Ranjan, G., Vasan, R. M., Charan, H. D., 1994: Behaviour of plastic-fibre-reinforced sand. *Geotextiles and Geomembranes*, Vol. **13**, No.8, pp. 555-565.

Santoni, R. L., Tingle, J. S., and Webster, S., 2001:. Engineering properties of sand-fiber mixtures for road construction, *Journal of Geotechnical and Geoenvironmental Engineering*, Vol. **127**, No. 3, pp. 258-268.

Sawicki, A., and Swidzinski, W., 1998: Elastic moduli of non-cohesive particulate materials. *Powder Technology* , pp. 24-32.

Seiken Inc.*, Pneumatic Cyclic Triaxial Test Apparatus, Two Unit Type Model DTC-311 Instruction Manual.*

Silver, M. L., 1976: Cyclic triaxial strength of standard test sand, *Journal of Geotechnical Engineering Divison,* ASCE, Vol. **102**, GT5

Srbulov, M., 2008: Geotechnical Earthquake Engineering Simplified Analysis with Case Studied and Examples. United Kingdom: Springer.

Tatsuoka, F., Teachavarorasinskun, S., Dong, J., Kohata, Y., Sato, T. 1994: Importance of measuring local strains in cyclic triaxial tests on granular materials in *Dynamic Geotechnical Testing II*, Eds. R. J. Ebelhar, V. P. Drenevich, B. L. Kutter, Philadelphia, ASTM, pp.288-302

Terzaghi, K., Peck, R. B., Mesri, G., 1996: *S*oil Mechanics in Engineering Practice. Canada: John Wiley& Sons. Inc.

Welsh and Burke, 1991: Jet Grouting-Uses for Soil Improvement, *Geotechnical Engineering Congresss*, American Society of Civil Engineers, GSP 27, pp.334-345

Waldron, L. J., 1977: Shear resistance of root-permeated homogeneous and statified soil, Soil Science Society of America Proceedings, **41**, 843-849

Yetimoglu, T., and Salbas, O., 2003: A study on shear strength of sands reinforced with randomly distributed discrete fiber. *Geotextiles and Geomembranes*, Vol. **21**, No.2, pp. 103-110.

APPENDICES

APPENDIX A : Cyclic Triaxial Test Results

APPENDIX B: Static Triaxial Test Results

APPENDIX C: Direct Shear Test Results

APPENDIX A

Table A. 1: Properties of Test No 8

Sample No	Cell Pressure (kPa)	Back Pressure (kPa)	Confining Pressure (kPa)	Fiber Content (%)	Saturation (%)	Relative Density (%)
8	330	300	30	0	97.5	55
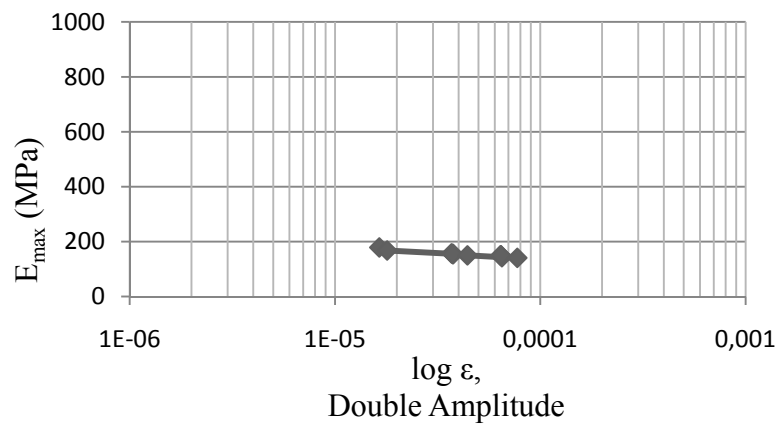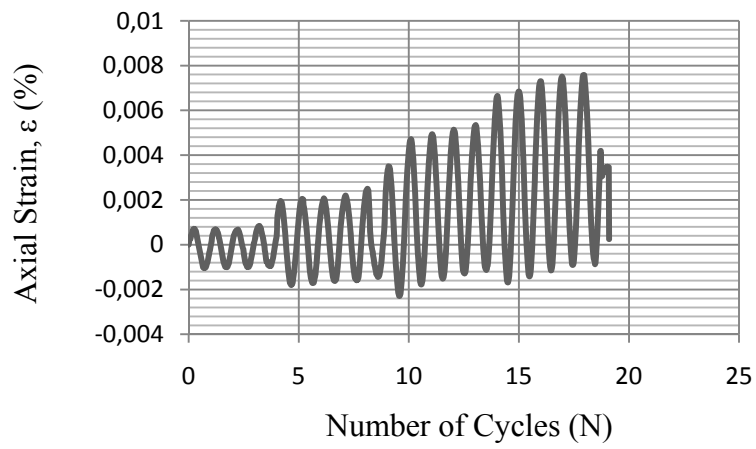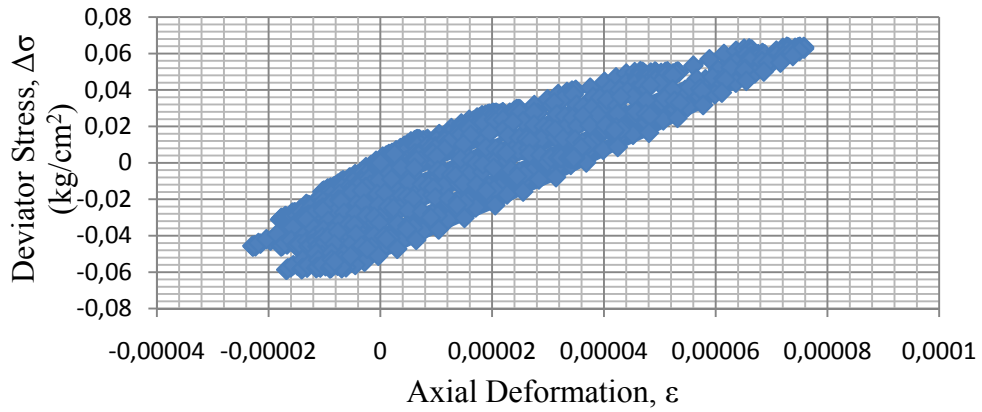
Figure A. 1: Test Results for Test No 8

Properties of Tests No 9

Sample No	Cell Pressure (kPa)	Back Pressure (kPa)	Confining Pressure (kPa)	Fiber Content (%)	Saturation (%)	Relative Density (%)
8	500	400	100	0	97.5	55
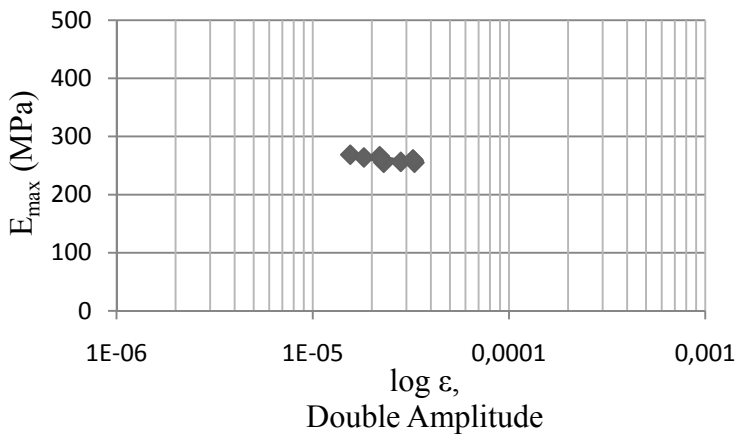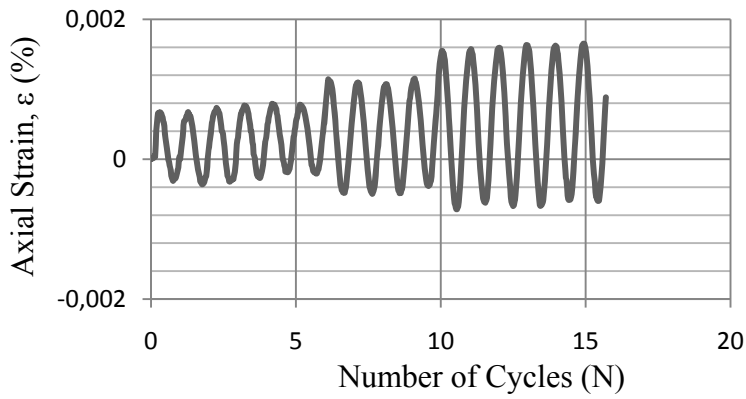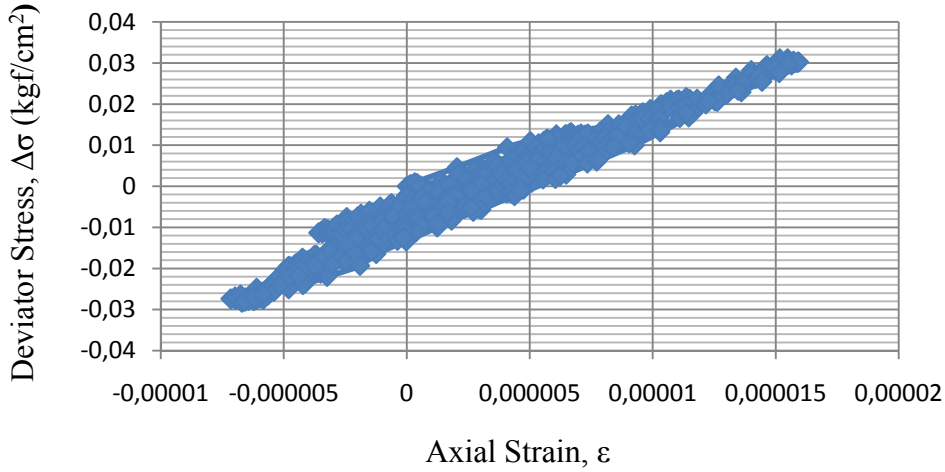
Figure A. 2: Test Results for Test No 9

Table A. 3: Properties of Sample No 7

Sample No	Cell Pressure (kPa)	Back Pressure (kPa)	Confining Pressure (kPa)	Fiber Content (%)	Saturation (%)	Relative Density (%)
7	330	300	30	0.1	98	57
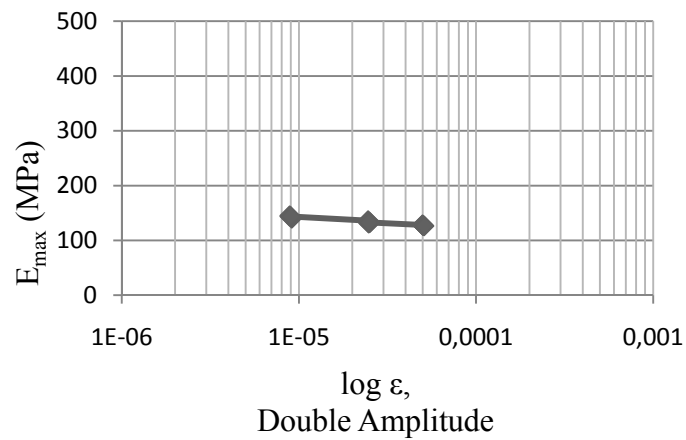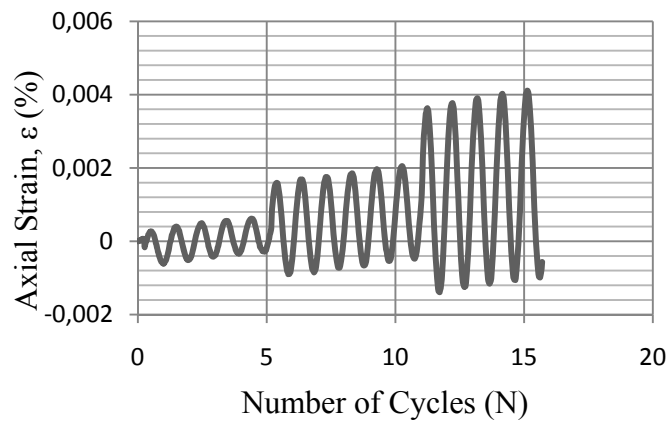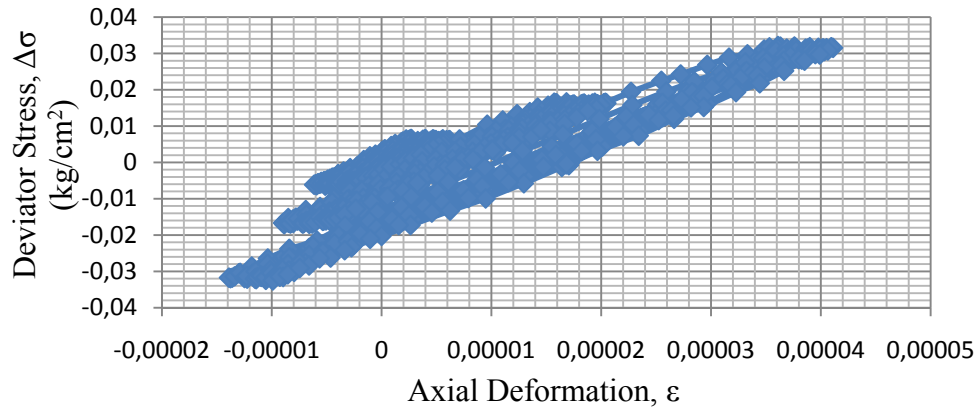
Figure A. 3: Test Results for Test No 7

Table A. 4: Properties of Test No 10

Sample No	Cell Pressure (kPa)	Back Pressure (kPa)	Confining Pressure (kPa)	Fiber Content (%)	Saturation (%)	Relative Density (%)
7	500	400	100	0.1	98	57
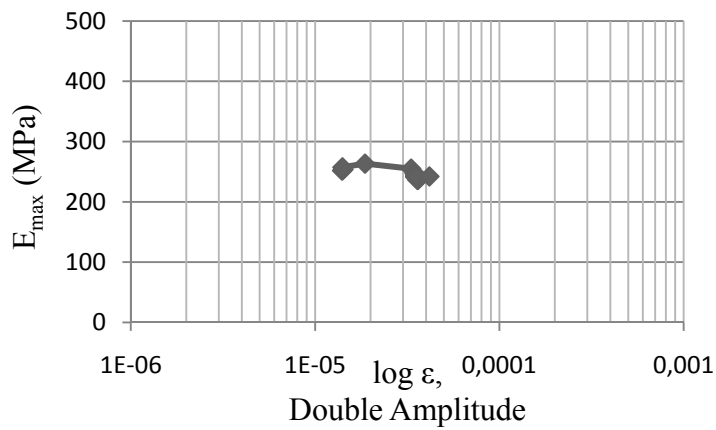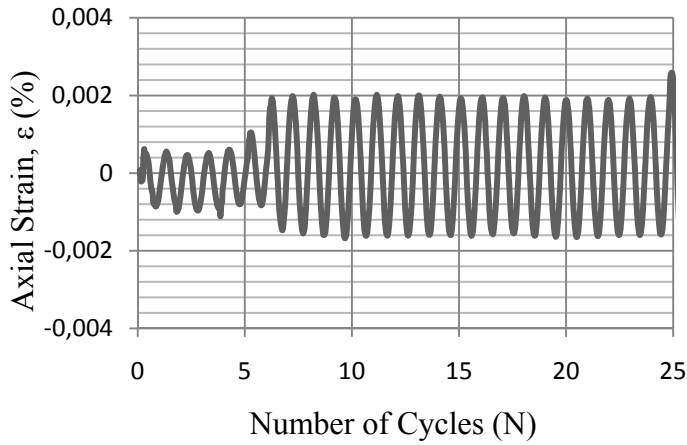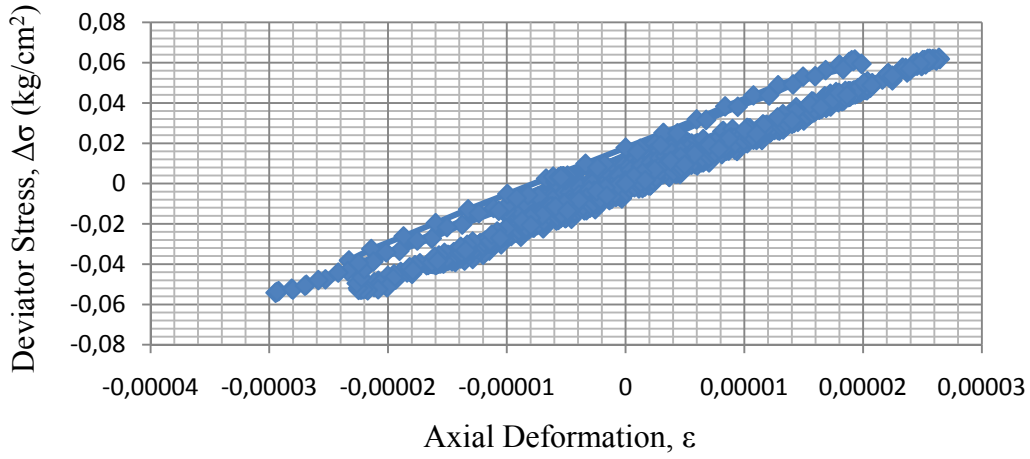
Figure A. 4: Test Results for Test No 10

Table A. 5: Properties of Test No 5

Sample No	Cell Pressure (kPa)	Back Pressure (kPa)	Confining Pressure (kPa)	Fiber Content (%)	Saturation (%)	Relative Density (%)
5	330	300	30	0.5	97	55
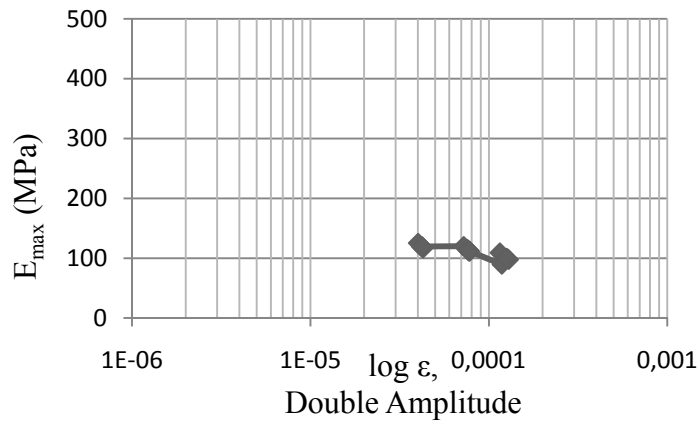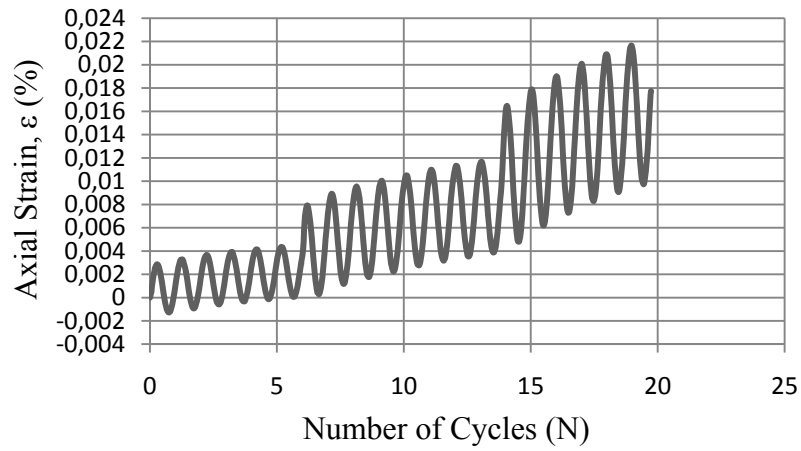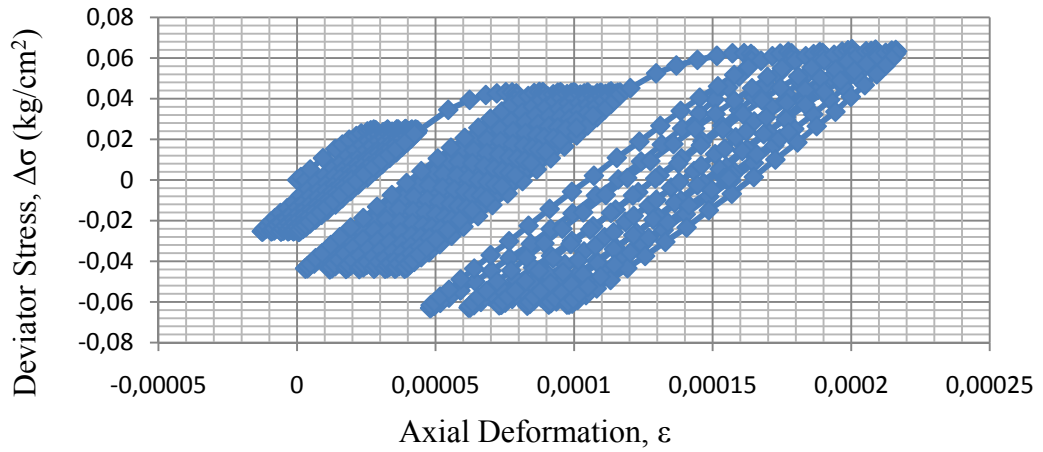
Figure A. 5: Test Results for Test No 5

Table A. 6: Properties of Test No 11

Sample No	Cell Pressure (kPa)	Back Pressure (kPa)	Confining Pressure (kPa)	Fiber Content (%)	Saturation (%)	Relative Density (%)
5	500	400	100	0.5	97	55
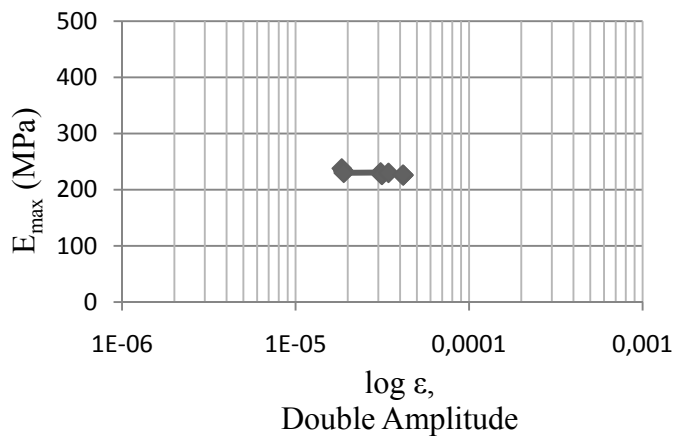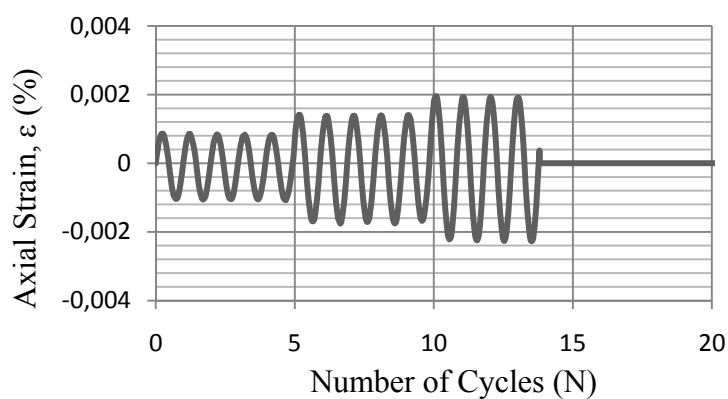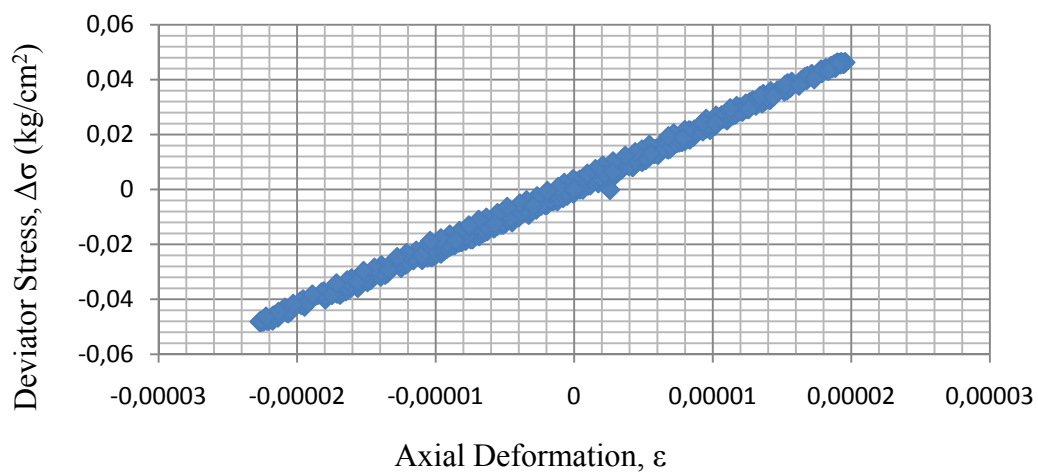
Figure A. 6: Test Results for Test No 11

Table A. 7: Properties of Test No 1

Sample No	Cell Pressure (kPa)	Back Pressure (kPa)	Confining Pressure (kPa)	Fiber Content (%)	Saturation (%)	Relative Density (%)
1	330	300	30	1.0	97	57
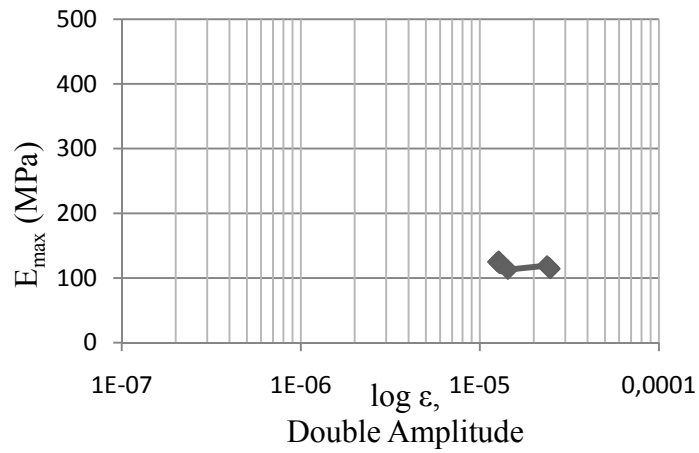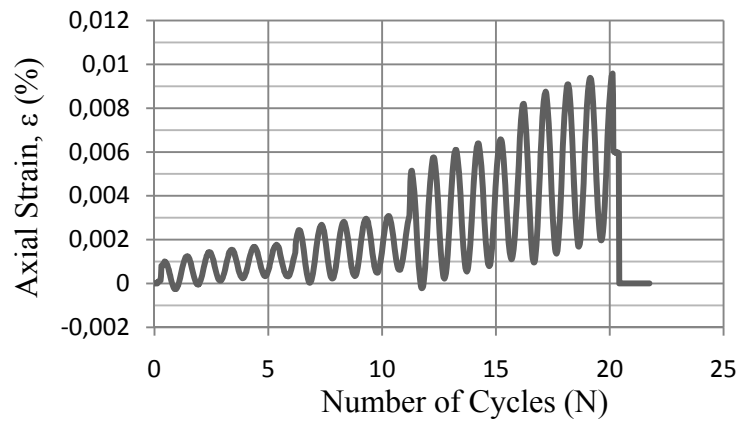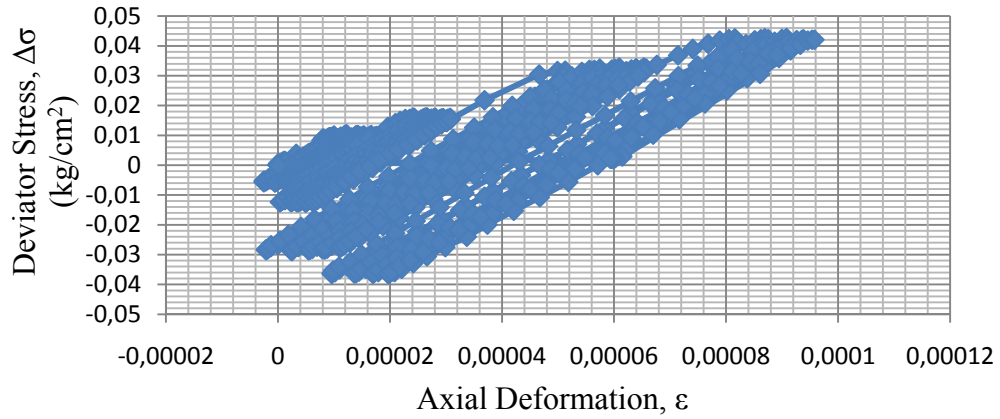
Figure A. 7: Test Results for Test No 1

Table A. 8: Properties of Test No 2

Sample No	Cell Pressure (kPa)	Back Pressure (kPa)	Confining Pressure (kPa)	Fiber Content (%)	Saturation (%)	Relative Density (%)
1	500	400	100	1.0	97	57
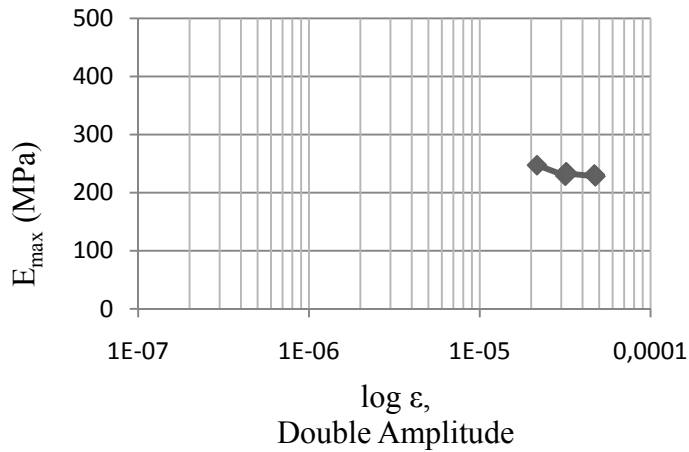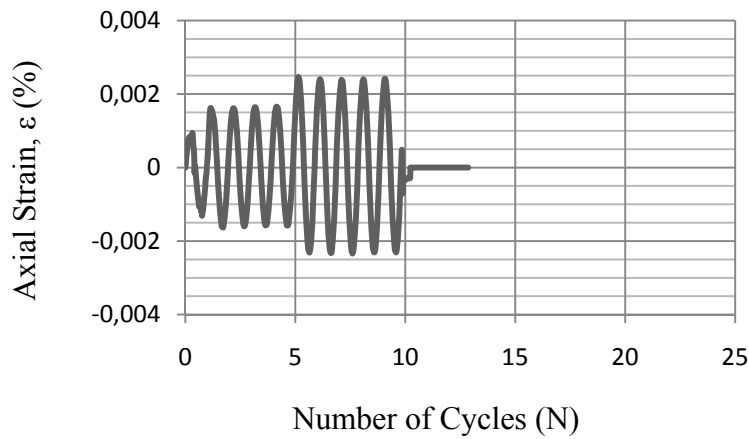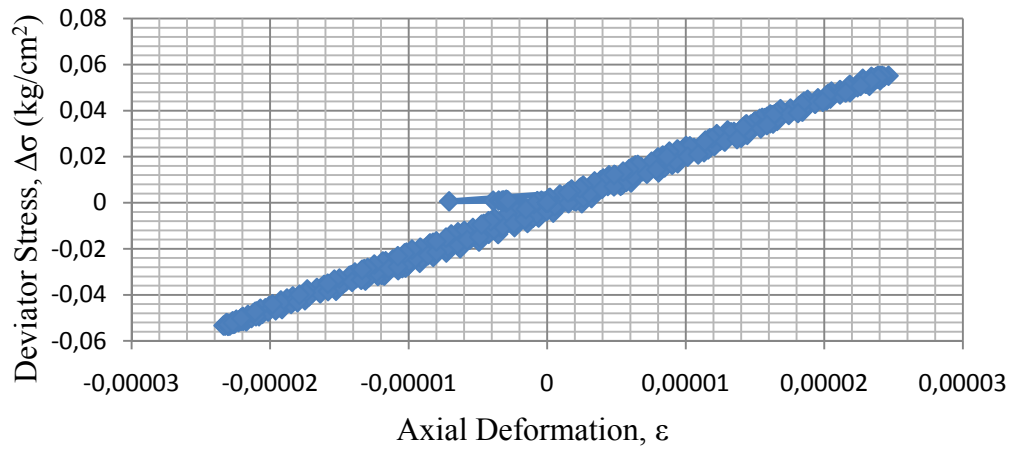
Figure A. 8: Test Results for Test No 2

Table B. 1: Properties of Sample No 75

Sample No	75
$A_0 \, (\text{cm}^2)$	19.37
$V_0 \, (\text{cm}^3)$	193.48
$\gamma_{dry} \, (\text{g/cm}^3)$	1.60
Cell Pressure (kPa)	500
Back Pressure (kPa)	400
Confining Pressure (kPa)	100
Fiber Content (%)	0
Saturation(%)	97.5
Relative Density, Dr (%)	55
Strain rate (mm/min)	1.00
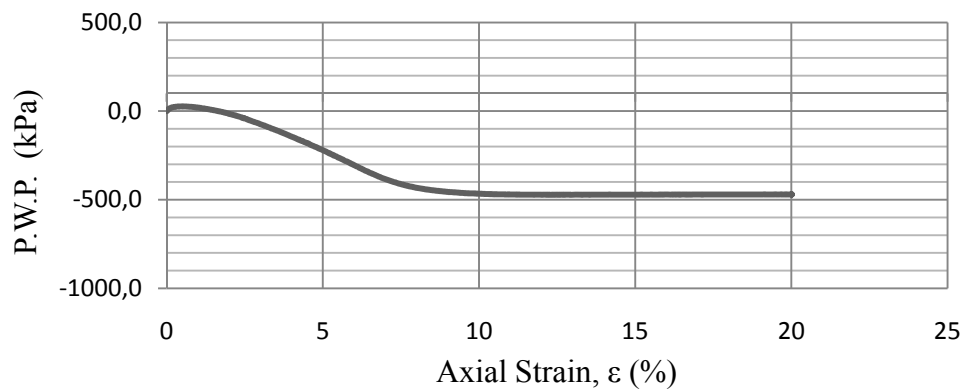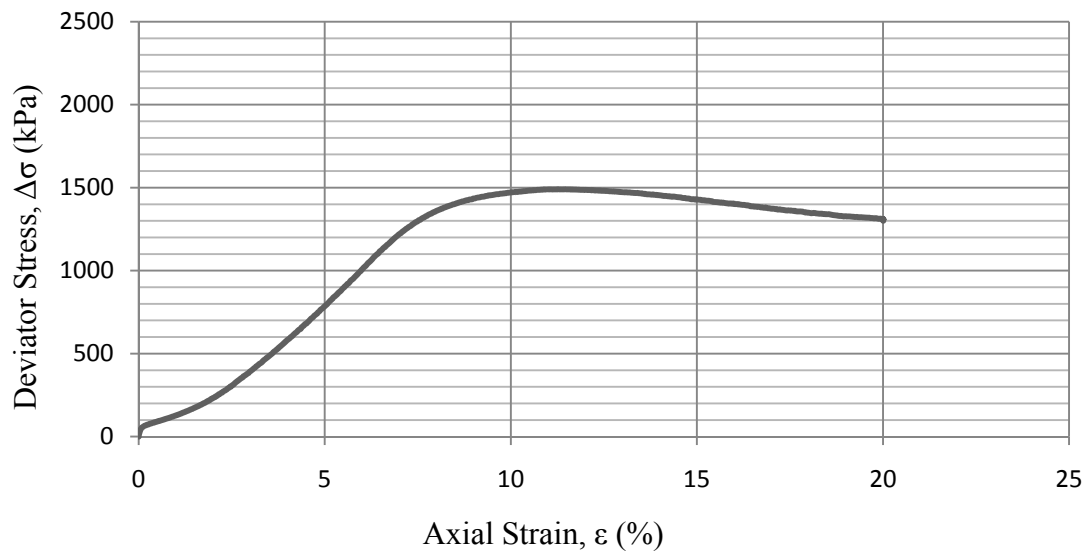
Figure B. 1: Test Results for Sample No 75

Table B. 2: Properties of Sample No 44

Sample	44
$A_0 \, (\text{cm}^2)$	19.39
$V_0 \, (\text{cm}^3)$	193.55
$\gamma_{dry} \, (\text{g/cm}^3)$	1.60
Cell Pressure (kPa)	500
Back Pressure (kPa)	400
Confining Pressure (kPa)	100
Fiber Content (%)	0
Saturation(%)	98
Relative Density, Dr (%)	55
Strain rate (mm/min)	1.25
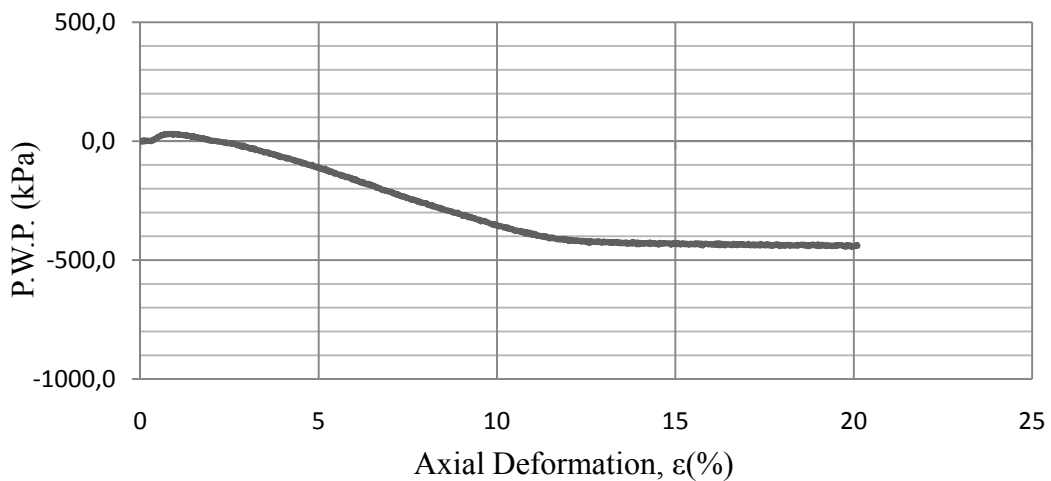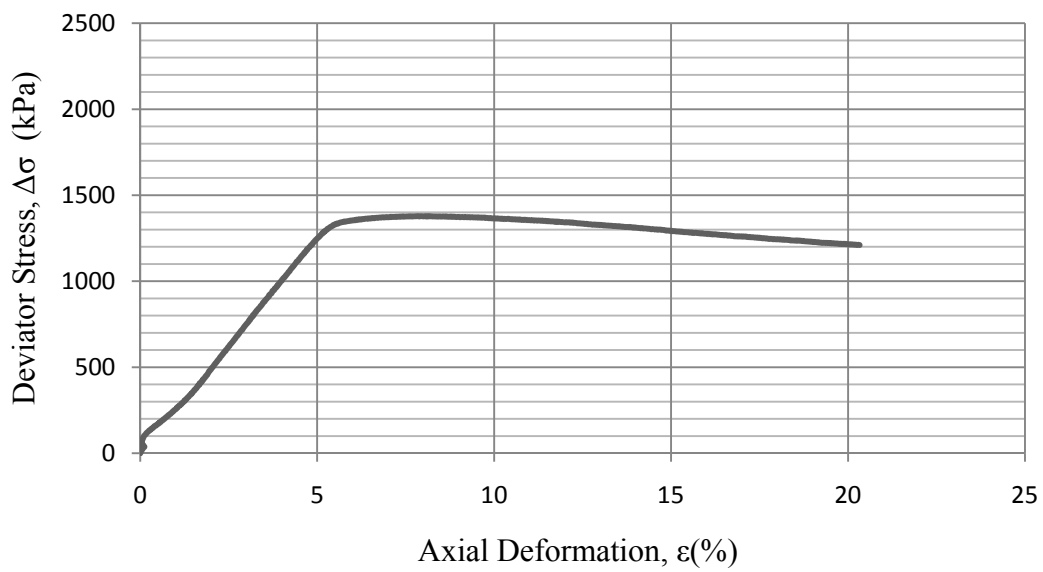
Figure B. 2: Test Results for Sample No 44

Table B. 3: Properties of Sample No 73

Sample	73
A_0 (cm^2)	19.37
V_0 (cm^3)	193.49
γ_{dry} (g/cm^3)	1.60
Cell Pressure (kPa)	500
Back Pressure (kPa)	400
Confining Pressure (kPa)	100
Fiber Content (%)	0
Saturation (%)	97
Relative Density, Dr (%)	55
Strain rate (mm/min)	1.50
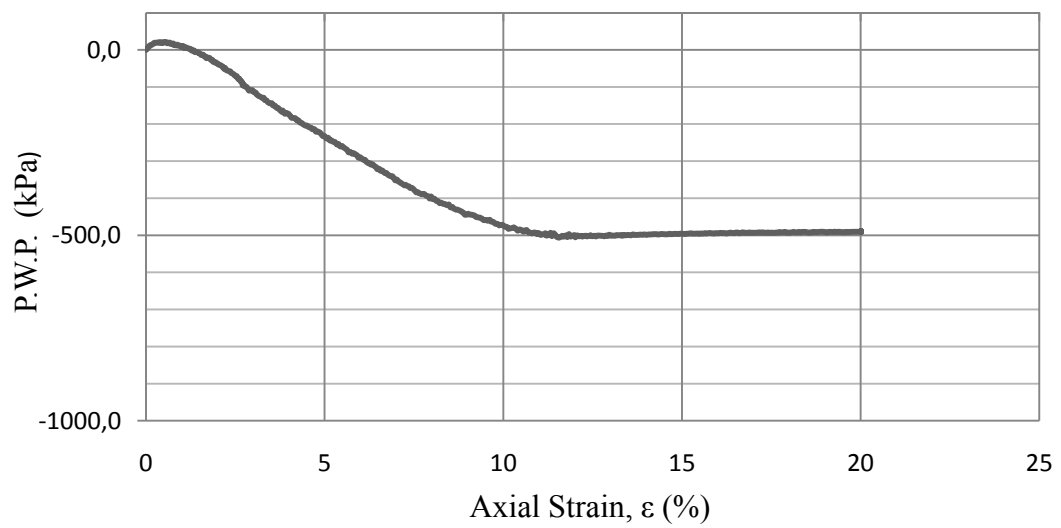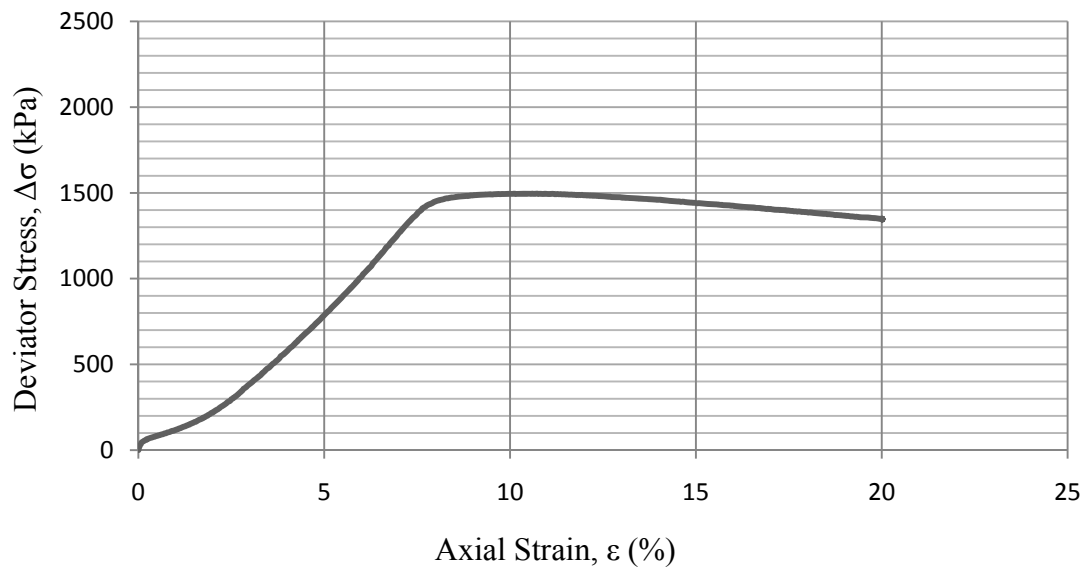
Figure B. 3: Test Results for Sample No 73

Table B. 4: Properties of Sample No 55

Sample No	55
A_0 (cm^2)	19.37
V_0 (cm^3)	193.23
γ_{dry} (g/cm^3)	1.604
Cell Pressure (kPa)	500
Back Pressure (kPa)	400
Confining Pressure (kPa)	100
Fiber Content (%)	0.1
Saturation(%)	98
Relative Density, Dr (%)	56
Strain rate (mm/min)	1.00
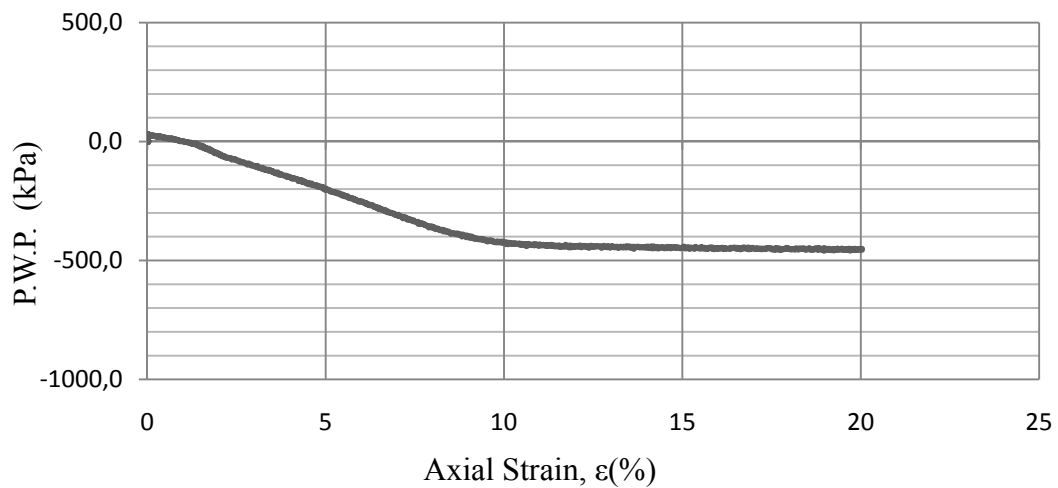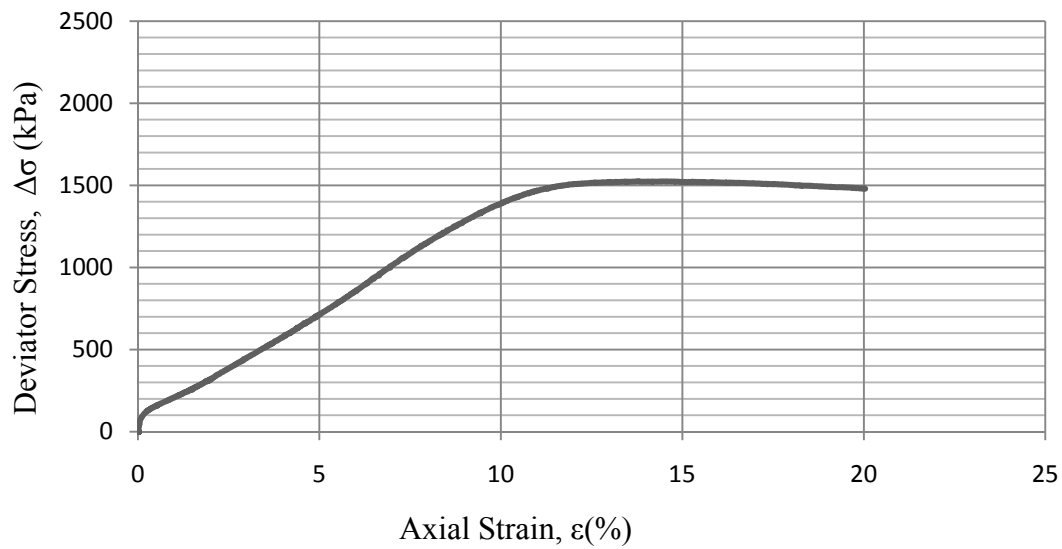
Figure B. 4: Test Results for Sample No 55

Table B. 5: Properties of Sample No 72

Sample No	72
A_0 (cm^2)	19.42
V_0 (cm^3)	193.56
γ_{dry} (g/cm^3)	1.603
Cell Pressure (kPa)	500
Back Pressure (kPa)	400
Confining Pressure (kPa)	100
Fiber Content (%)	0.1
Saturation(%)	98
Relative Density, Dr (%)	55
Strain rate (mm/min)	1.25
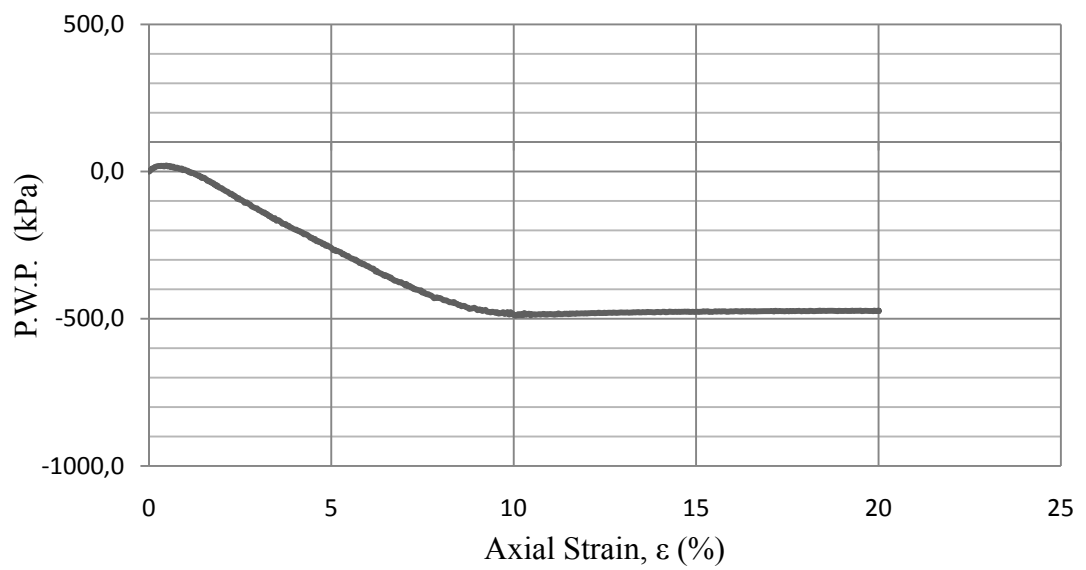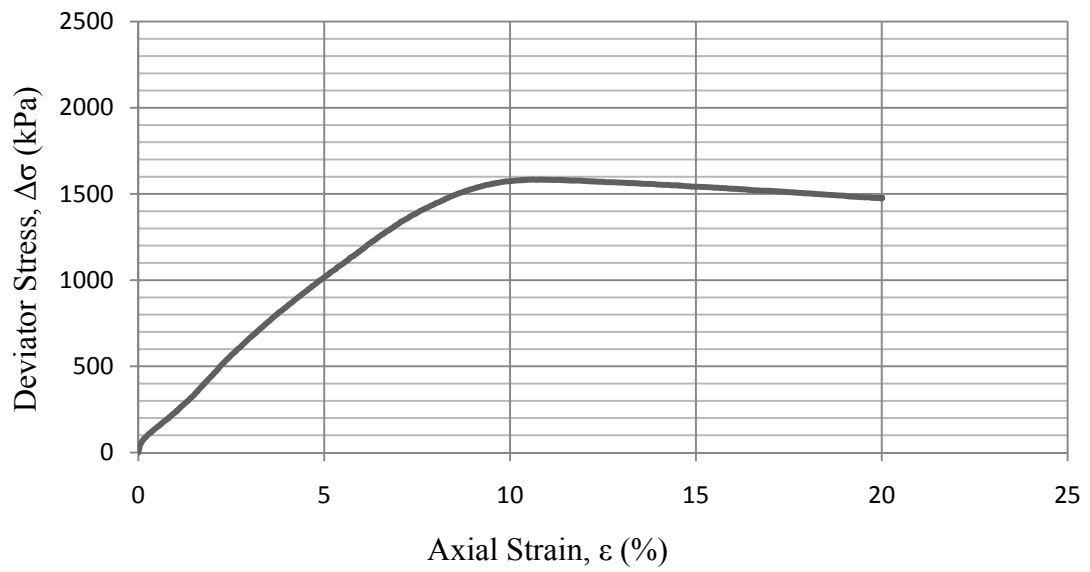
Figure B. 5: Test Results for Sample No 72

Table B. 6 : Properties of Sample No 78

Sample No	78
$A_0 \, (\text{cm}^2)$	19.39
$V_0 \, (\text{cm}^3)$	193.36
$\gamma_{dry} \, (\text{g/cm}^3)$	1.605
Cell Pressure (kPa)	500
Back Pressure (kPa)	400
Confining Pressure (kPa)	100
Fiber Content (%)	0.1
Saturation(%)	98
Relative Density, Dr (%)	56
Strain rate (mm/min)	1.50
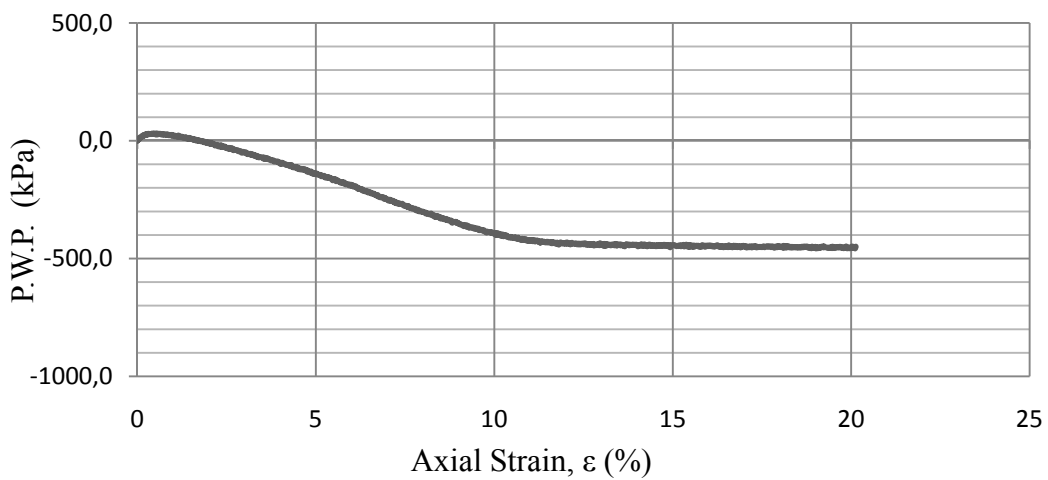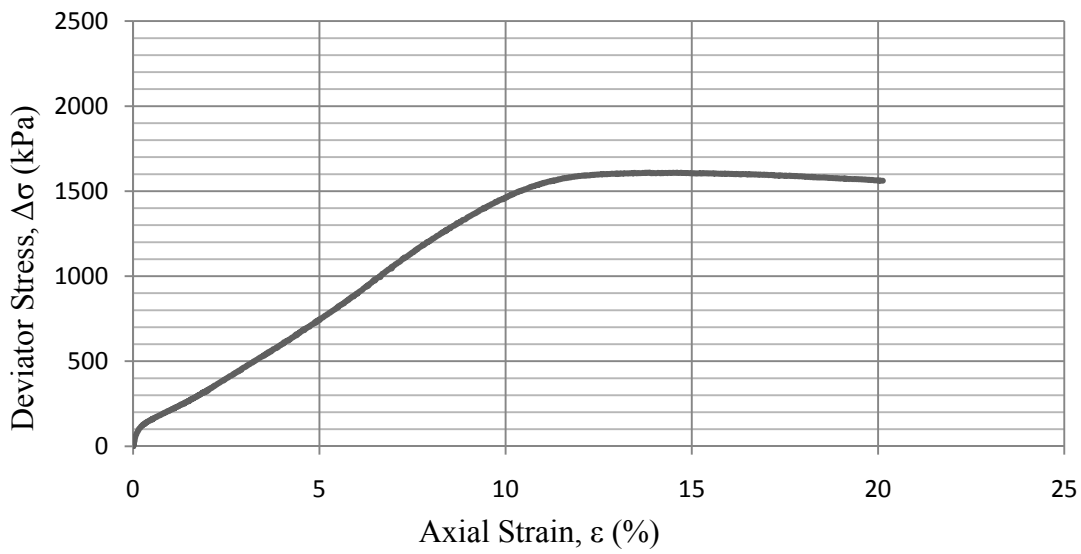
Figure B. 6 : Test Results for Sample No 78

Table B. 7 : Properties of Sample No 56

Sample No	56
$A_0\,(cm^2)$	19.44
$V_0\,(cm^3)$	194.08
$\gamma_{dry}\,(g/cm^3)$	1.602
Cell Pressure (kPa)	500
Back Pressure (kPa)	400
Confining Pressure (kPa)	100
Fiber Content (%)	0.5
Saturation(%)	98
Relative Density, Dr (%)	57
Strain rate (mm/min)	1.00
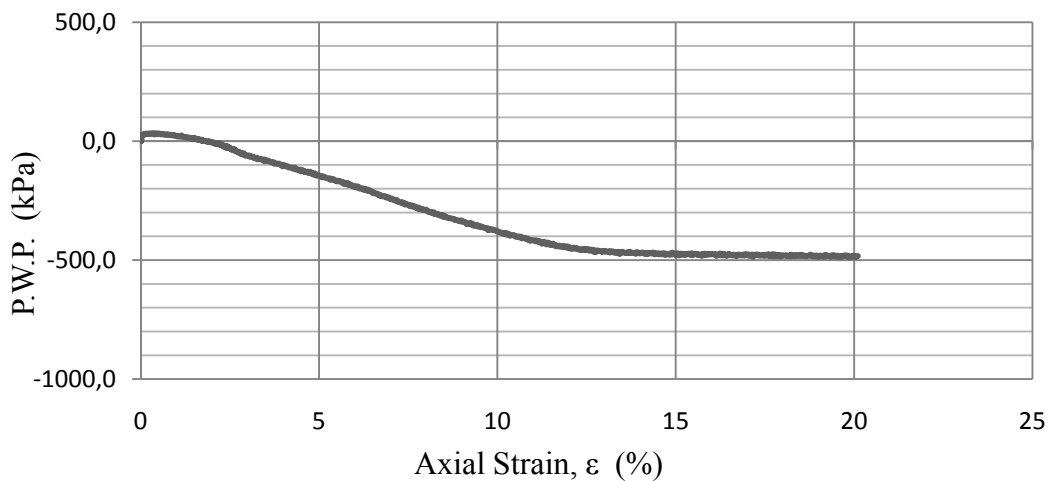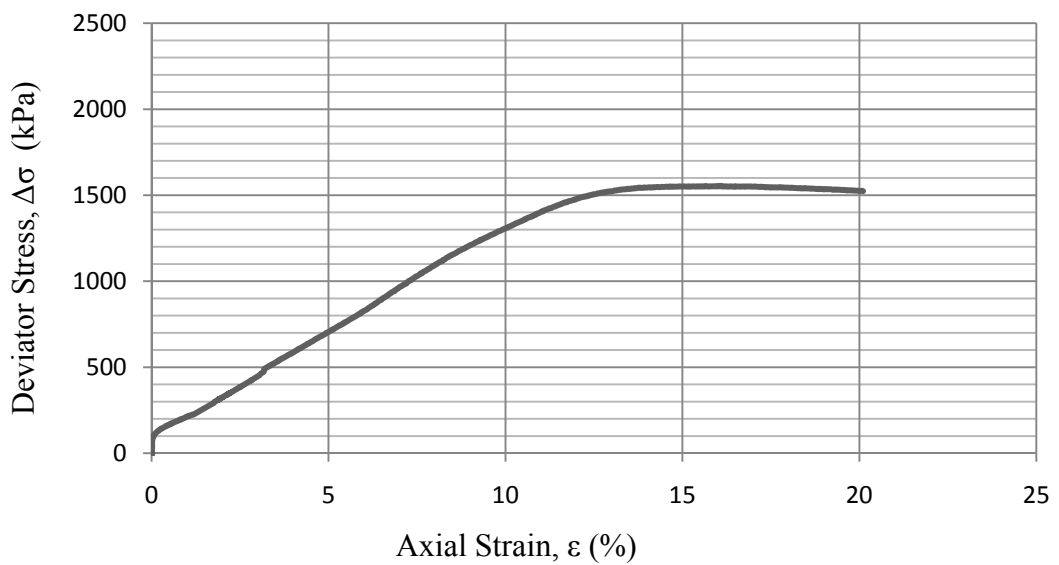
Figure B. 7 : Test Results for Sample No 56

Table B. 8 : Properties of Sample No 68

Sample No	68
A_0 (cm^2)	19.38
V_0 (cm^3)	193.55
γ_{dry} (g/cm^3)	1.612
Cell Pressure (kPa)	500
Back Pressure (kPa)	400
Confining Pressure (kPa)	100
Fiber Content (%)	0.5
Saturation(%)	98
Relative Density, Dr (%)	58
Strain rate (mm/min)	1.25
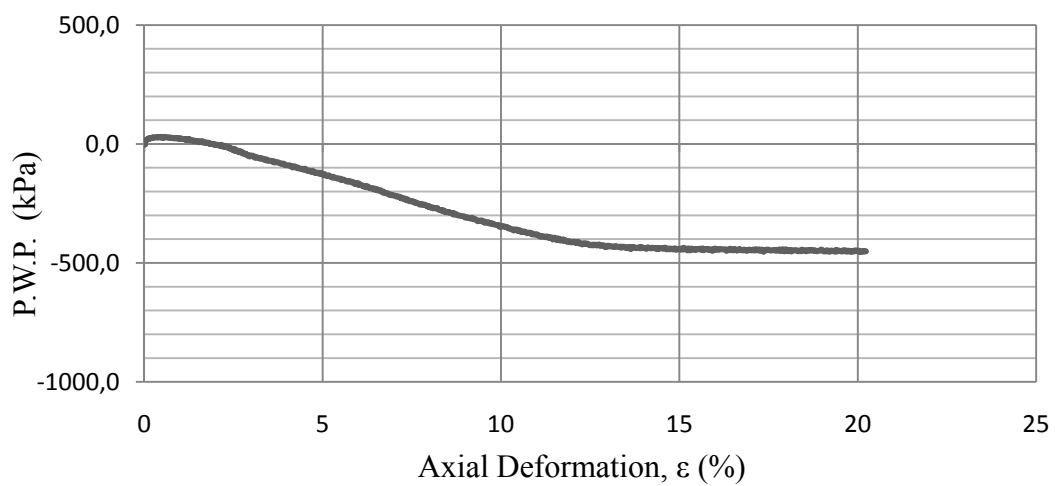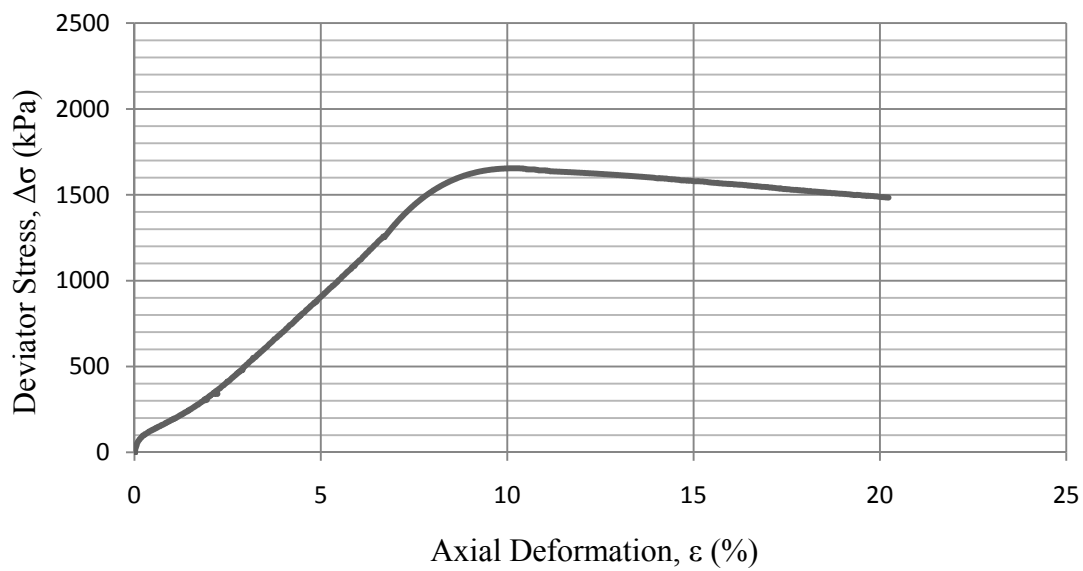
Figure B. 8 : Test Results for Sample No 68

114

Table B. 9 : Properties of Sample No 57

Sample No	57
$A_0 (cm^2)$	19.44
$V_0 (cm^3)$	194.27
$\gamma_{dry} (g/cm^3)$	1.606
Cell Pressure (kPa)	500
Back Pressure (kPa)	400
Confining Pressure (kPa)	100
Fiber Content (%)	0.5
Saturation(%)	98
Relative Density, Dr (%)	56
Strain rate (mm/min)	1.50
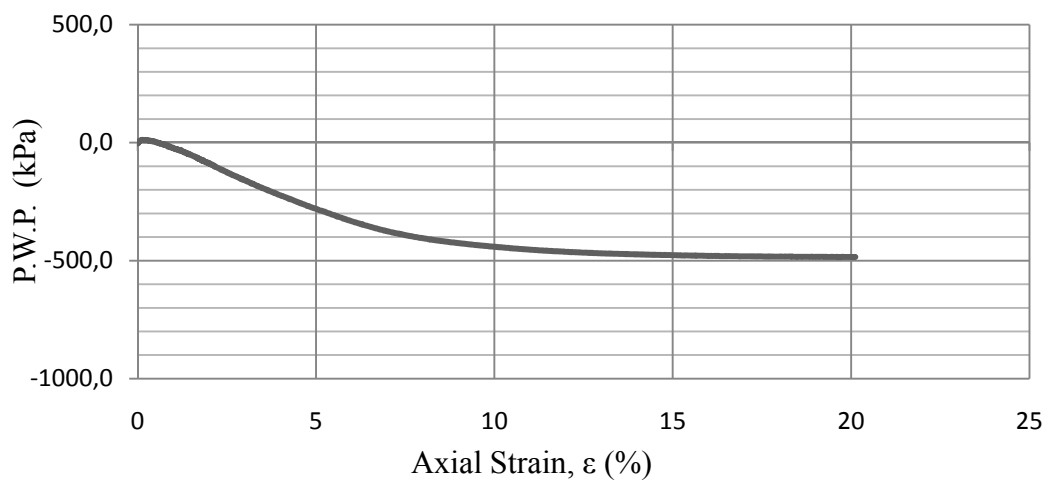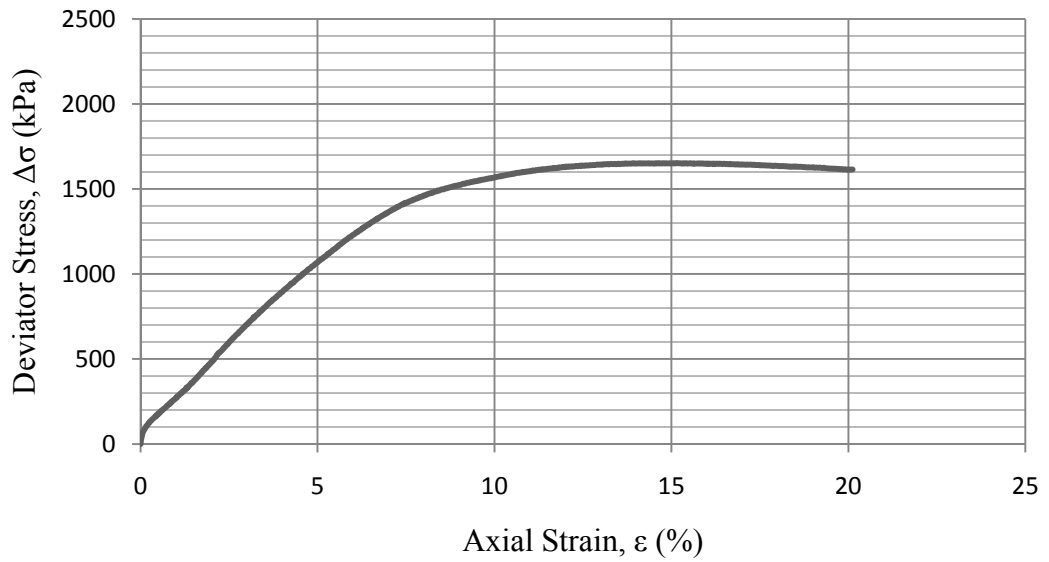
Figure B. 9 : Test Results for Sample No 57

Table B. 10 : Properties of Sample No 47

Sample No	47
A_0 (cm^2)	19.43
V_0 (cm^3)	194.00
γ_{dry} (g/cm^3)	1.613
Cell Pressure (kPa)	500
Back Pressure (kPa)	400
Confining Pressure (kPa)	100
Fiber Content (%)	1.0
Saturation (%)	97
Relative Density, Dr (%)	58
Strain rate (mm/min)	1.00
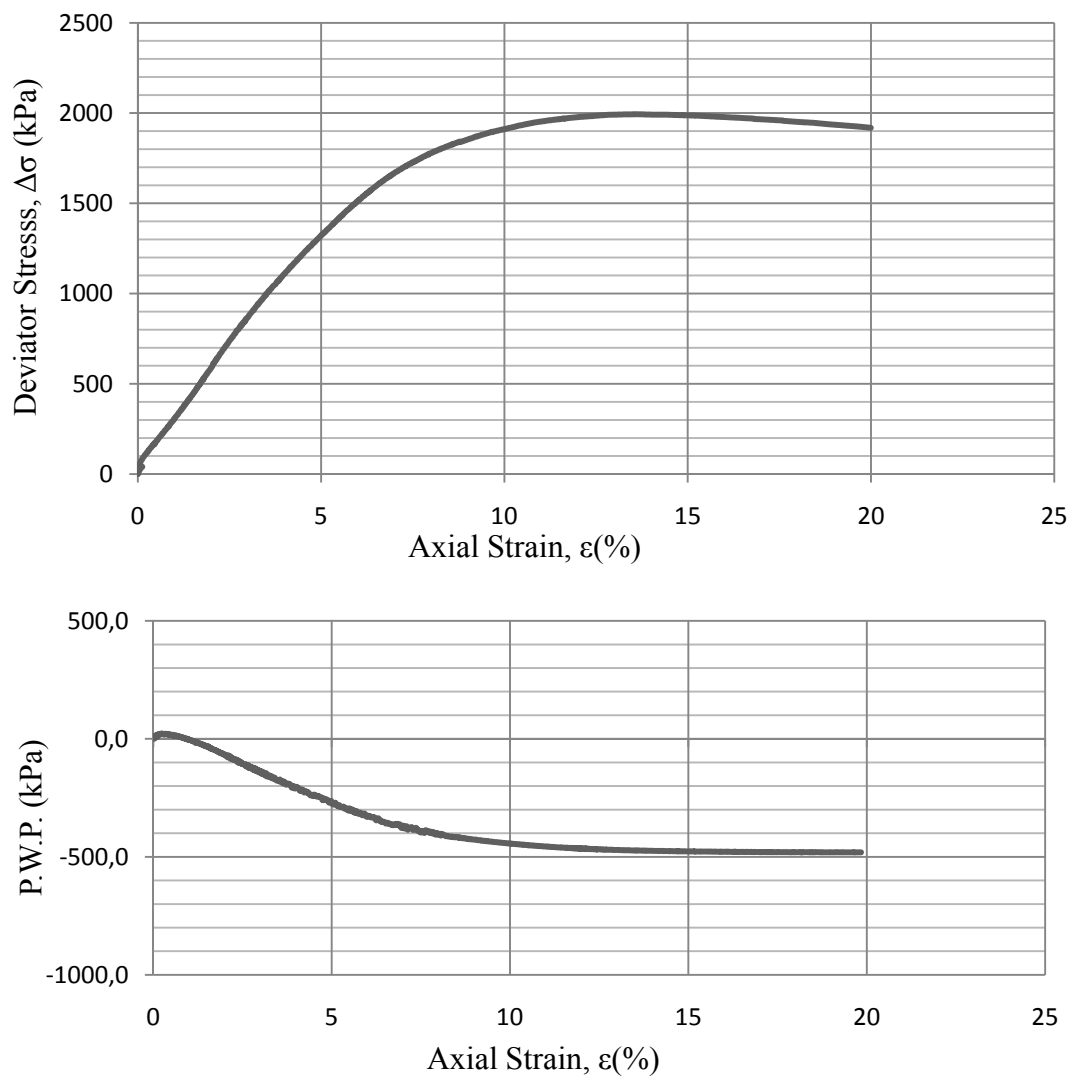
Figure B. 10 : Test Results for Sample No 47

Table B. 11 : Properties of Sample No 1

Sample No	1
$A_0 \, (cm^2)$	19.46
$V_0 \, (cm^3)$	194.40
$\gamma_{dry} \, (g/cm^3)$	1.610
Cell Pressure (kPa)	500
Back Pressure (kPa)	400
Confining Pressure (kPa)	100
Fiber Content (%)	1.0
Saturation (%)	97
Relative Density, Dr (%)	57
Strain rate (mm/min)	1.25
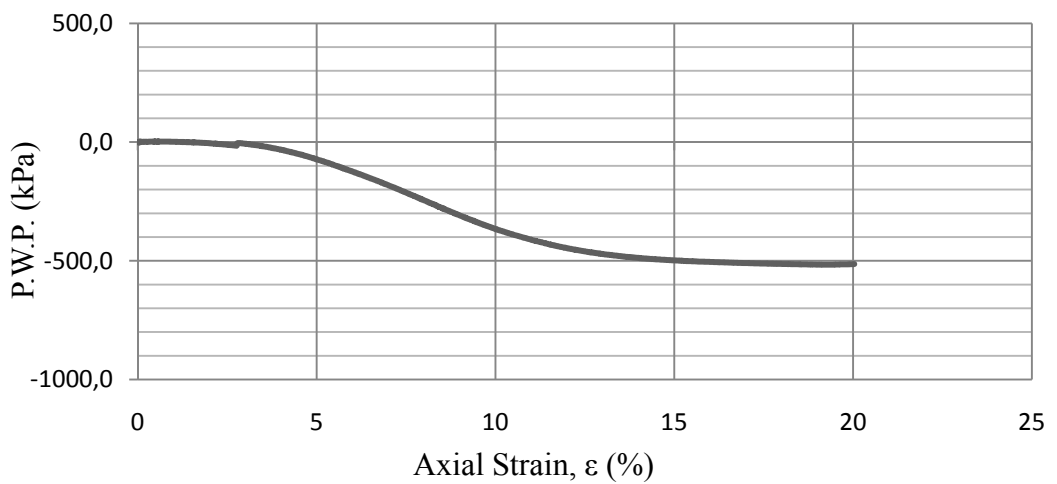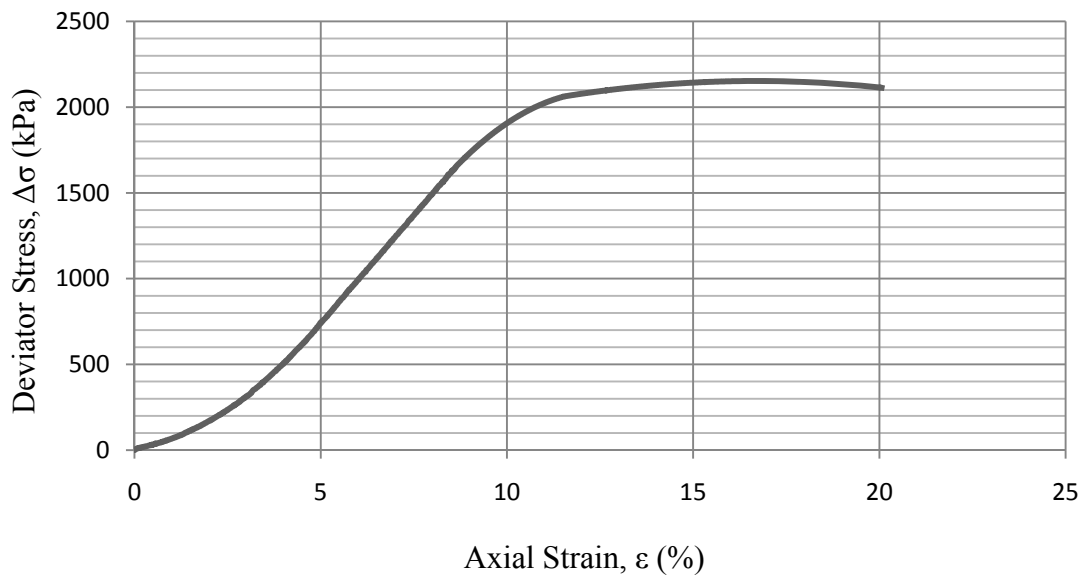
Figure B. 11 : Test Results for Sample No 58

Table B. 12 : Properties of Sample No 50

Sample No	50
$A_0 \, (cm^2)$	19.42
$V_0 \, (cm^3)$	194.07
$\gamma_{dry} \, (g/cm^3)$	1.613
Cell Pressure (kPa)	500
Back Pressure (kPa)	400
Confining Pressure (kPa)	100
Fiber Content (%)	1.0
Saturation (%)	99
Relative Density, Dr (%)	58
Strain rate (mm/min)	1.50
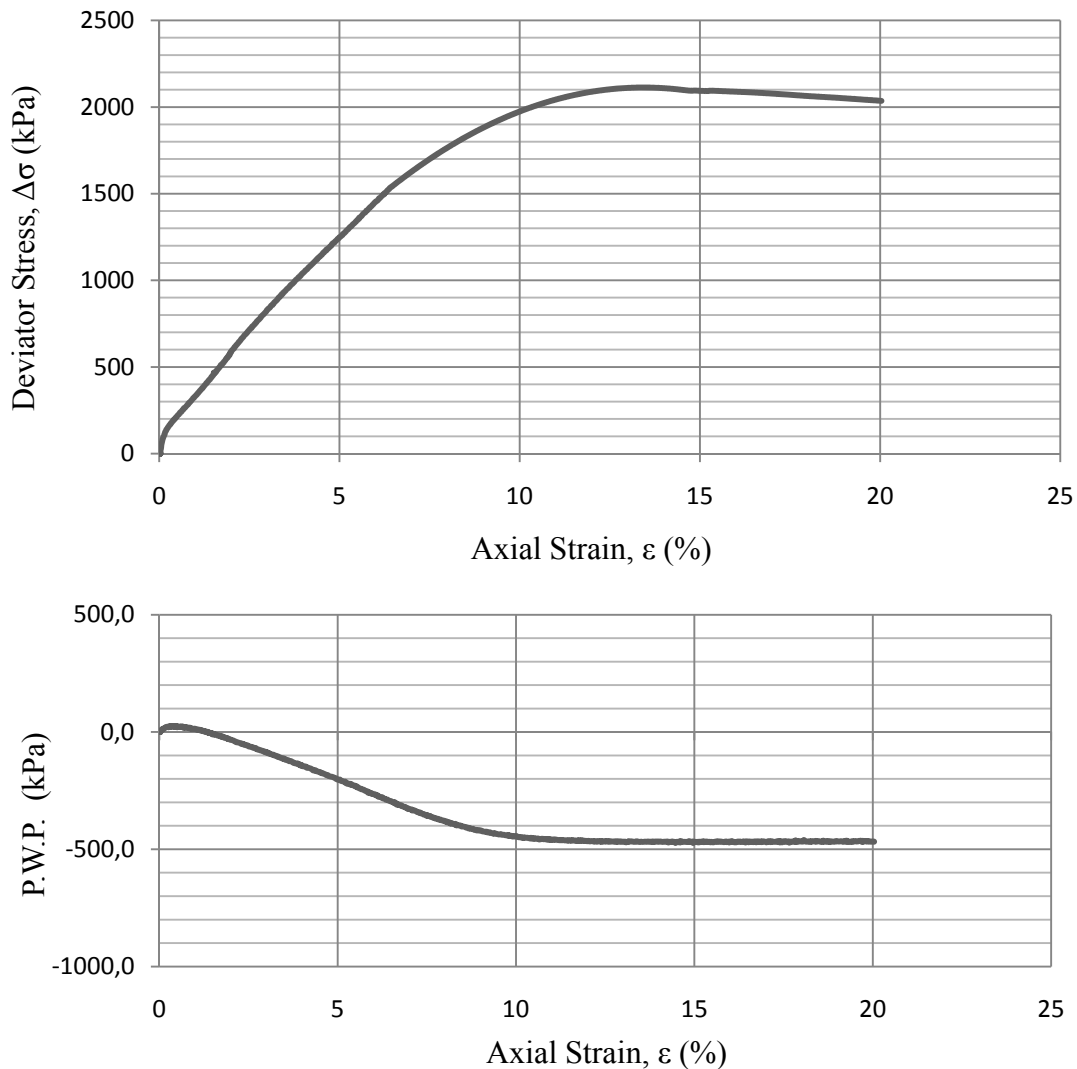
Figure B. 12 : Test Results for Sample No 50

Table B. 13 : Properties of Sample No 90

Sample No	90
A_0 (cm^2)	19.37
V_0 (cm^3)	193.42
γ_{dry} (g/cm^3)	1.60
Cell Pressure (kPa)	100
Back Pressure (kPa)	0
Confining Pressure (kPa)	100
Fiber Content (%)	0
Relative Density, Dr (%)	55
Strain rate (mm/min)	1.00

w= 10 %
Δu=0
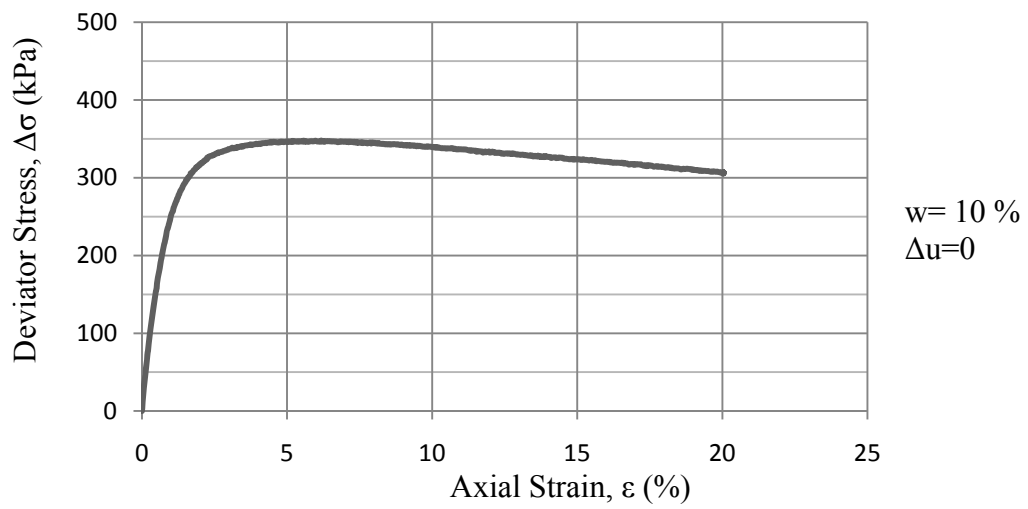
Figure B. 13: Test Results for Sample No 90

Table B. 14 : Properties of Sample No 19

Sample No	19
$A_0 (cm^2)$	19.47
$V_0 (cm^3)$	194.27
$\gamma_{dry} (g/cm^3)$	1.596
Cell Pressure (kPa)	100
Back Pressure (kPa)	0
Confining Pressure (kPa)	100
Fiber Content (%)	0.1
Relative Density, Dr (%)	54
Strain rate (mm/min)	1.00

w=10 %
$\Delta u=0$
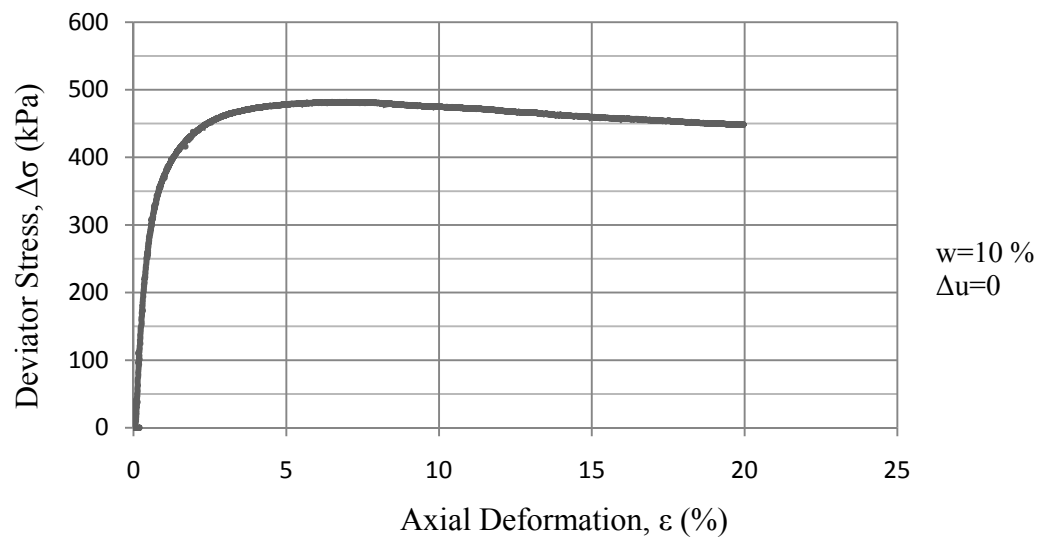
Figure B. 14 : Test Results for Sample No 19

Table B. 15 : Properties of Sample No 23

Sample No	23
A_0 (cm^2)	19.41
V_0 (cm^3)	194.00
γ_{dry} (g/cm^3)	1.603
Cell Pressure (kPa)	100
Back Pressure (kPa)	0
Confining Pressure (kPa)	100
Fiber Content (%)	0.5
Relative Density, Dr (%)	55
Strain rate (mm/min)	1.00

w= 10%
Δu=0
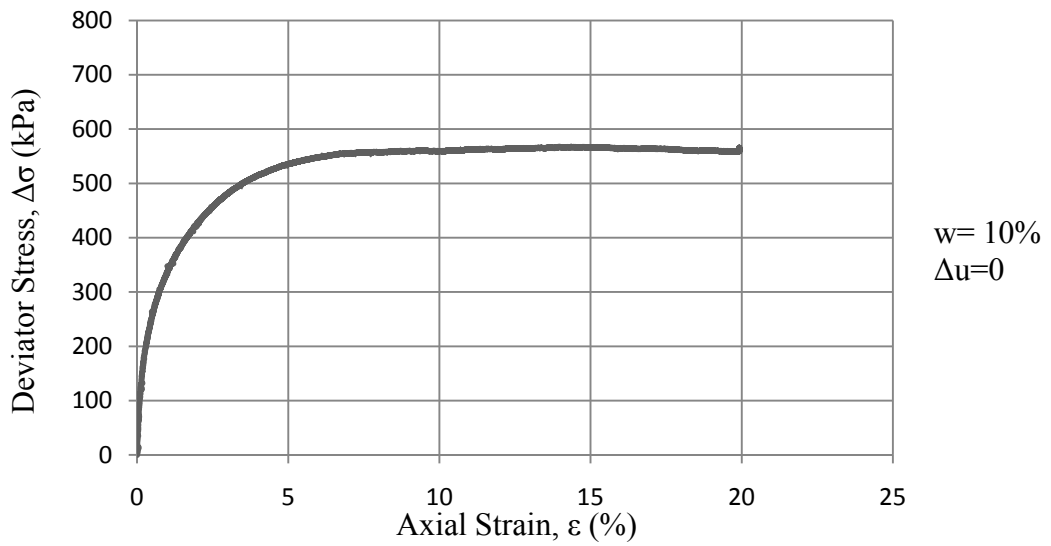
Figure B. 15 : Test Results for Sample No 23

Table B. 16 : Properties of Sample No 80

Sample No	80
A_0 (cm^2)	19.47
V_0 (cm^3)	194.53
γ_{dry} (g/cm^3)	1.609
Confining Pressure (kPa)	100
Back Pressure (kPa)	0
Confining Pressure (kPa)	100
Fiber Content (%)	1.0
Relative Density, Dr (%)	57
Strain rate (mm/min)	1.00

w= 10%
$\Delta u=0$
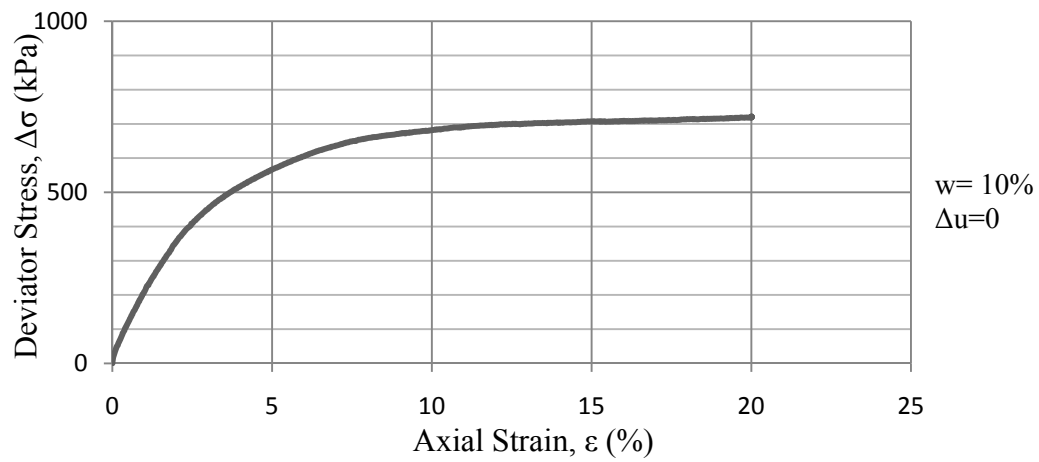
Figure B. 16 : Test Results for Sample No 80

Table B. 17 : Properties of Sample No 79

Sample No	79
A_0 (cm^2)	19.39
V_0 (cm^3)	193.81
γ_{dry} (g/cm^3)	1.599
Cell Pressure (kPa)	200
Back Pressure (kPa)	0
Confining Pressure (kPa)	200
Fiber Content (%)	0
Relative Density, Dr (%)	55
Strain rate (mm/min)	1.00

w=10%
Δu=0
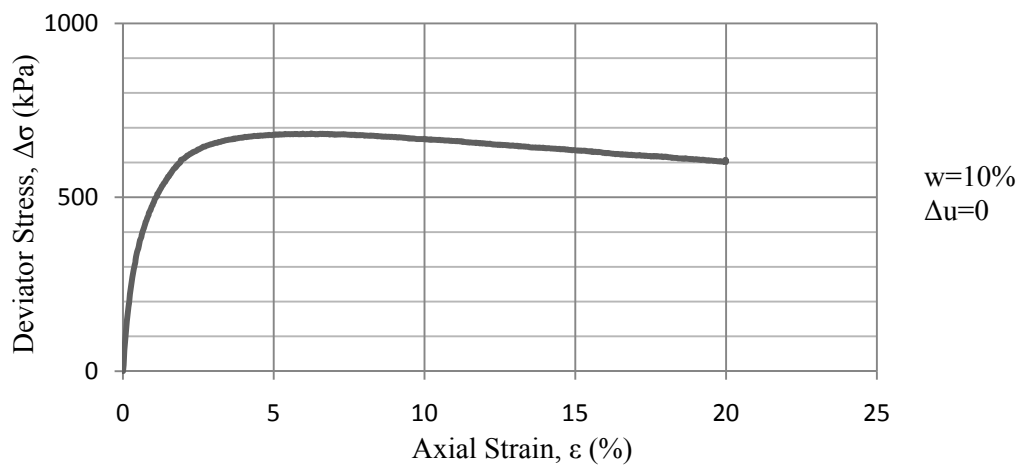
Figure B. 17 : Test Results for Sample No 79

Table B. 18 : Properties of Sample No 76

Sample No	76
$A_0 \, (cm^2)$	19.37
$V_0 \, (cm^3)$	193.49
$\gamma_{dry} \, (g/cm^3)$	1.602
Cell Pressure (kPa)	300
Back Pressure (kPa)	0
Confining Pressure (kPa)	300
Fiber Content (%)	0
Relative Density, Dr (%)	55
Strain rate (mm/min)	1.00

w= 10%
Δu=0
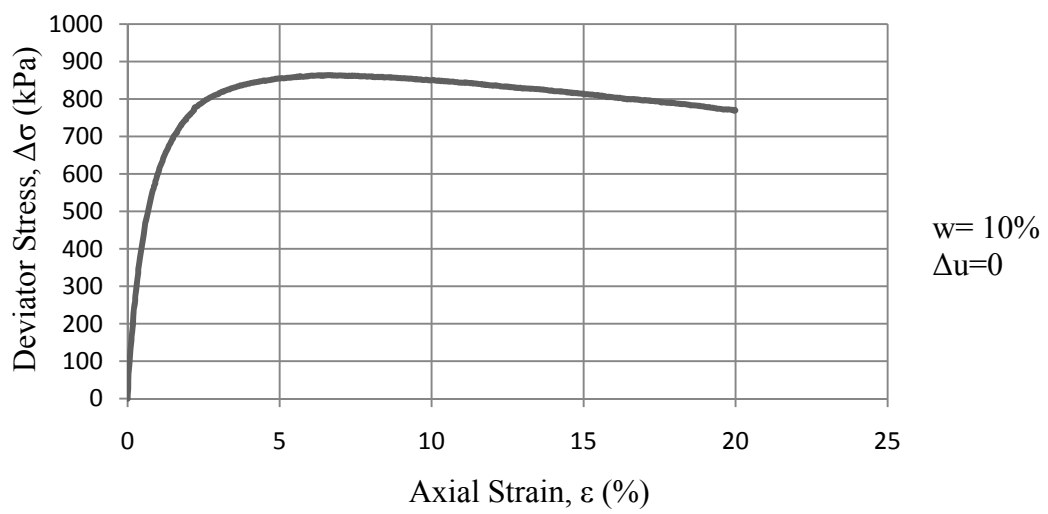
Figure B. 18 : Test Results for Sample No 76

Table B. 19: Properties of Sample No 82

Sample No	82
A_0 (cm^2)	19.36
V_0 (cm^3)	193.45
γ_{dry} (g/cm^3)	1.608
Cell Pressure (kPa)	200
Back Pressure (kPa)	0
Confining Pressure (kPa)	200
Fiber Content (%)	0.5
Relative Density, Dr (%)	57
Strain rate (mm/min)	1.00

w =10 %
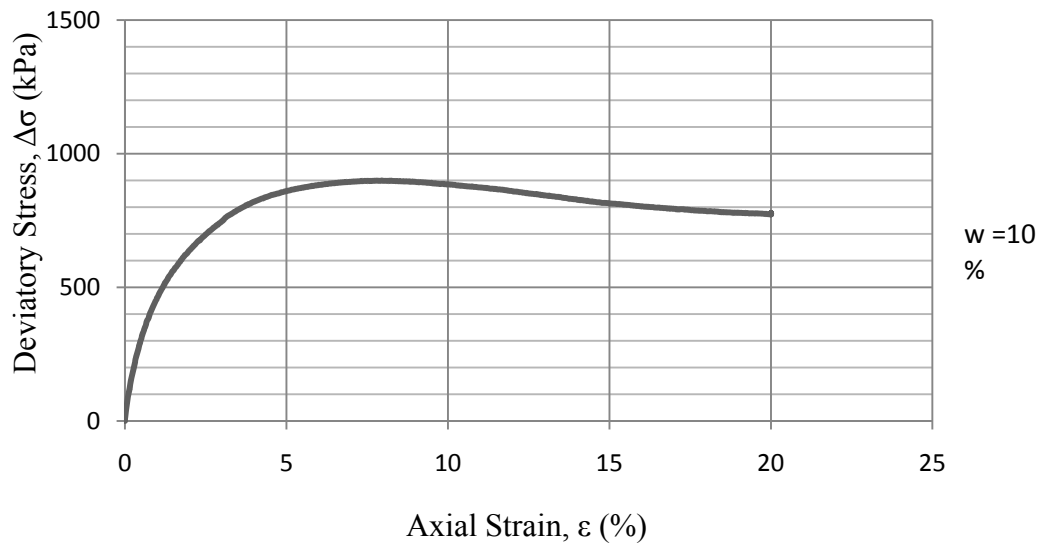
Figure B. 19: Test Results for Sample No 82

Table B. 20: Properties of Sample No 83

Sample No	83
$A_0 (cm^2)$	19.36
$V_0 (cm^3)$	193.50
$\gamma_{dry} (g/cm^3)$	1,608
Cell Pressure (kPa)	300
Back Pressure (kPa)	0
Confining Pressure (kPa)	300
Fiber Content (%)	0.5
Relative Density, Dr (%)	58
Strain rate (mm/min)	1.00
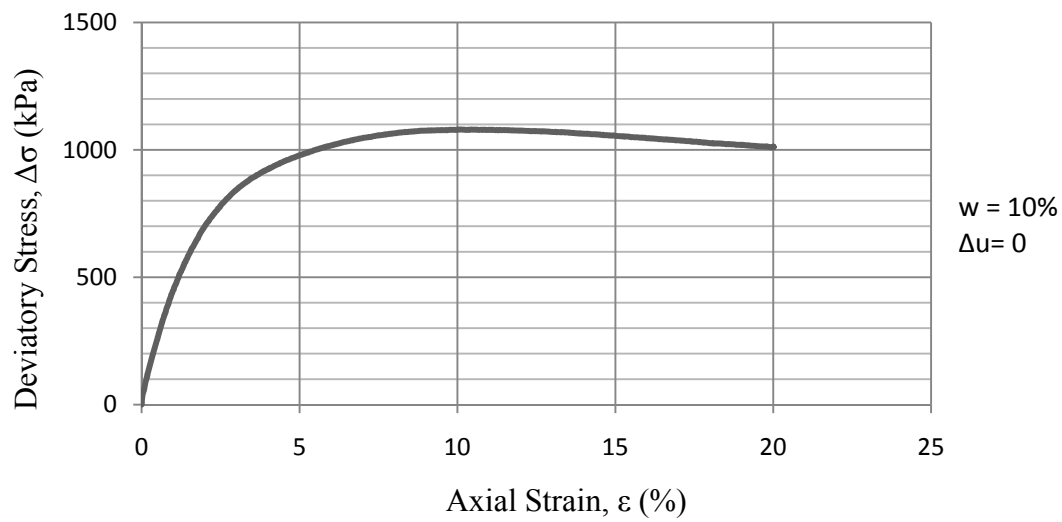
Figure B. 20: Test Results for Sample No 83

Table B. 21 : Properties of Sample No 81

Sample No	81
$A_0 (cm^2)$	19.47
$V_0 (cm^3)$	194.14
$\gamma_{dry} (g/cm^3)$	1.610
Cell Pressure (kPa)	200
Back Pressure (kPa)	0
Confining Pressure (kPa)	200
Fiber Content (%)	1.0
Relative Density, Dr (%)	58
Strain rate (mm/min)	1.00

w = 10%
Δu=0
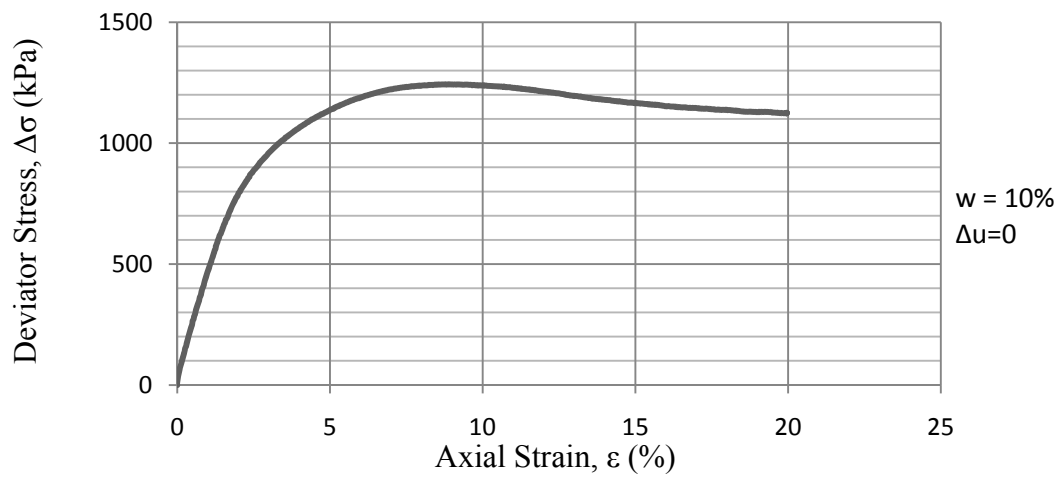
Figure B. 21 : Test Results for Sample No 81

Table B. 22 : Properties of Sample No 77

Sample No	77
A_0 (cm^2)	19.47
V_0 (cm^3)	194.60
γ_{dry} (g/cm^3)	1.608
Cell Pressure (kPa)	300
Back Pressure (kPa)	0
Confining Pressure (kPa)	300
Fiber Content (%)	1.0
Relative Density, Dr (%)	57
Strain rate (mm/min)	1.00

w= 10%
Δu=0
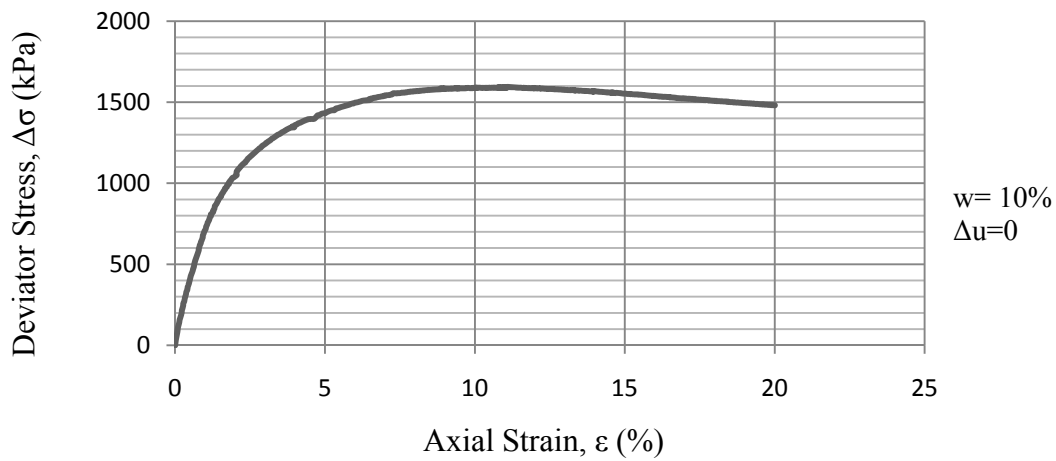
Figure B. 22 : Test Results for Sample No 77

Table B. 23: Properties of Sample No 87

Sample No	87
$A_0 (cm^2)$	19.37
$V_0 (cm^3)$	193.42
$\gamma_{dry} (g/cm^3)$	1.603
Confining Pressure (kPa)	500
Back Pressure (kPa)	400
Fiber Content (%)	0
Saturation(%)	97
Test Type	CD
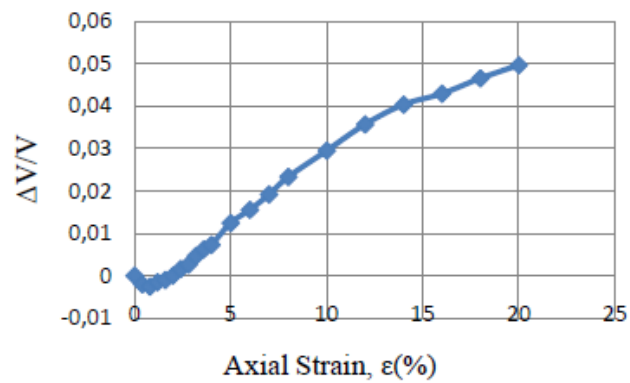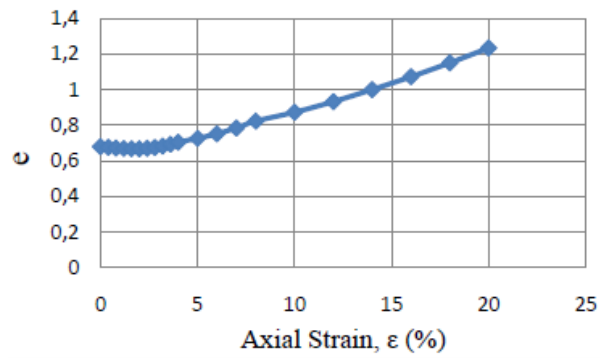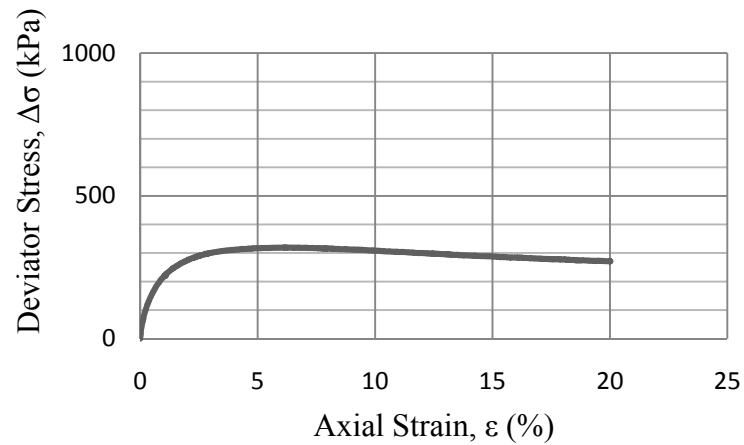
Figure B. 23: Test Results for Sample No 87

Table B. 24: Properties of Sample No 86

Sample No	86
$A_0 \, (cm^2)$	19.43
$V_0 \, (cm^3)$	194.02
$\gamma_{dry} \, (g/cm^3)$	1.601
Confining Pressure (kPa)	500
Back Pressure (kPa)	400
Net Pressure (kPa)	100
Fiber Content (%)	0
Saturation(%)	98
Relative Density, Dr (%)	55
Strain rate (mm/min)	1.00
Test Type	CD
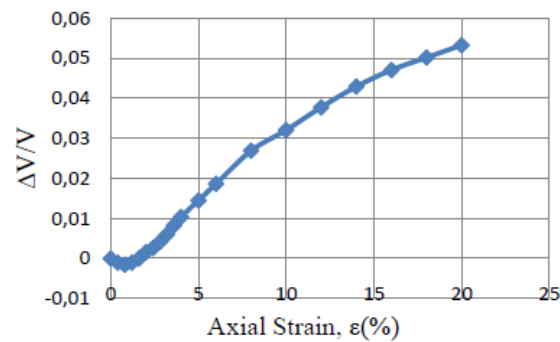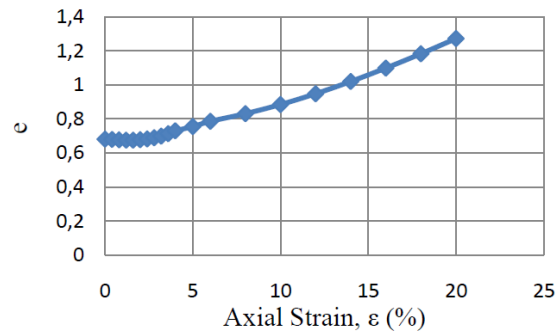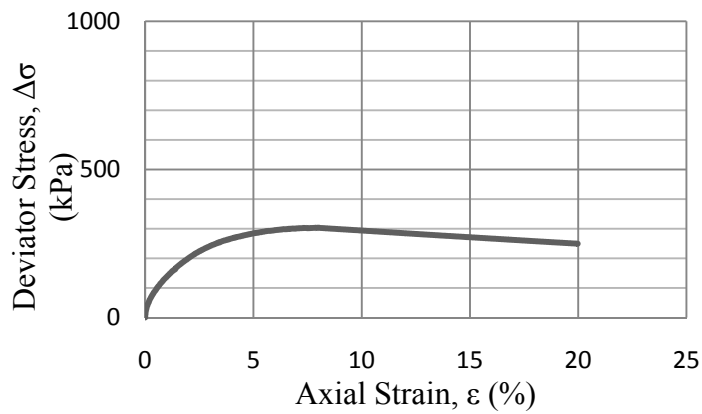
Figure B. 24: Test Results for Sample No 86

Table B. 25: Properties of Sample No 88

Sample No	88
A_0 (cm^2)	19.40
V_0 (cm^3)	193.62
γ_{dry} (g/cm^3)	1.601
Confining Pressure (kPa)	500
Back Pressure (kPa)	400
Net Pressure (kPa)	100
Fiber Content (%)	0
Saturation(%)	97
Relative Density, Dr (%)	55
Strain rate (mm/min)	2.00
Test Type	CD
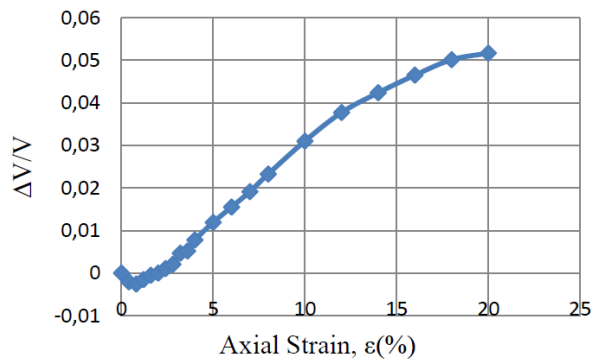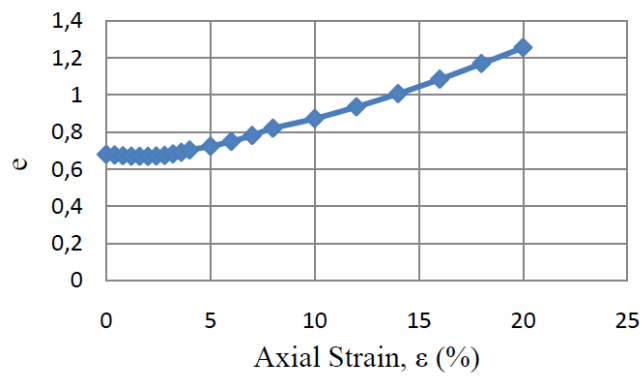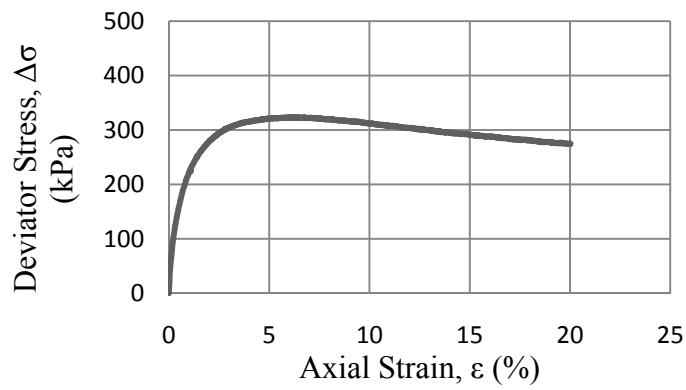
Figure B. 25: Test Results for Sample No 88

131

Table B. 26: Properties of Sample No 89

Sample No	89
$A_0\,(cm^2)$	19.39
$V_0\,(cm^3)$	193.84
$\gamma_{dry}\,(g/cm^3)$	1.607
Confining Pressure (kPa)	500
Back Pressure (kPa)	400
Net Pressure (kPa)	100
Fiber Content (%)	0.5
Saturation(%)	98
Relative Density, Dr (%)	57
Strain rate (mm/min)	1.00
Test Type	CD
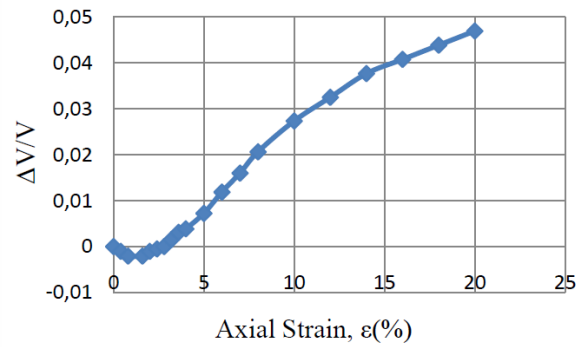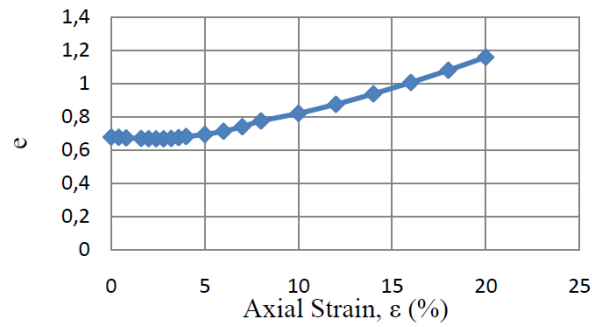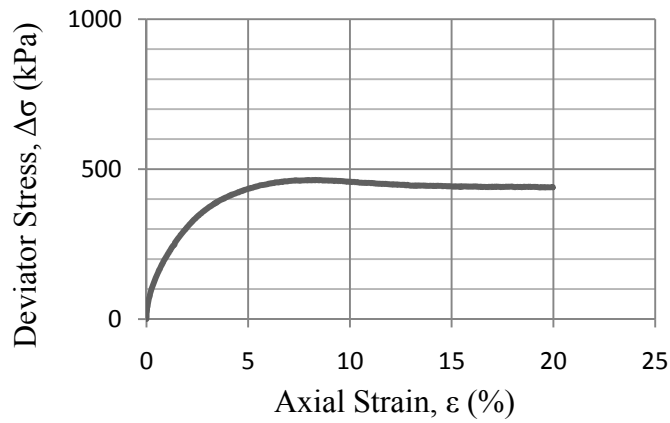
Figure B. 26: Test Results for Sample No 89

Table B. 27: Properties of Sample No 90

Sample No	90
A_0 (cm^2)	19.41
V_0 (cm^3)	194.203
γ_{dry} (g/cm^3)	1.612
Confining Pressure (kPa)	500
Back Pressure (kPa)	400
Net Pressure (kPa)	100
Fiber Content (%)	1.0
Saturation(%)	97
Relative Density, Dr (%)	58
Strain rate (mm/min)	1.00
Test Type	CD
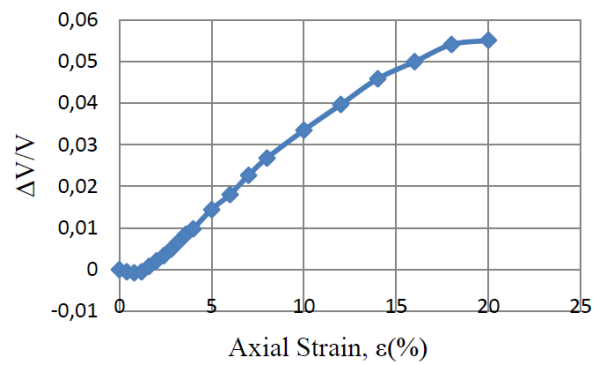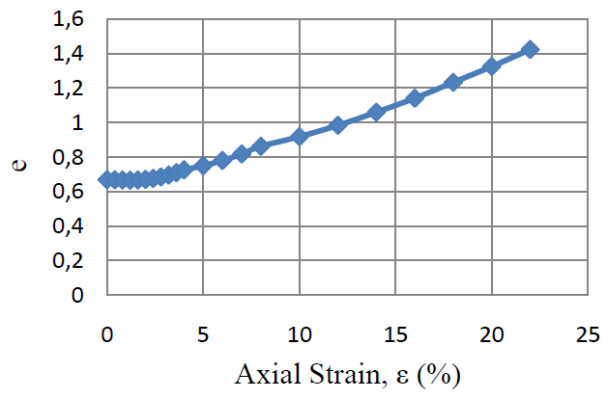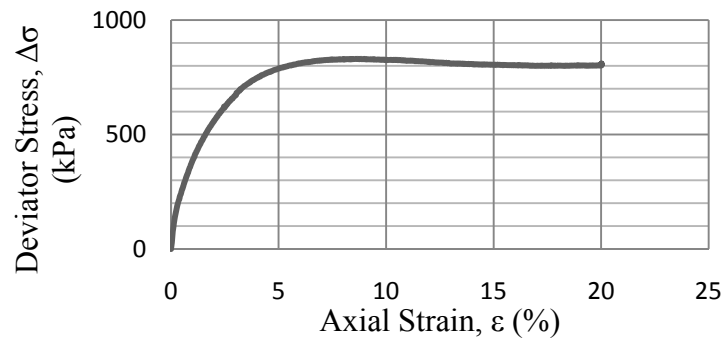
Figure B. 27: Test Results for Sample No 90

APPENDIX C
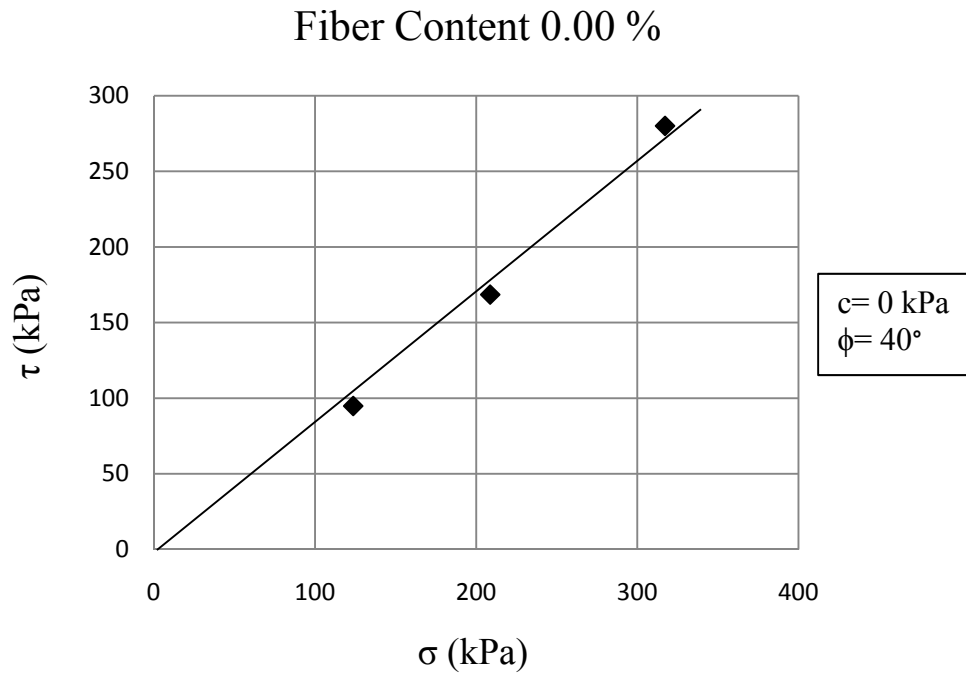
Fiber Content 0.00 %

Figure C. 1 : Shear Stress-Normal Stress graph for unreinforced sand
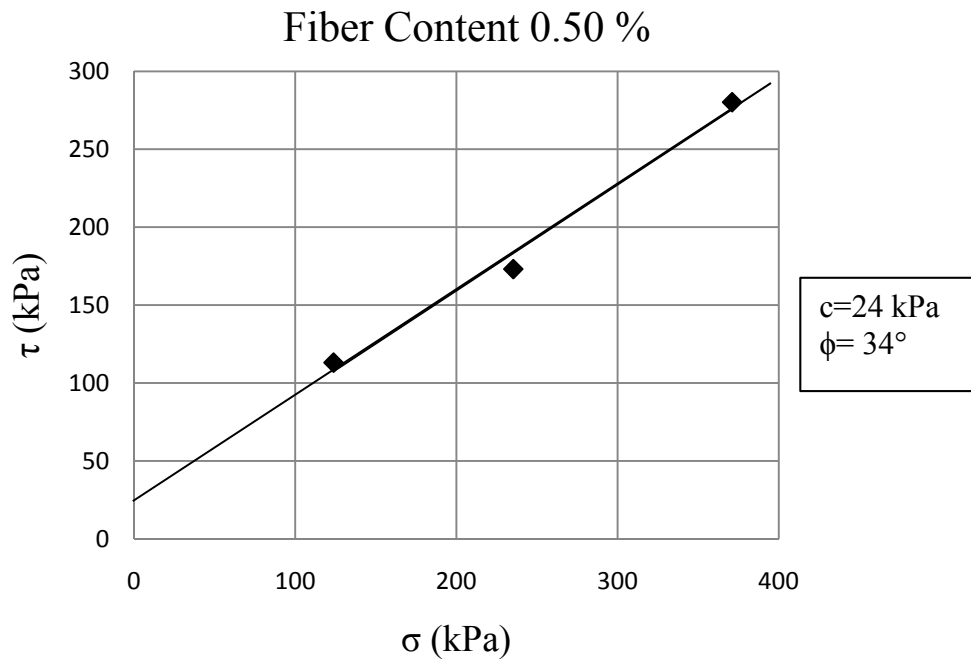
Fiber Content 0.50 %

Figure C. 2 : Shear Stress-Normal Stress graph for sand including 0.50 % fiber content
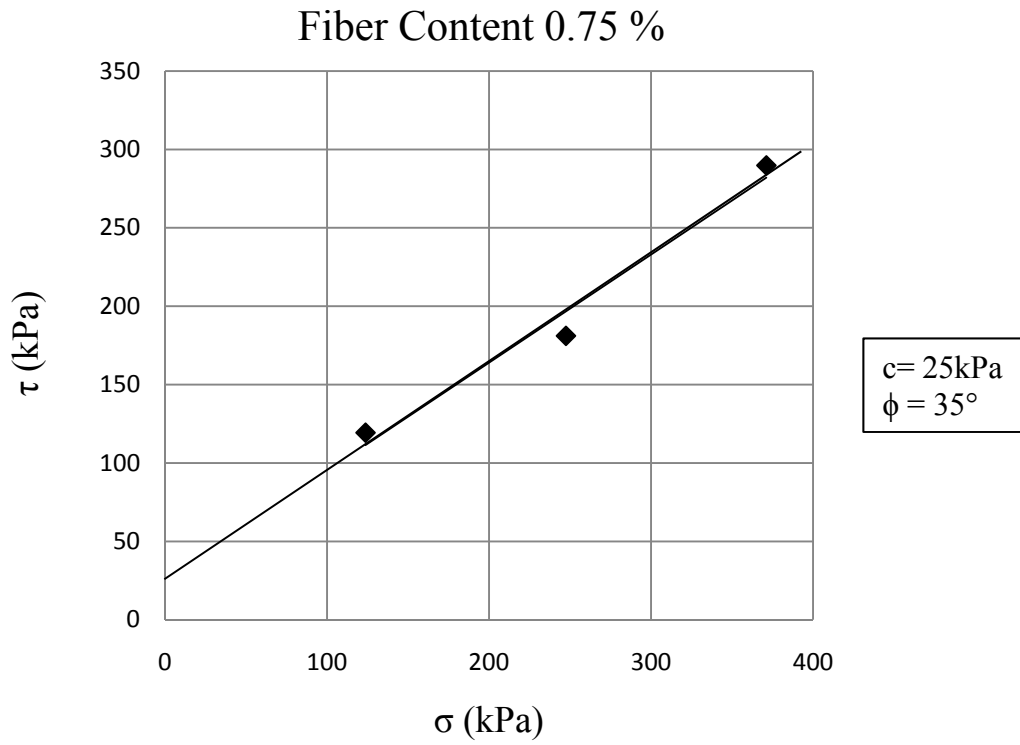
Figure C. 3 : Shear Stress-Normal Stress graph for sand including 0.75 % fiber content
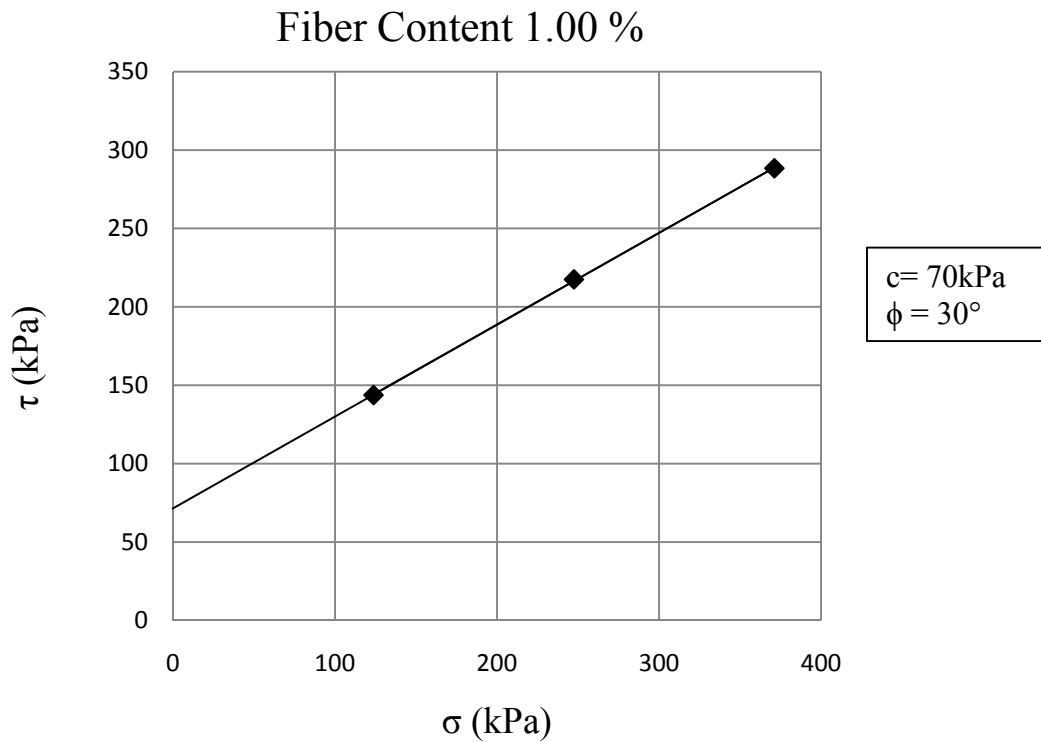

Figure C. 4 : Shear Stress-Normal Stress graph for sand including 1.00 % fiber content
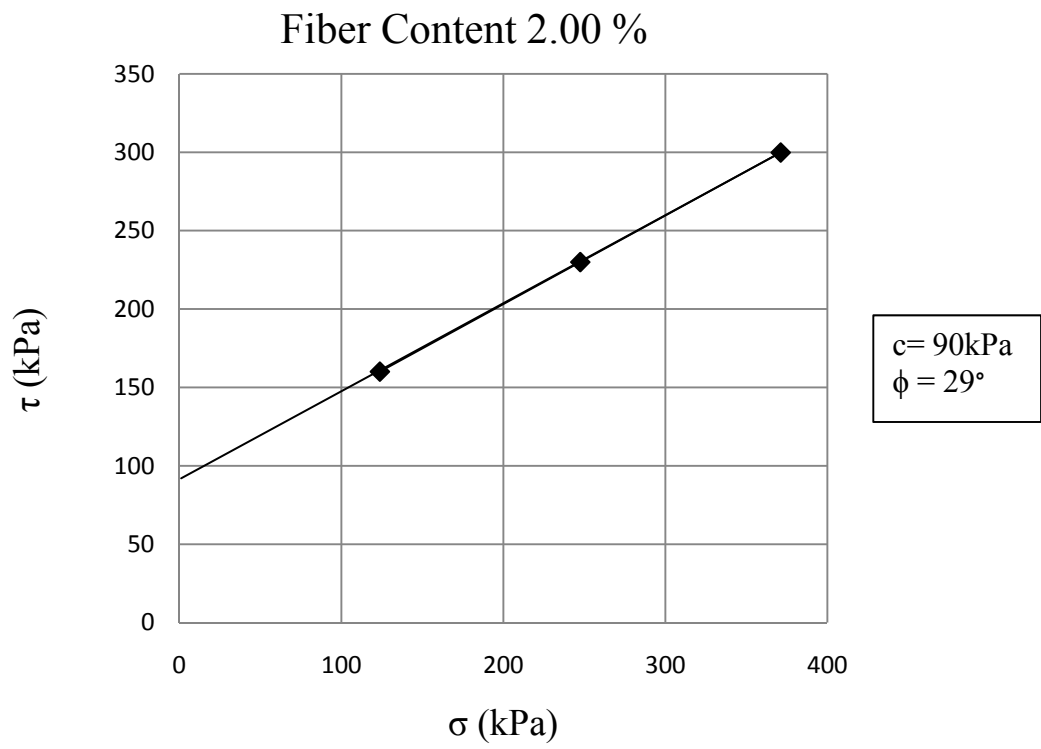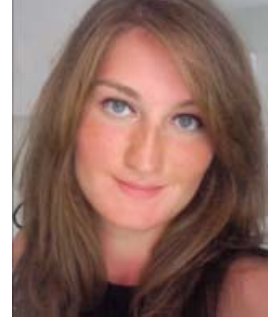
Figure C. 5 : Shear Stress-Normal Stress graph for sand including 2.00 % fiber content

CURRICULUM VITAE

Candidate's full name:	Hande Gerkuş
Place and date of birth:	İstanbul 27.04.1988
Permanent Address:	Kozyatağı Sok. Parlar Başoğlu B. Blok No:28 D.14 Kadıköy İSTANBUL
Universities and Colleges attended:	Istanbul Technical University (2005-2009)